Supporting Information for

Reversible photo-control over transmembrane anion transport using visible-light responsive supramolecular carriers

Aidan Kerckhoffs and Matthew J. Langton*

Contents

1 Materials and methods

All reagents and solvents were purchased from commercial sources and used without further purification. Lipids were purchased from Avanti Polar Lipids and used without further purification. Where necessary, solvents were dried by passing through an MBraun MPSP-800 column and degassed with nitrogen. Triethylamine was distilled from and stored over potassium hydroxide. Column chromatography was carried out on Merck® silica gel 60 under a positive pressure of nitrogen. Where mixtures of solvents were used, ratios are reported by volume. NMR spectra were recorded on a Bruker AVIII 400, Bruker AVII 500 (with cryoprobe) and Bruker AVIII 500 spectrometers. Chemical shifts are reported as δ values in ppm. Mass spectra were carried out on a Waters Micromass LCT and Bruker microTOF spectrometers. Fluorescence spectroscopic data were recorded using a Horiba Duetta fluorescence spectrophotometer, equipped with Peltier temperature controller and stirrer. UV-Vis spectra were recorded on a V-770 UV-Visible/NIR Spectrophotometer equipped with Peltier temperature controller and stirrer using quartz cuvettes of 1 cm path length. Experiments were conducted at 25°C unless otherwise stated. Vesicles were prepared as described below using Avestin "LiposoFast" extruder apparatus, equipped with polycarbonate membranes with 200 nm pores. GPC purification of vesicles was carried out using GE Healthcare PD-10 desalting columns prepacked with Sephadex G 25 medium.

Abbreviations

Boc: tert-butyloxycarbonyl; CF: 5(6)-Carboxyfluorescein; DBU: 1,8-Diazabicyclo[5.4.0]undec-7-ene; DCM: Dichloromethane; DIPEA: *N*,*N*-Diisopropylethylamine; DMF: *N*,*N*-Dimethylformamide; DMSO: Dimethylsulfoxide; DPPC: 1,2-dipalmitoyl-*sn*-glycero-3-phosphocholine; EYPG: egg-yolk phosphatidylglycerol; HEPES: *N*-(2- hydroxyethyl)piperazine-*N*'-(2-ethanesulfonic acid); HPTS: 8-hydroxy-1,3,6-pyrenetrisulfonate; HRMS: High resolution mass spectrometry; KF: Potassium Fluoride; KOH: Potassium hydroxide; LUVs: large unilamellar vesicles; MeCN: Acetonitrile; MeOH: Methanol; NCS: *N*-Chlorosuccinimide; POPC: 1-palmitoyl-2-oleoyl-*sn*-glycero-3-phosphocholine; rt: Room temperature; TFA: Trifluoroacetic acid; THF: Tetrahydrofuran.

2 Synthesis and characterization

General comments.

Compounds **6a-f** were prepared according to literature procedures.[1-2]

All novel compounds were characterised by ^{1}H and ^{13}C NMR, UV-Vis and high-resolution mass spectrometry. Azobenzene derivatives were formed as a mixture of *E* and *Z* isomers. Peaks for the *E* isomer are reported (major product). Thermal relaxation to achieve 100% *E* isomer was achieved by heating the sample in DMSO at 80 °C prior to NMR titration experiments or anion transport assays. For carriers **5a-i**, ^{1}H NMR spectra are provided for both 100% *E*-azobenzene isomer (heated dark state) and where available, 77% cis isomer (red light photostationary state for carriers **1a-i**). For ^{13}C spectra of carriers **5a-i**, spectra were run at 80 °C to improve solubility, and the *trans* isomer is the main species present. Where applicable, rotameric signals are labelled with a blue asterisk (*).

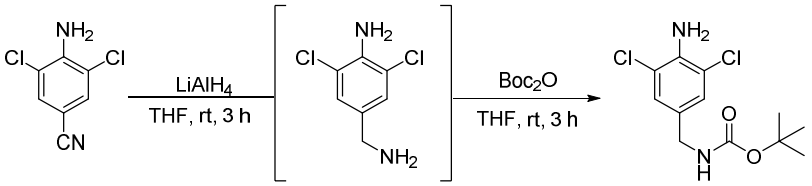

4-(aminomethyl)-2,6-dichloroaniline 3. To a suspension of $LiAlH_4$ (3.62 g, 95.3 mmol, 2.2 eq) in dry THF (90 mL) was added dropwise 3,5-dichloro-4-aminobenzonitrile **2** (8.1 g, 43.31 mmol, 1.0 eq) in THF (130 mL) at rt. THF (100 mL) was added to break up the thick solids. The suspension was stirred at rt for 3 hours. The reaction mixture was diluted in Et_2O (350 mL), then water (2 mL), 2.5M NaOH (4 mL), and water (8 mL) was added dropwise. The suspension was stirred for 15 minutes, and then anhydrous $MgSO_4$ was added. The solution was filtered, and filtrate concentrated. The off-white solid was redissolved in THF (75 mL). Boc_2O (8.4 g, 38.5 mmol, 1.05 eq.) was added and the reaction was stirred for 3 hours. The solution was concentrated and purified by silica gel flash chromatography (18% Acetone in hexane), then recrystallized from Et_2O and petroleum ether to afford the title compound (7.4 g, 3.37 mmol, 59% over two steps). ^{1}H NMR (400 MHz, Chloroform-*d*) δ 7.11 (s, 2H), 4.78 (s, 1H), 4.51 – 4.28 (br s, 2H), 4.15 (d, *J* = 6.0 Hz, 2H), 1.46 (s, 9H). ^{13}C NMR (126 MHz, Chloroform-d) δ 155.63, 139.11, 129.15, 126.88, 119.45, 79.63, 43.39, 28.27. HRMS-ESI (m/z) Calculated for $C_{12}H_{16}Cl_2N_2O_2$ $[M+H]^+$, 291.0661; found 291.0662.

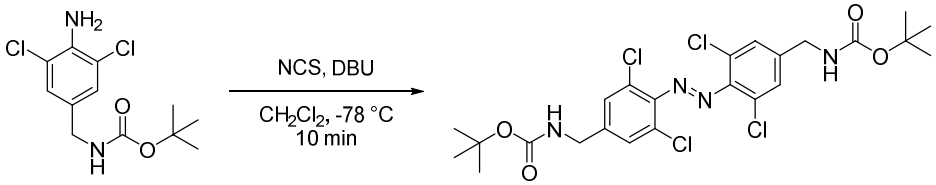

Azobenzene 4. To a solution of **3** (3.77 g, 12.9 mmol) in CH_2Cl_2 (200 mL) was added DBU (3.95 g, 25.9 mmol, 2 eq). The solution was stirred at room temperature for 5 min before being cooled down to −78 °C. N-Chlorosuccinimide (3.45 g, 25.9 mmol, 2 eq) was added. The dark solution was stirred for 10 min at −78 °C before quenching by addition of a saturated bicarbonate solution (200 mL). The organic layer was separated, washed sequentially with water (3 × 200 mL) and 1M HCl (200 mL) and concentrated to dryness in vacuo. The residue was purified by silica gel flash chromatography (1 to 3% EtOAc in CH_2Cl_2) to afford the title compound as a brown solid as a mixture of isomers (1.61 g, 5.55 mmol, 43%, 3:2 ratio of ***E*-4** and ***Z*-4** as indicated by ^{1}H NMR analysis). ***E*-4:** ^{1}H NMR (400 MHz, Chloroform-d) δ 7.37 (s, 4H), 4.99 (br s, 2H), 4.32 (d, *J* = 6.2 Hz, 4H), 1.48 (s, 18H) ^{13}C NMR (126 MHz, DMSO-d_6) δ 155.80, 144.97, 144.32, 128.11, 126.13, 78.34, 42.36, 28.16. HRMS-ESI (m/z) Calculated for $C_{24}H_{28}Cl_4N_4O_4$ $[M+H]^+$, 577.0937; found 577.0936.

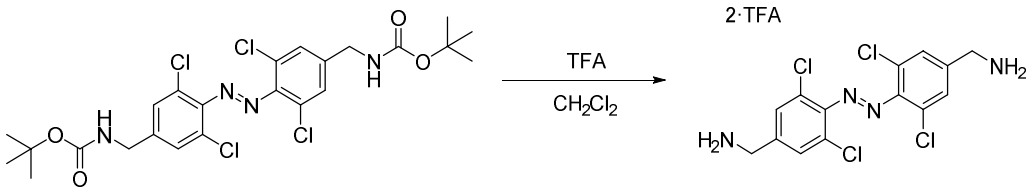

Amine 5. To a solution of **4** (2.00 g, 3.46 mmol) in CH_2Cl_2 (40 mL) was added TFA (5 mL). The reaction was stirred at room temperature for 4 hours. The TFA was removed under a stream of nitrogen, then dried in vacuo to afford the title compound as a brown solid (2.10 g, 3.46 mmol, 100%, 4:1 ratio of ***E*-5** and ***Z*-5** as indicated by ^{1}H NMR analysis). ***E*-5:** ^{1}H NMR (400 MHz, Methanol-d_4) δ 7.74 (s, 4H), 4.23 (s, 4H). ^{13}C NMR (101 MHz, Methanol-d_4) δ 148.73, 137.49, 131.33, 128.58, 42.86. HRMS-ESI (m/z) Calculated for $C_{14}H_{12}Cl_4N_4$ $[M+H]^+$, 376.9889; found 376.9888.

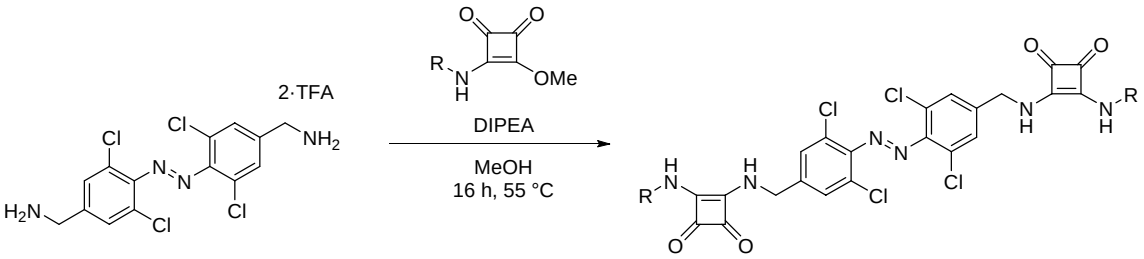

General Procedure 1. Amine **5** (50 mg, 82.5 µmol) was dissolved in MeOH (1 mL). DIPEA (86.2 µL, 0.5 mmol, 6 eq) was added dropwise. Monosquaramide **6a-i** (165 µmol, 2 eq) in MeCN (1 mL) was added, and the solution heated at 55 °C for 16 hours. The reaction was cooled to rt and the solid precipitate was filtered and washed sequentially with MeOH and MeCN, then collected and dried under high vacuum to afford the title compound as an orange/brown solid.

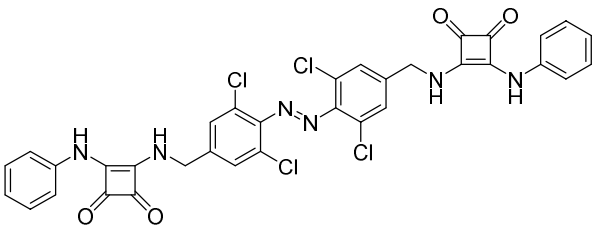

Transporter 1a. Synthesised according to general procedure 1 (31 mg, 44 µmol, 51%). ***E*-1a:** ^{1}H NMR (400 MHz, DMSO-d_6) δ 9.80 (s, 2H), 8.09 (br s, *J* = 6.3 Hz, 2H), 7.74 (s, 4H), 7.43 (m, 4H), 7.34 (m, 4H), 7.04 (t, *J* = 7.3 Hz, 2H), 4.90 (d, *J* = 6.3 Hz, 4H). ^{13}C NMR (126 MHz, DMSO-d_6) δ 183.81, 180.68, 168.50, 164.16, 145.24, 141.98, 138.46, 128.62, 128.32, 126.10, 122.34, 118.06, 45.50. HRMS-ESI (m/z) Calculated for $C_{34}H_{22}Cl_4N_6O_4$ $[M-H]^-$, 717.0373; found 717.0376.

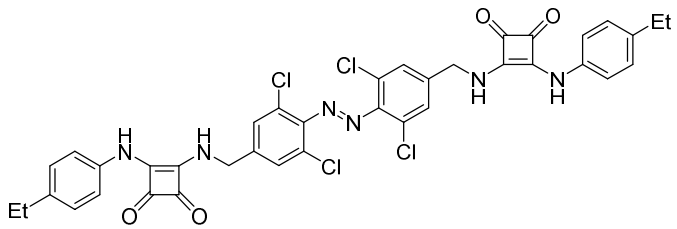

Transporter 1b. Synthesised according to general procedure 1 (39.1 mg, 50.3 µmol, 61%). ***E*-1b:** ^{1}H NMR (400 MHz, DMSO-d_6) δ 9.74 (s, 2H), 8.04 (t, *J* = 5.54 Hz, 1H), 7.74 (s, 4H), 7.33 (d, *J* = 8.25 Hz), 7.18 (d, *J* = 8.25 Hz) 4.90 (d, *J* = 5.54 Hz, 4H), 2.57 (q, *J* = 7.61 Hz, 4H), 1.17 (t, *J* = 7.61 Hz, 6H). ^{13}C NMR (126 MHz, DMSO-d_6) δ 183.79, 180.89, 168.57, 164.36, 145.50, 142.76, 138.43, 136.53, 128.84, 128.57, 126.37, 118.44, 45.78, 27.50, 15.70. HRMS-ESI (m/z) Calculated for $C_{38}H_{30}Cl_4N_6O_4$ [M-H]$^-$, 773.1010; found 773.1017

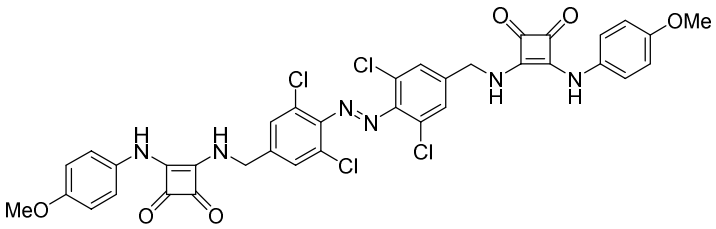

Transporter 1c. Synthesised according to general procedure 1 (32 mg, 44 µmol, 53%). ***E*-1c:** ^{1}H NMR (400 MHz, DMSO-d_6) δ 9.67 (s, 2H), 7.94 (s, 2H), 7.73 (s, 4H), 7.34 (d, *J* = 8.5 Hz, 4H), 6.96 – 6.91 (m, 4H), 4.88 (d, *J* = 6.1 Hz, 4H), 4.80 (s, 1H), 3.74 (s, 6H). ^{13}C NMR (126 MHz, DMSO-d_6) δ 183.23, 180.92, 168.05, 164.34, 155.40, 145.24, 142.14, 131.69, 128.32, 126.11, 119.91, 114.32, 55.06, 45.50. HRMS-ESI (m/z) Calculated for $C_{36}H_{26}Cl_4N_6O_6$ [M-H]$^-$, 777.0584; found 777.0591.

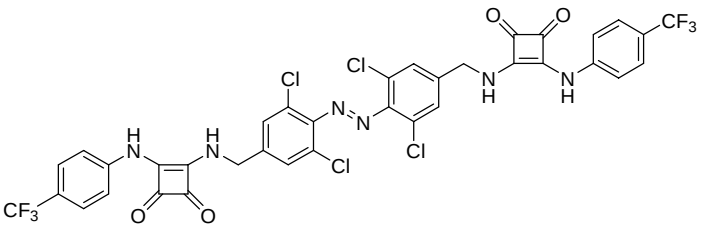

Transporter 1d. Synthesised according to general procedure 1 (34.5 mg, 40.2 µmol, 49%). ***E*-1d:** ^{1}H NMR (400 MHz, DMSO-d_6) δ 10.07 (s, 2H), 8.17 (t, *J* = 5.43 Hz, 1H), 7.75 (s, 4H), 7.69 (d, *J* = 8.69 Hz), 7.60 (d, *J* = 8.69 Hz), 4.91 (d, *J* = 5.43 Hz, 4H). ^{13}C NMR (126 MHz, DMSO-d_6) δ 184.54, 180.62, 169.22, 163.46, 145.31, 142.08, 128.37, 125.92, 124.48 (q, *J* = 271.3 Hz), 122.48 (q, *J* = 32.13 Hz), 117.94, 45.60. HRMS-ESI (m/z) Calculated for $C_{36}H_{20}Cl_4F_6N_6O_4$ [M-H]$^-$, 855.0115; found 855.0107

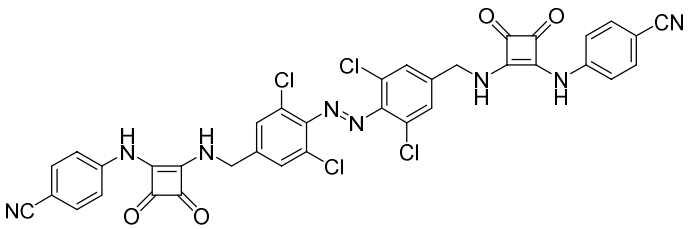

Transporter 1e. Synthesised according to general procedure 1 (40 mg, 52 µmol, 63%). ***E*-1e:** ^{1}H NMR (400 MHz, DMSO-d_6) δ 10.12 (s, 2H), 8.21 (m, 2H), 7.80 (d, *J* = 8.01 Hz, 4H), 7.75 (s, 4H), 7.58 (d, *J* = 8.01 Hz), 4.91 (d, *J* = 4.38 Hz, 4H). ^{13}C NMR (126 MHz, DMSO-d_6) δ 184.71, 180.52, 169.45, 162.98, 145.29, 142.68, 141.68, 132.97, 128.35, 126.09, 118.32, 118.00, 103.86, 45.59. Calculated for $C_{36}H_{20}Cl_4N_8O_4$ [M-H]$^-$, 767.0278, found 767.0301.

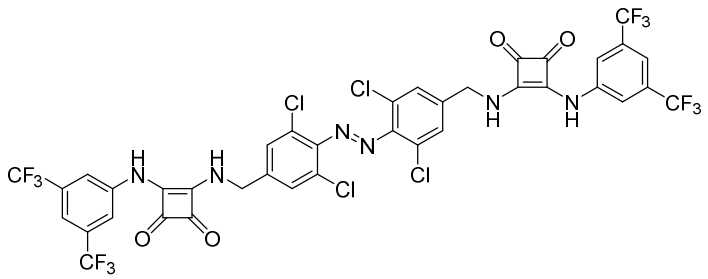

Transporter 1f. Synthesised according to general procedure 1 (34 mg, 46.2 µmol, 70%). ***E*-1f:** ^{1}H NMR (400 MHz, DMSO-d_6) δ 10.37 (br s, 2H), 8.20 (br s, 2H), 8.02 (s, 4H), 7.74 (s, 4H), 7.69 (s, 2H), 4.91 (s, 4H). ^{13}C NMR (101 MHz, DMSO-d_6) δ 184.69, 180.87, 169.42, 162.86, 145.33, 141.80, 140.72, 131.05 (q, *J* = 33.08 Hz), 128.43, 126.12, 122.74 (q, *J* = 274 Hz), 118.03, 114.34, 45.66. HRMS-ESI (m/z) Calculated for $C_{38}H_{18}Cl_4N_6O_4$ $[M-H]^-$, 988.9879; found 988.9863.

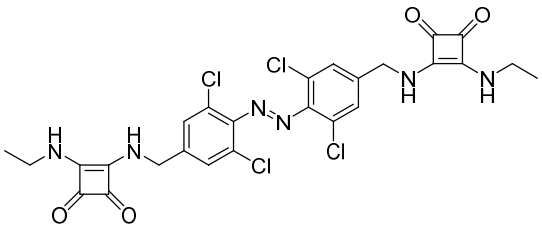

Transporter 1g. Synthesised according to general procedure 1 (34.6 mg, 55 µmol, 67%). ***E*-1g:** ^{1}H NMR (400 MHz, DMSO-d_6) δ 7.87 (br s, 2H), 7.67 (s, 4H), 7.49 (br s, 2H), 4.78 (d, *J* = 6.2 Hz, 4H), 3.52 (m, 4H), 1.16 (t, *J* = 7.2 Hz, 6H). ^{13}C NMR (126 MHz, DMSO) δ 182.76, 182.19, 168.05, 166.90, 145.14, 142.53, 128.27, 126.07, 45.19, 38.01, 15.80. HRMS-ESI (m/z) Calculated for $C_{26}H_{22}Cl_4N_6O_4$ $[M-H]^-$, 621.0384; found 621.0384

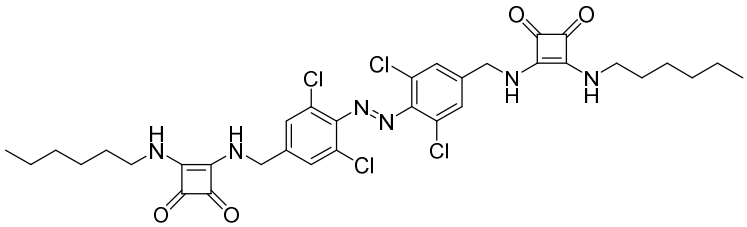

Transporter 1h. Synthesised according to general procedure 1 (50 mg, 68.4 µmol, 83%). ***E*-1h:** ^{1}H NMR (400 MHz, DMSO-d_6) δ 7.83 (br s, 2H), 7.66 (s, 4H), (br m, 2H) 4.79 (d, *J* = 5.54 Hz, 4H), 3.50 (m, 4H), 1.51 (m, 4H), 1.27 (m, 12H), 0.84 (m, 6H). ^{13}C NMR (126 MHz, DMSO-d_6) δ 182.77, 182.16, 168.20, 166.81, 145.10, 142.53, 128.19, 126.05, 45.12, 43.04, 30.21, 30.06, 24.89, 21.25, 12.99. HRMS-ESI (m/z) Calculated for $C_{34}H_{38}Cl_4N_6O_4$ $[M-H]^-$, 733.1625; found 733.1632.

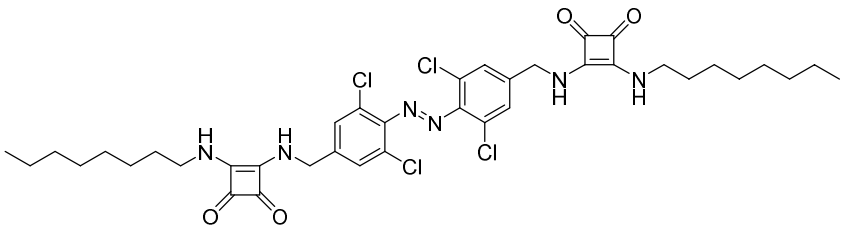

Transporter 1i. Synthesised according to general procedure 1 (55.6 mg, 68.4 µmol, 83%). ***E*-1i:** ^{1}H NMR (400 MHz, DMSO-d_6) δ 7.62 (s, 4H), 4.75 (s, 4H), 3.56 (m, 4H), 1.48 (m, 4H), 1.22 (m, 20H), 0.80 (t, *J* = 6.5 Hz, 6H). ^{13}C NMR (126 MHz, DMSO-d_6) δ 182.79, 182.18, 168.22, 166.84, 145.13, 142.57, 128.22, 126.08, 45.15, 43.07, 30.57, 30.12, 27.98, 27.91, 25.30, 21.34, 13.10. HRMS-ESI (m/z) Calculated for $C_{38}H_{46}Cl_4N_6O_4$ $[M-H]^-$, 789.2251; found 789.2254.

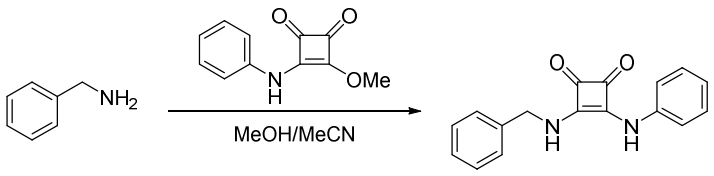

Transporter S1. Benzylamine (17 mg, 158 µmol) was dissolved in MeOH (0.5 mL). **6a** (21 mg, 104 µmol, 1.0 eq) dissolved in MeCN (1.5 mL) was added, and the reaction was stirred at room temperature, after which a white precipitate had formed. The solid precipitate was filtered and washed sequentially with MeOH and MeCN, then collected and dried under high vacuum to afford the title compound as a white solid (19 mg, 68 µmol, 43.03%). ^{1}H NMR (500 MHz, DMSO-d_6) δ 9.64 (s, 1H), 8.01 (s, 1H), 7.45 – 7.37 (m, 6H), 7.33 (m, 3H), 7.02 (t, *J* = 7.4 Hz, 1H), 4.82 (s, 2H). ^{13}C NMR (126 MHz, DMSO) δ 184.00, 180.36, 168.83, 163.78, 138.96, 138.45, 129.35, 128.75, 127.69, 127.63, 122.68, 118.01, 47.20. HRMS-ESI (m/z) Calculated for $C_{17}H_{15}N_2O_2$ $[M+H]^+$, 279.1128; found 279.1130.

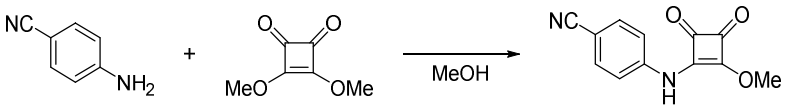

Monosquaramide 6e. To a stirred solution of 3,4-dimethoxy-3-cyclobutene-1,2-dione (100 mg, 0.70 mmol, 1 eq) in methanol (1 mL) was added 4-aminobenzonitrile (87 mg, 0.77 mmol, 1.04 eq) and the mixture stirred for 24 hours at room temperature. The residue was concentrated, dry-loaded onto silica, then purified by silica gel flash chromatography (0% then 10% MeCN in CH_2Cl_2) afford the title compound (90 mg, 0.316 mmol, 56%) as a white solid. ^{1}H NMR (400 MHz, DMSO-d_6) δ 11.06 (s, 1H), 7.81 (d, *J* = 8.4 Hz, 2H), 7.53 (d, *J* = 8.3 Hz, 2H), 4.41 (s, 3H). ^{13}C NMR (101 MHz, DMSO-d_6) δ 187.37, 184.65, 180.04, 169.05, 142.33, 133.59, 119.31, 118.96, 105.36, 60.91. HRMS-ESI (m/z) Calculated for $C_{12}H_{10}NO_4$ $[M-H]^-$, 227.0462; found 227.0460.

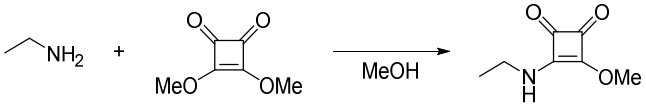

Monosquaramide 6g. To a stirred solution of 3,4-dimethoxy-3-cyclobutene-1,2-dione (100 mg, 0.77 mmol, 1 eq) in methanol (1 mL) was added 70% ethylamine in water (168 µl, 2.11 mmol, 3 eq) and the mixture was allowed to stir at room temperature for 20 hours. The residue was concentrated and purified by silica gel flash chromatography (7% MeCN in CH_2Cl_2) to afford the title compound (73 mg, 0.316 mmol, 72%) as a white solid. The compound exists as two rotamers in DMSO at room temperature in a 3:2 ratio. **Major rotamer:** ^{1}H NMR (400 MHz, DMSO-d_6). δ 8.78 (s, 1H), 4.29 (s, 3H), 3.29 (t, *J* = 6.9 Hz, 2H), 1.13 (t, *J* = 7.0 Hz, 3H). ^{13}C NMR (126 MHz, DMSO) δ 189.05, 182.25, 176.95, 171.89, 60.11, 38.54 15.68. HRMS-ESI (m/z) Calculated for $C_7H_9NO_3$ $[M-H]^-$, 154.0499; found 154.0503.

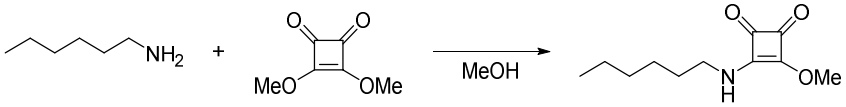

Monosquaramide 6h. To a stirred solution of 3,4-dimethoxy-3-cyclobutene-1,2-dione (100 mg, 0.70 mmol, 1 eq) in methanol (1 mL) was added hexylamine (78.3 mg, 0.77 mmol, 1.1 eq) and the mixture was stirred for 20 hours at room temperature, then concentrated. The residue was purified by silica gel flash chromatography (9% MeCN in CH_2Cl_2) to afford the title compound (133 mg, 0.629 mmol, 89%). The compound exists as two rotamers in DMSO at room temperature in a 3:1 ratio. **Major Rotamer**: ^{1}H NMR (400 MHz, Chloroform-d) δ 6.26 (br s, 1H), 4.41 (s, 3H), 3.46 – 3.36 (m, 2H), 1.60 (m, 2H), 1.39 – 1.25 (m, 6H), 0.95 – 0.83 (m, 3H), ^{13}C NMR (101 MHz, Chloroform-d) δ 189.85, 182.88, 177.72, 172.29, 60.56, 45.11, 31.36, 30.57, 26.09, 22.58, 14.06. HRMS-ESI (m/z) Calculated for $C_{11}H_{17}NO_3$ $[M-H]^-$, 210.1136; found 210.1133.

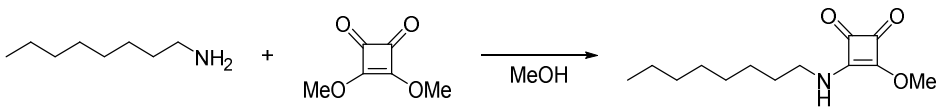

Monosquaramide 6i. To a stirred solution of 3,4-dimethoxy-3-cyclobutene-1,2-dione (100 mg, 0.70 mmol, 1 eq) in methanol (1 mL) was added octylamine (100 mg, 0.77 mmol, 1.1 eq) and the mixture was allowed to stir at room temperature for 20 hours, then concentrated. The residue was concentrated and purified by silica gel flash chromatography (10% MeCN in CH_2Cl_2), to afford the title compound as a white solid (100 mg, 0.629 mmol, 52%). The compound exists as two rotamers in DMSO at room temperature in a 4:1 ratio. **Major Rotamer:** ^{1}H NMR (400 MHz, Chloroform-d) δ 6.61 (br s, 1H), 4.40 (s, 3H), 3.41 (m, 2H), 1.61 (m, 2H), 1.29 (m, 10H), 0.87 (t, J = 6.7 Hz, 3H). δ ^{13}C NMR (101 MHz, Chloroform-d) δ 189.72, 183.02, 177.73, 172.32, 60.62, 45.13, 31.86, 30.65, 29.24, 29.18, 26.44, 22.73, 14.18. HRMS-ESI (m/z) Calculated for $C_{13}H_{21}NO_3$ $[M-H]^-$, 240.1596; found 240.1594.

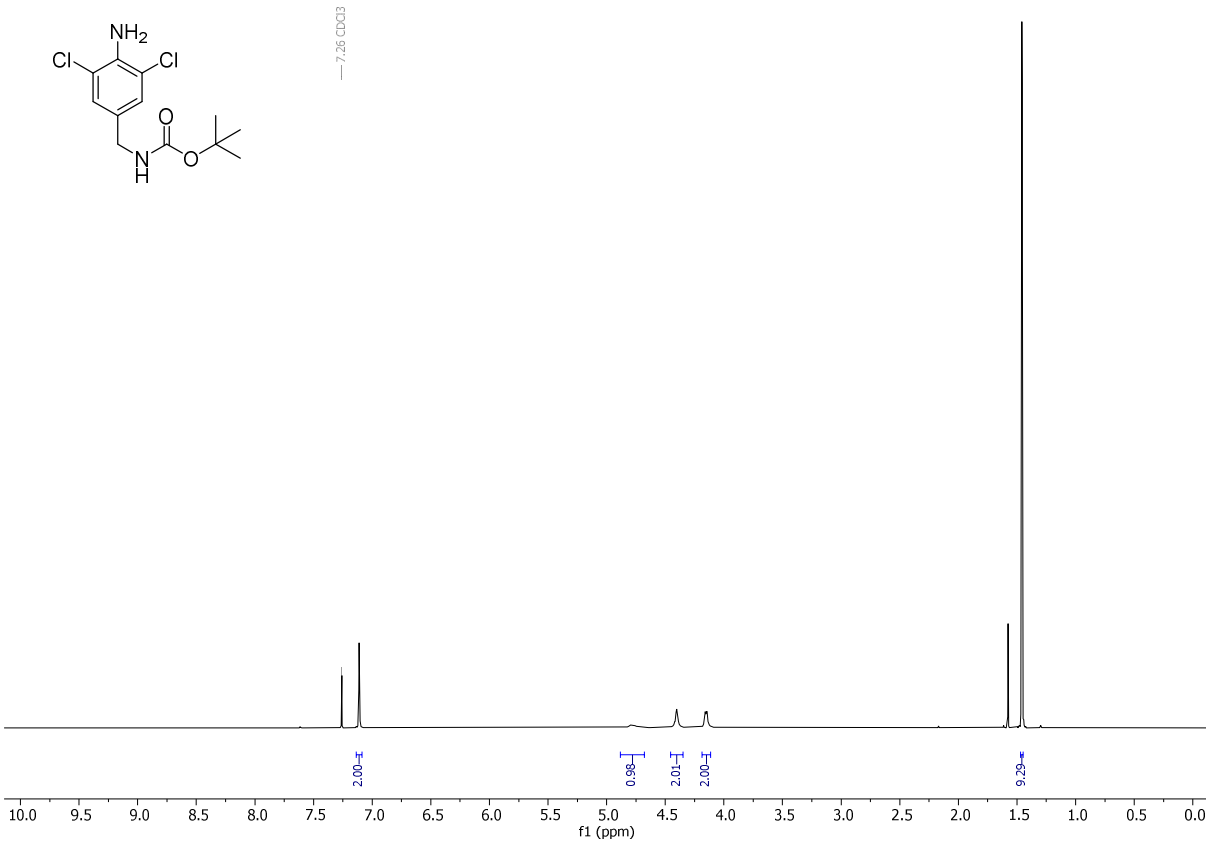

Figure S1. ^{1}H NMR Spectrum of **3** (Chloroform-*d*, 298 K).

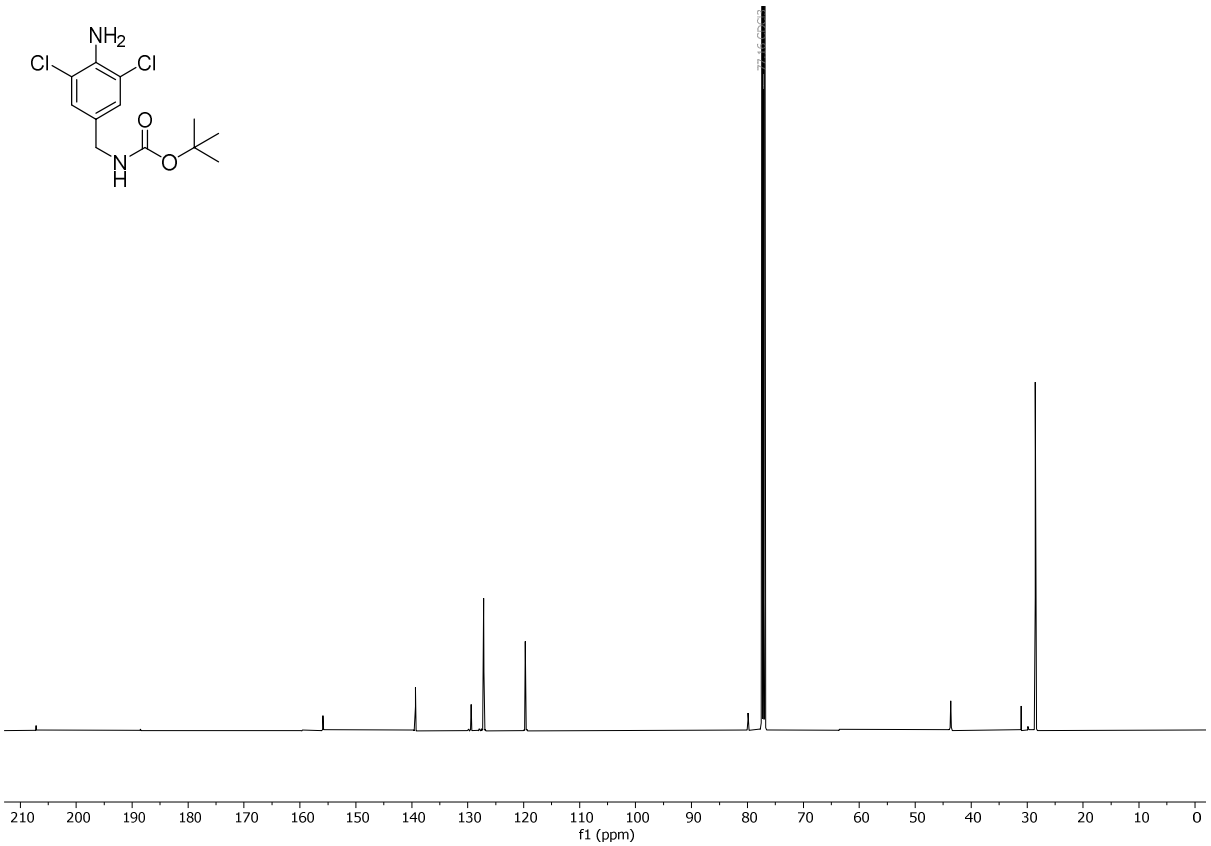

Figure S2. ^{13}C NMR Spectrum of **3** (Chloroform-*d*, 298 K).

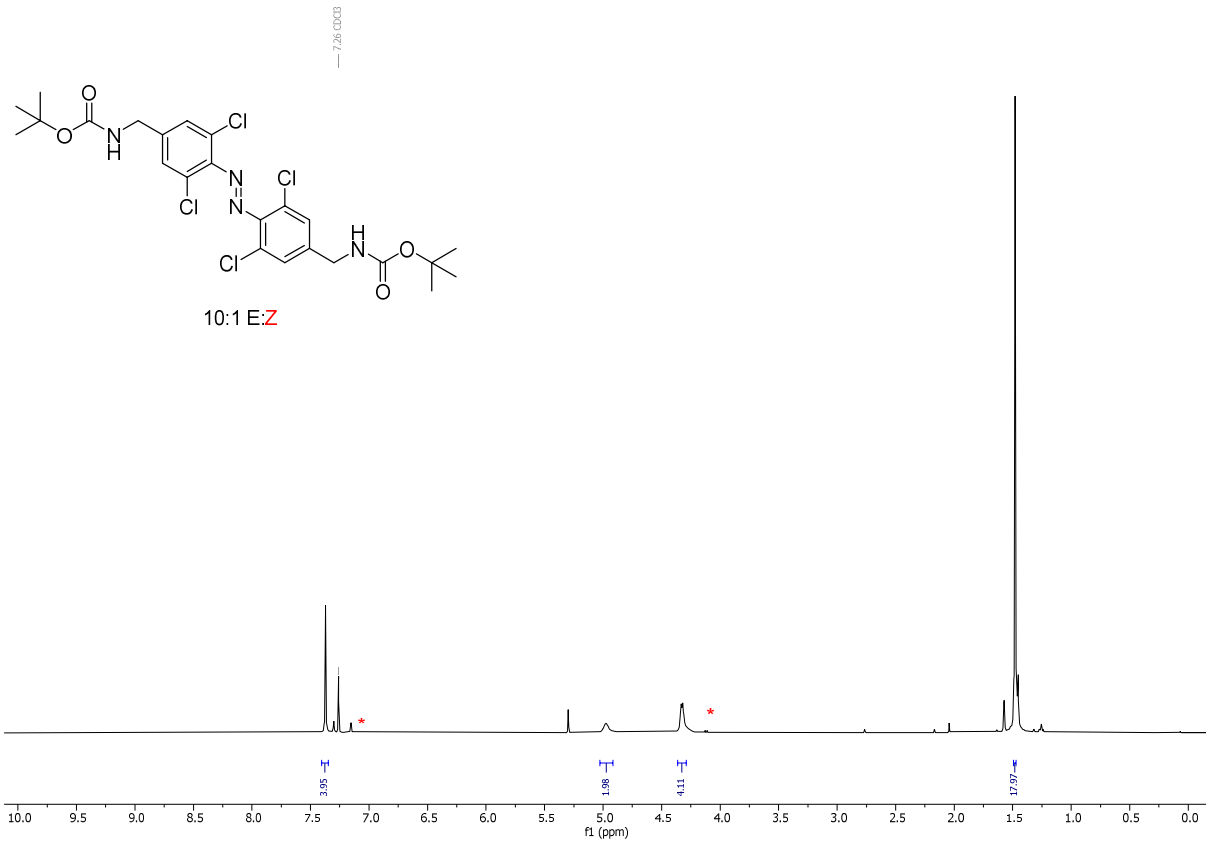

Figure S3. ^{1}H NMR Spectrum of **4** (Chloroform-*d*, 298 K).

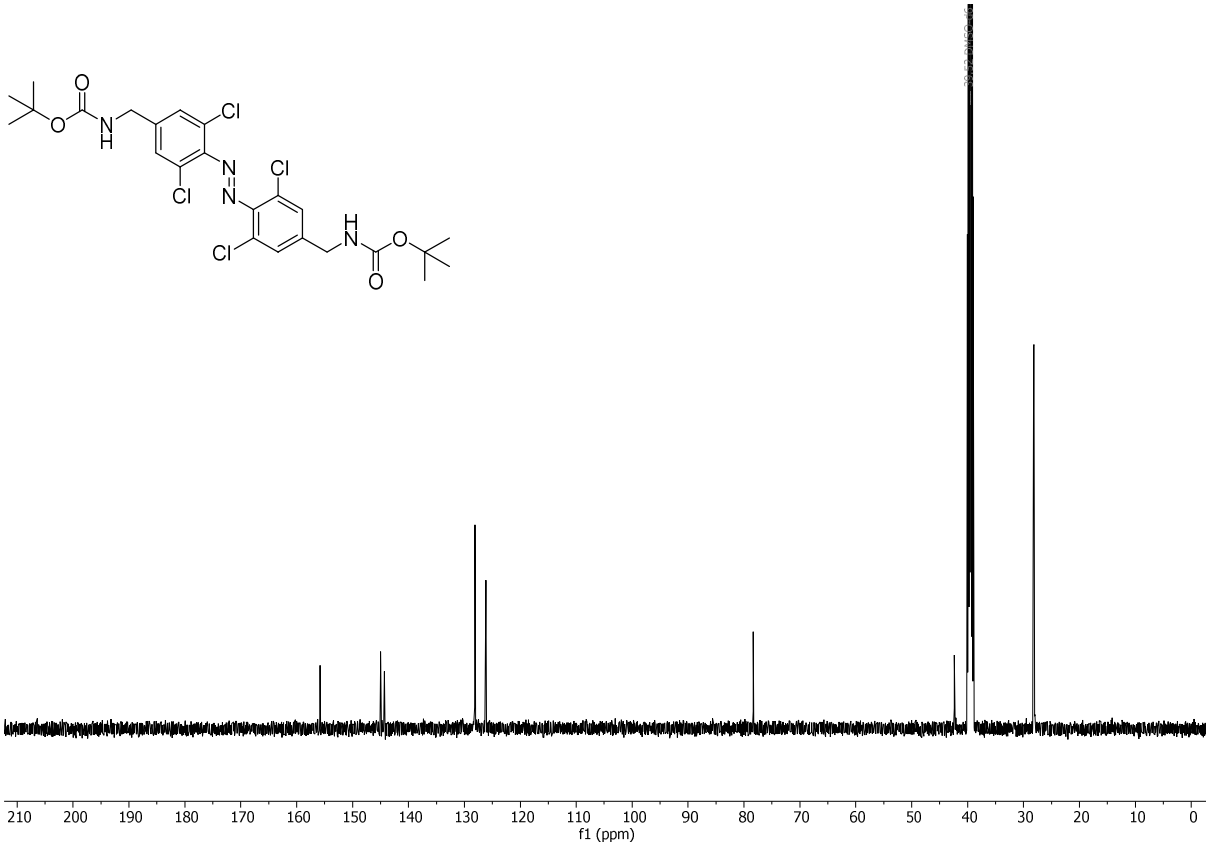

Figure S4. ^{13}C NMR Spectrum of **4** (Chloroform-*d*, 298 K).

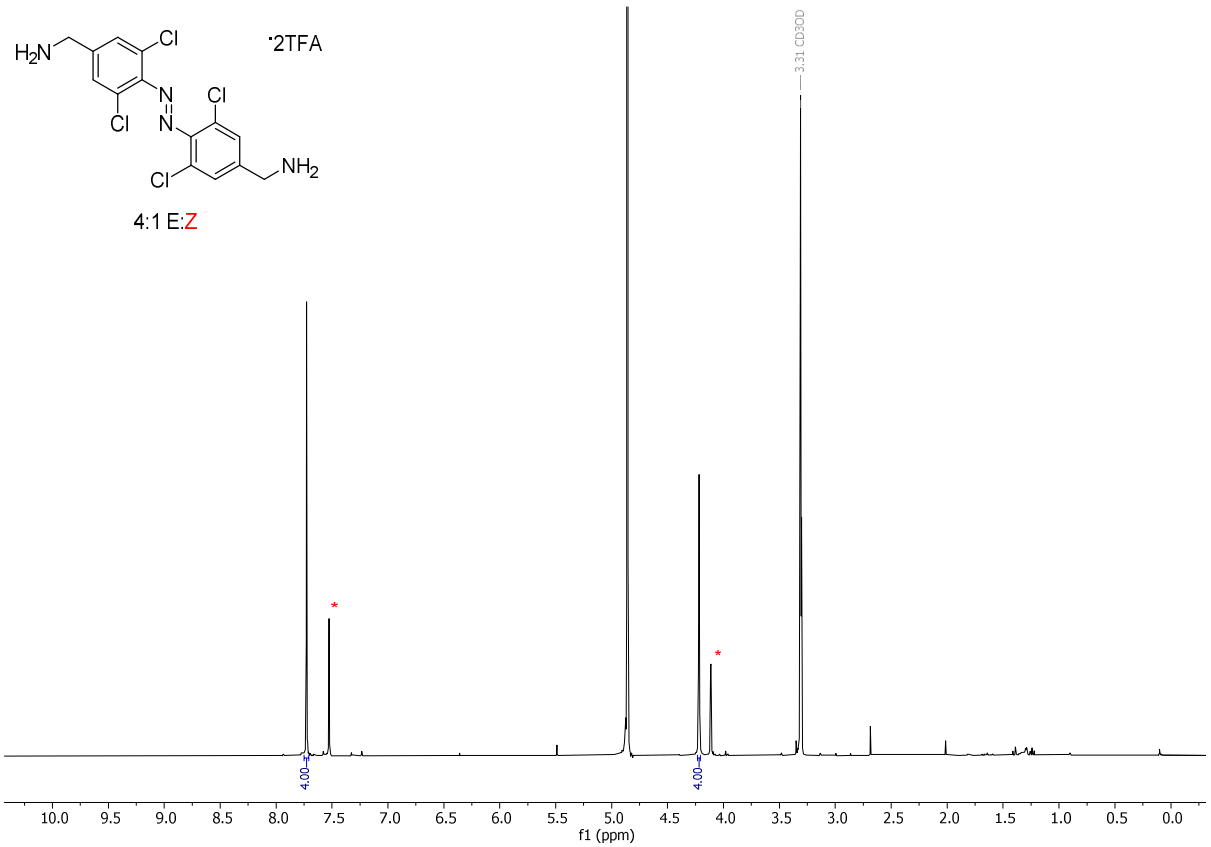

Figure S5. ^{1}H NMR Spectrum of **5**, (Methanol-d_4, 298 K).

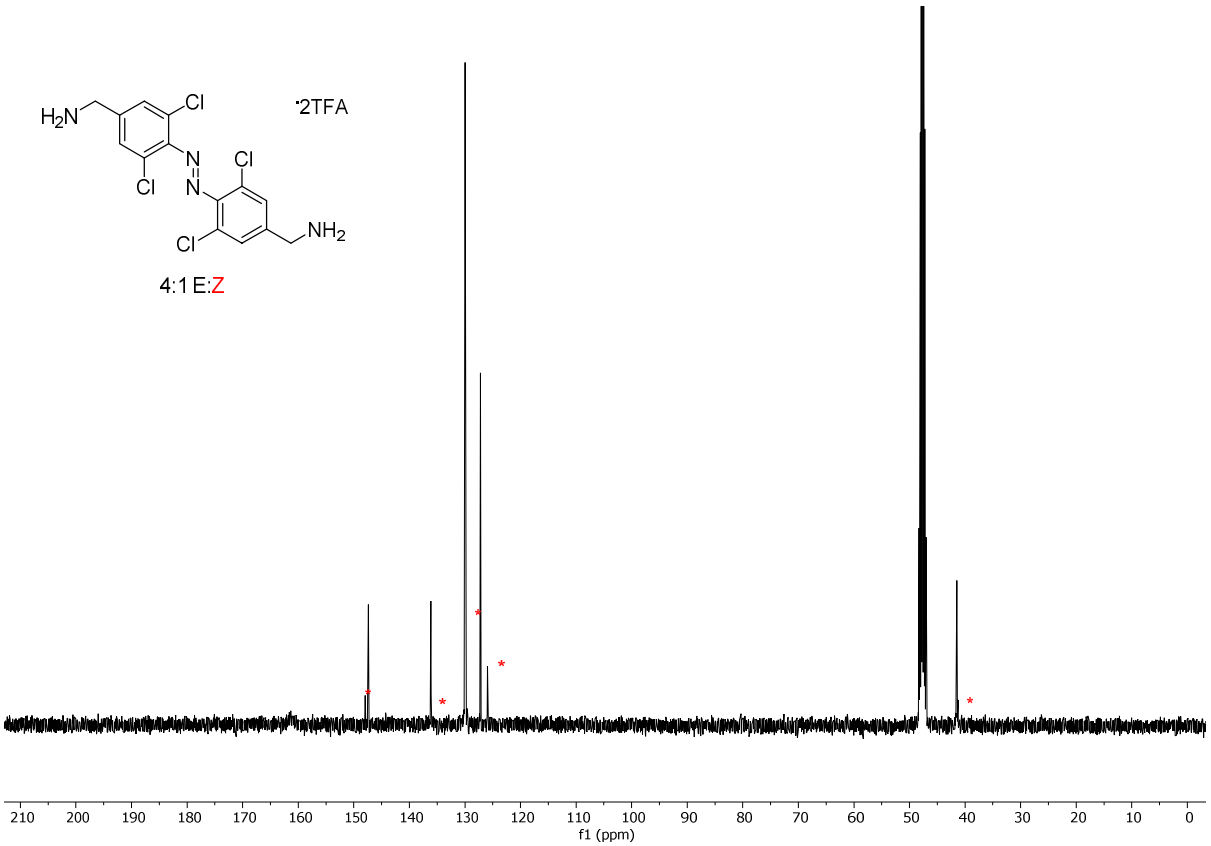

Figure S6. ^{13}C NMR Spectrum of **5**, (Methanol-d_4, 298 K).

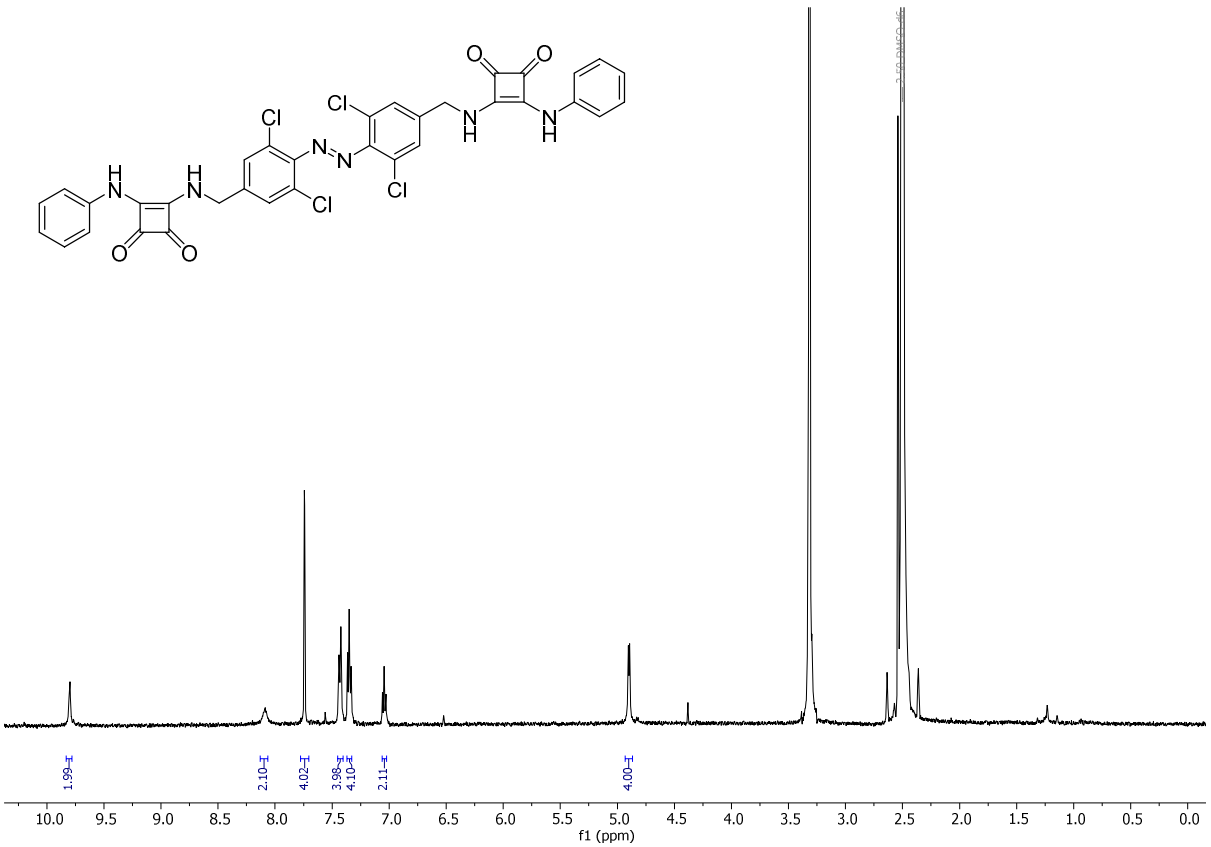

Figure S7. ^{1}H NMR Spectrum of ***E*-1a** (DMSO-d_6, 298 K).

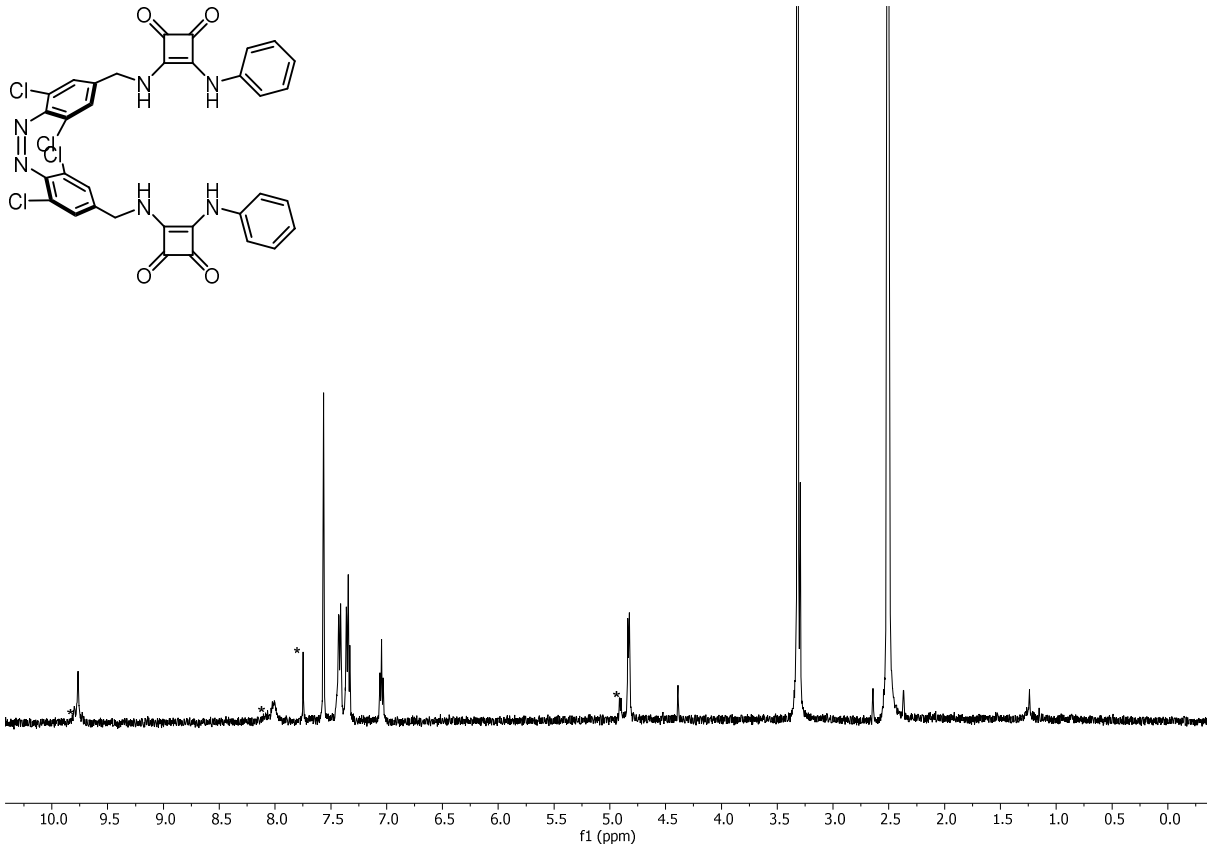

Figure S8. ^{1}H NMR Spectrum of ***Z*-1a** at photostationary state (77%). ***E*-1a** signals labelled as *. (DMSO-d_6, 298 K).

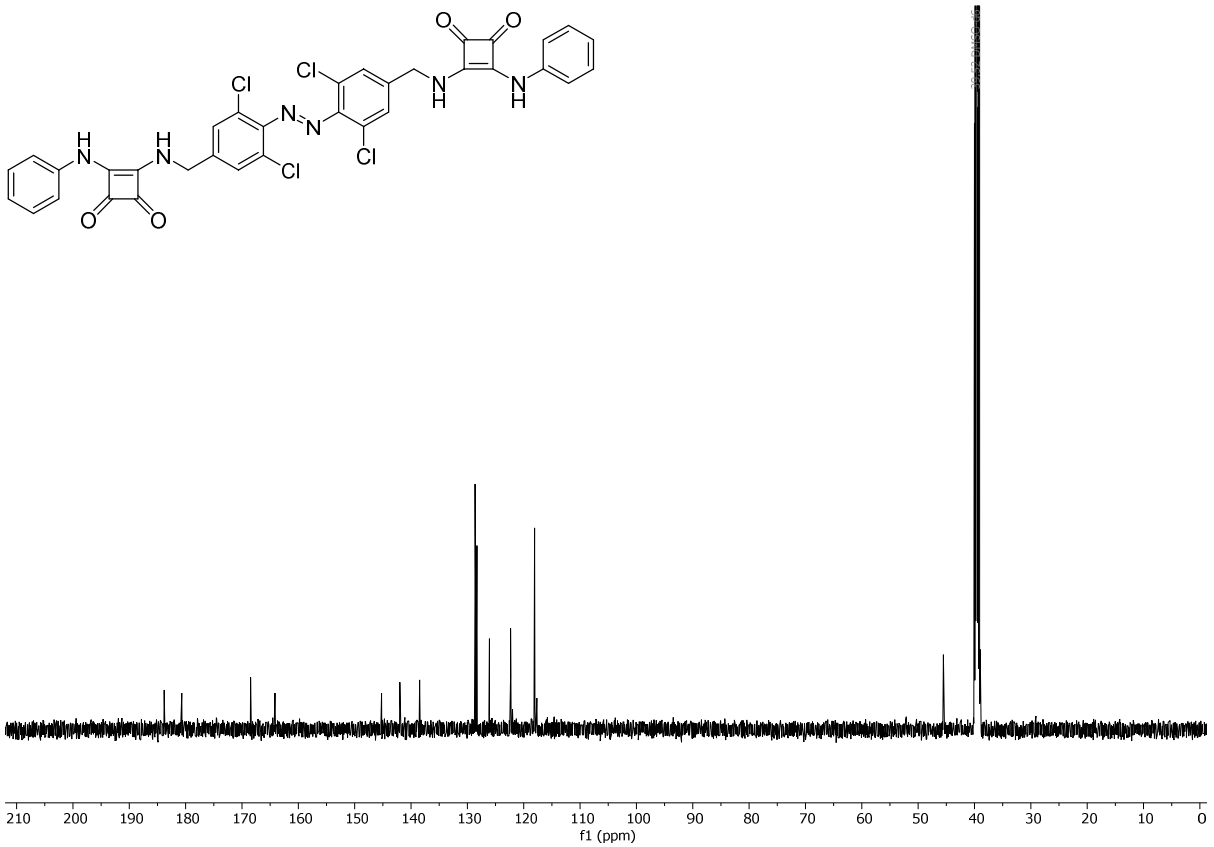

Figure S9. ^{13}C NMR Spectrum of ***E*-1a**. (DMSO-d_6, 378 K).

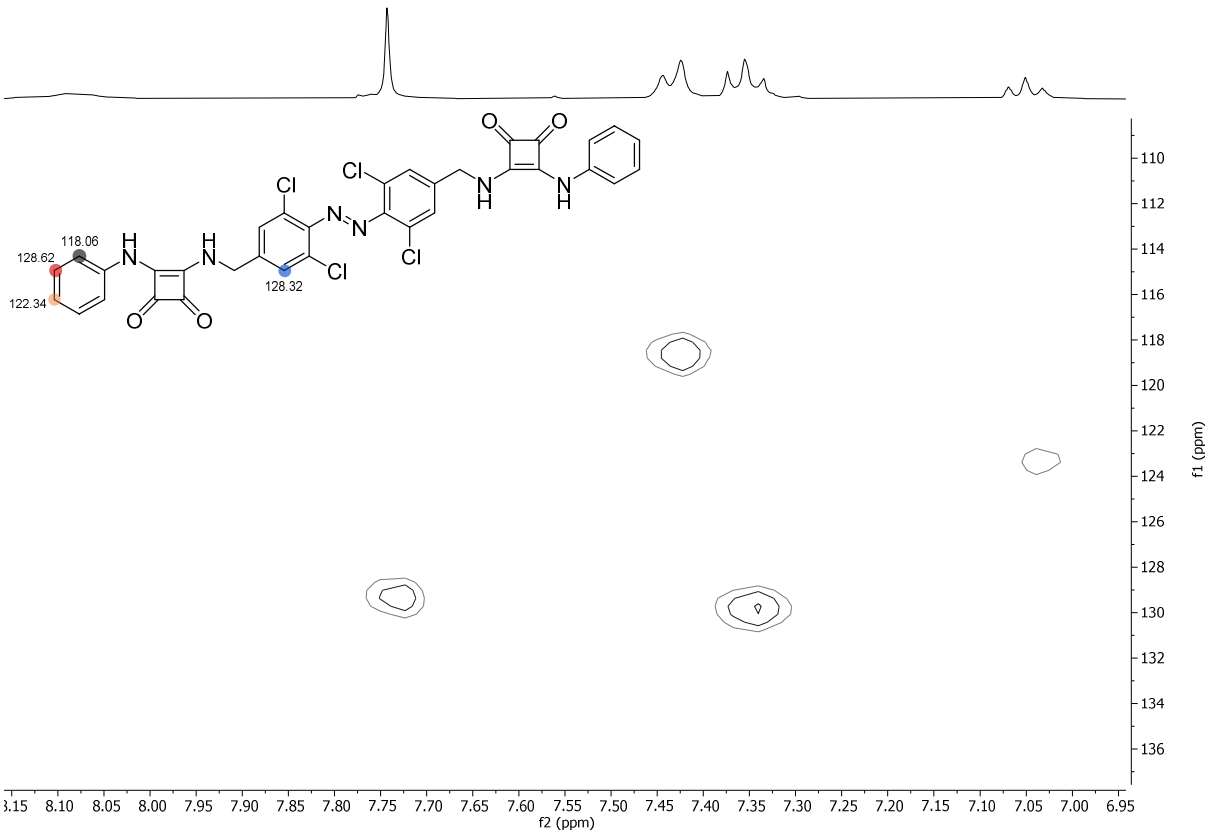

Figure S10. HSQC of **1a**. Key aromatic ^{1}H–^{13}C correlations highlighted. (DMSO-d_6, 298 K).

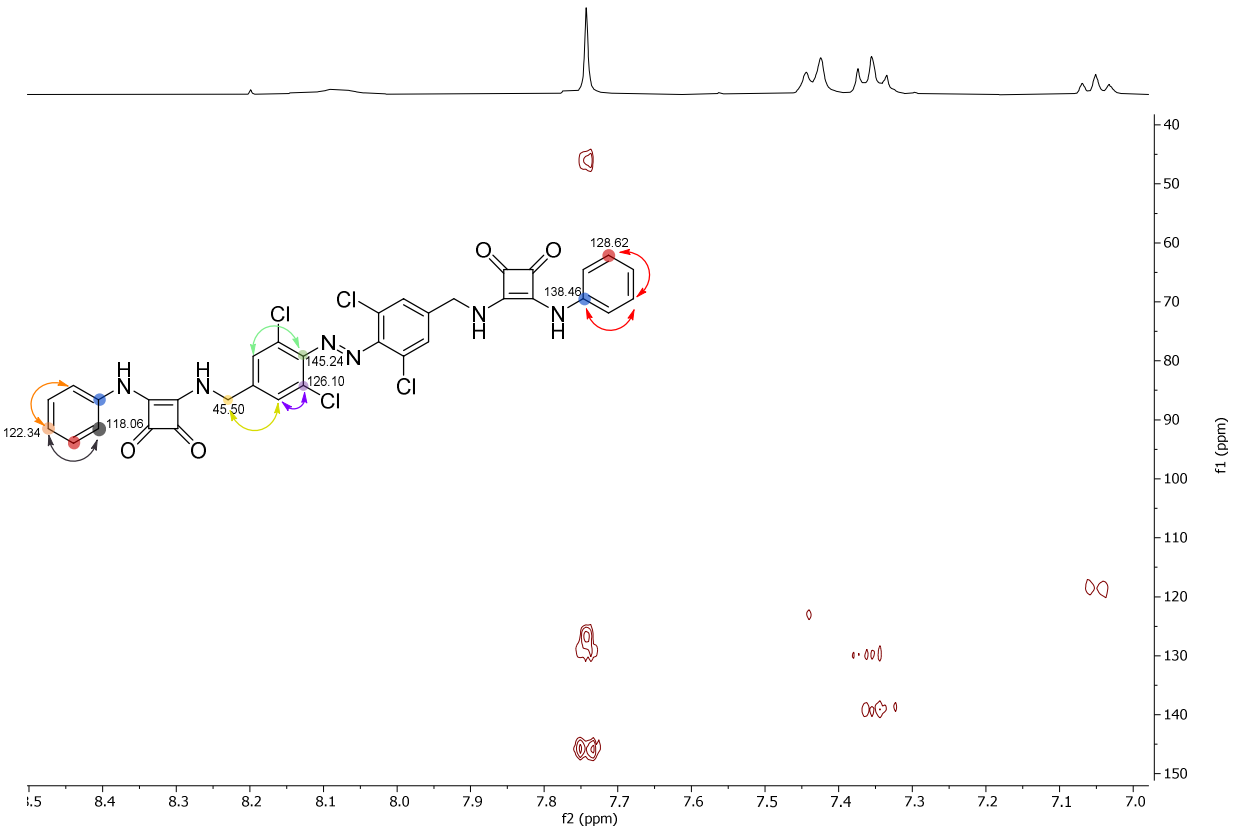

Figure S11. HMBC of **1a**. Key ^{1}H–^{13}C correlations highlighted. (DMSO-d_6, 298 K).

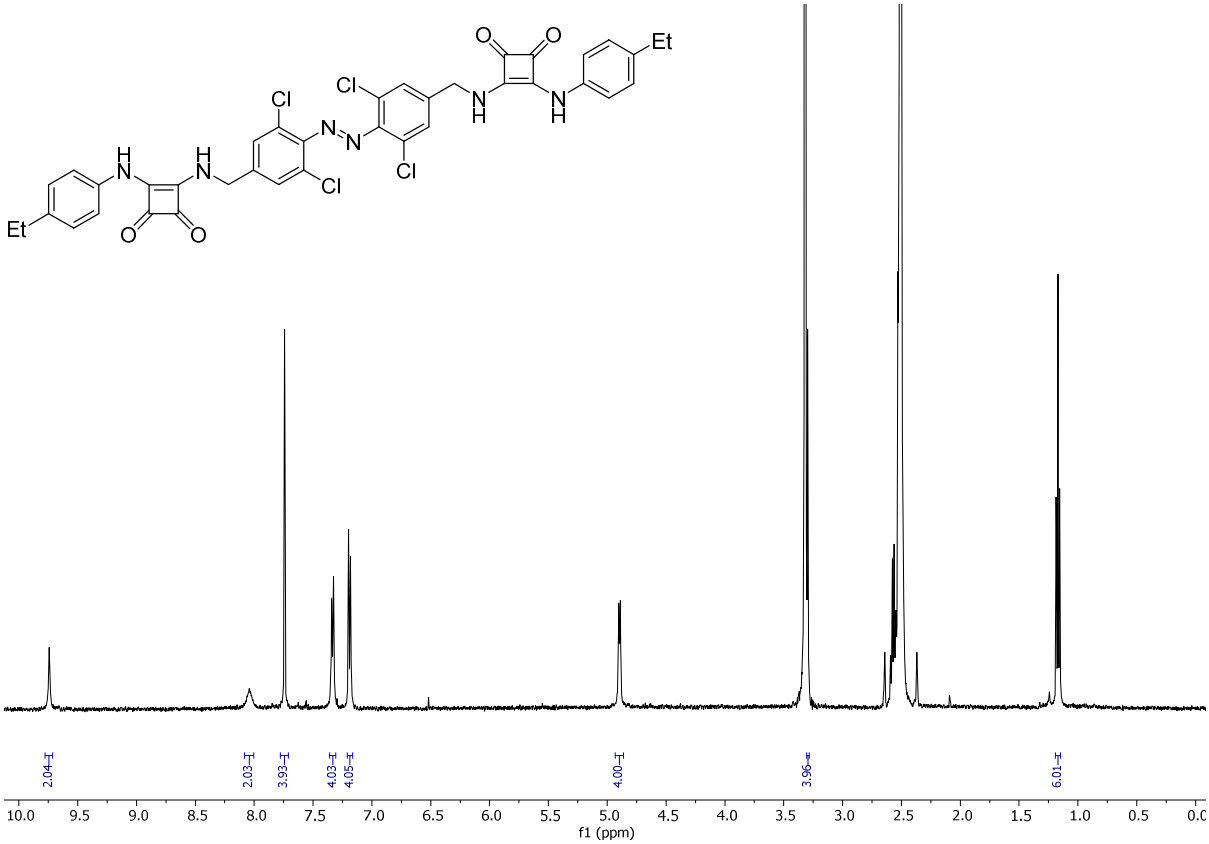

Figure S12. ^{1}H NMR Spectrum of ***E*-1b**. (DMSO-d_6, 298 K).

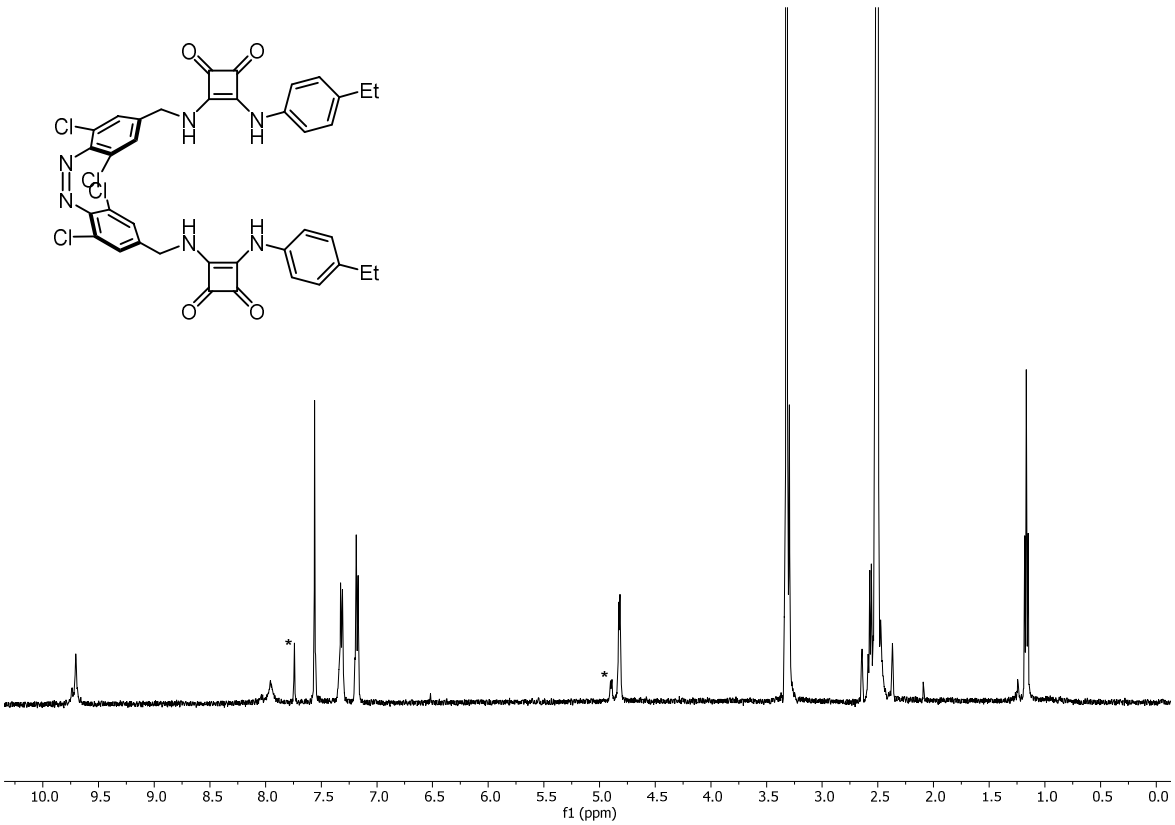

Figure S13. ^{1}H NMR Spectrum of ***Z*-1b** at photostationary state (77%). ***E*-1b** signals labelled as *. (DMSO-d_6, 298 K).

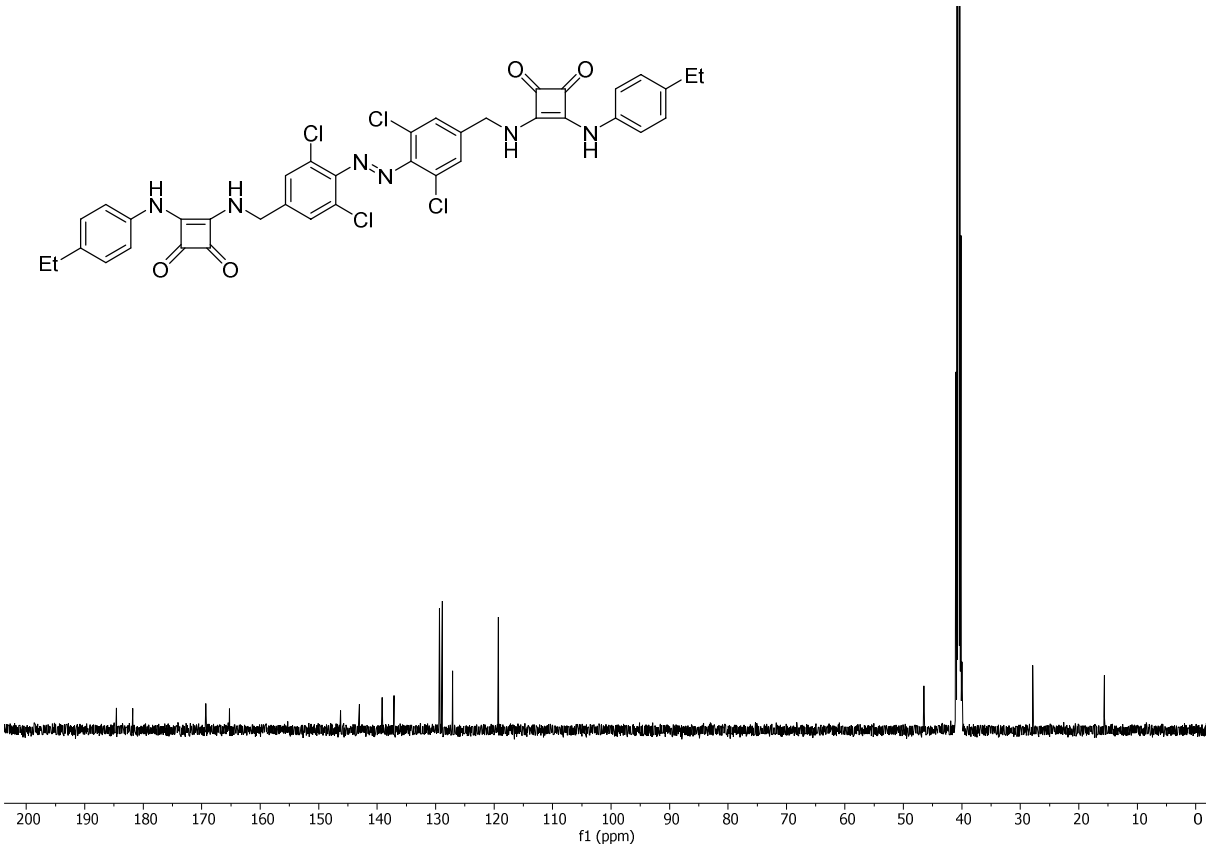

Figure S14. ^{13}C NMR Spectrum of ***E*-1b**. (DMSO-d_6, 378 K).

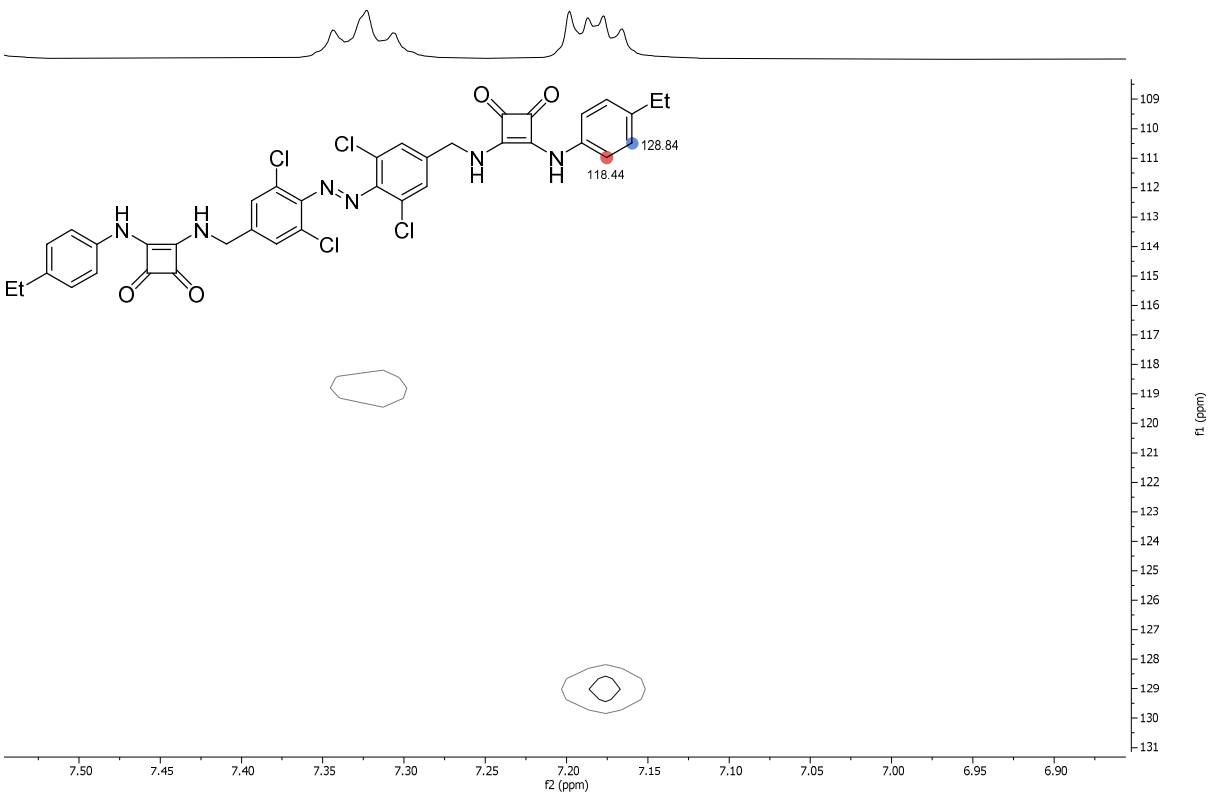

Figure S15. HSQC of **1b**. Key squaramide aromatic ^{1}H–^{13}C correlations highlighted (DMSO-d_6, 298K).

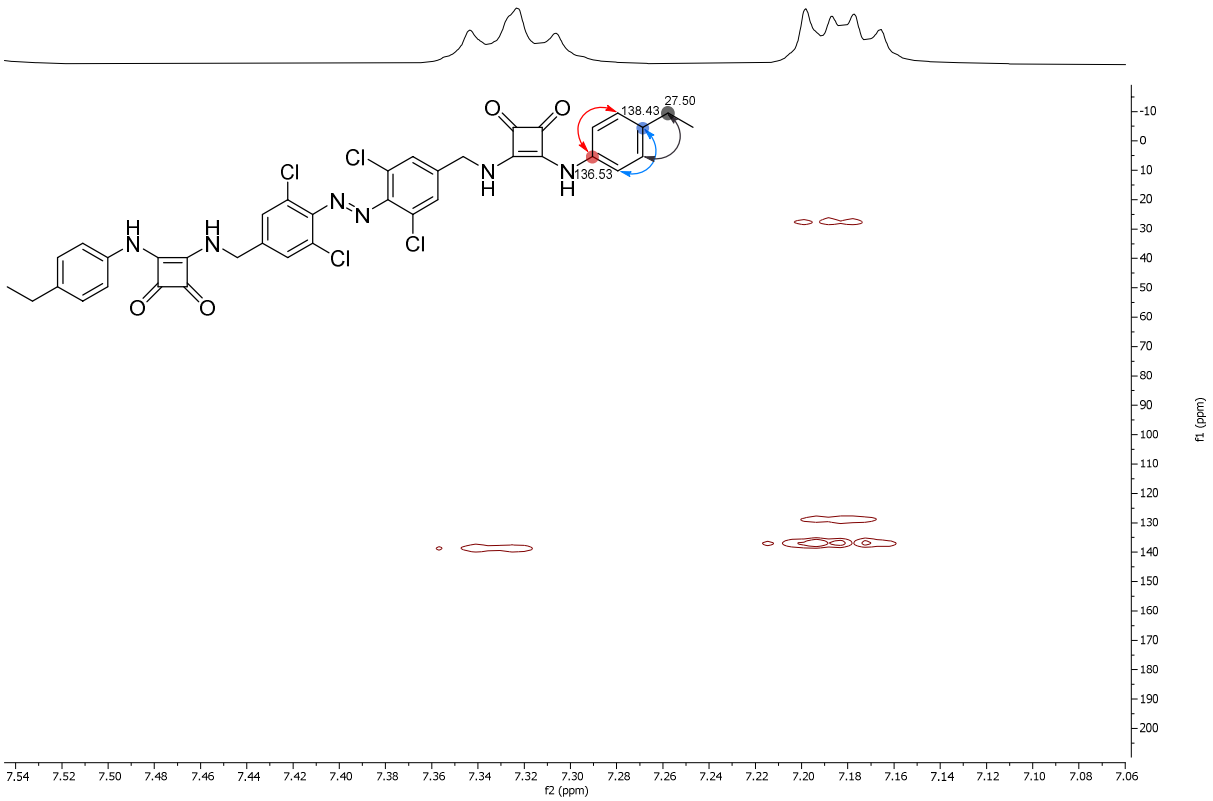

Figure S16. HMBC of **1b**. Key squaramide $^{1}H–^{13}C$ correlations highlighted. (DMSO-d_6, 298K).

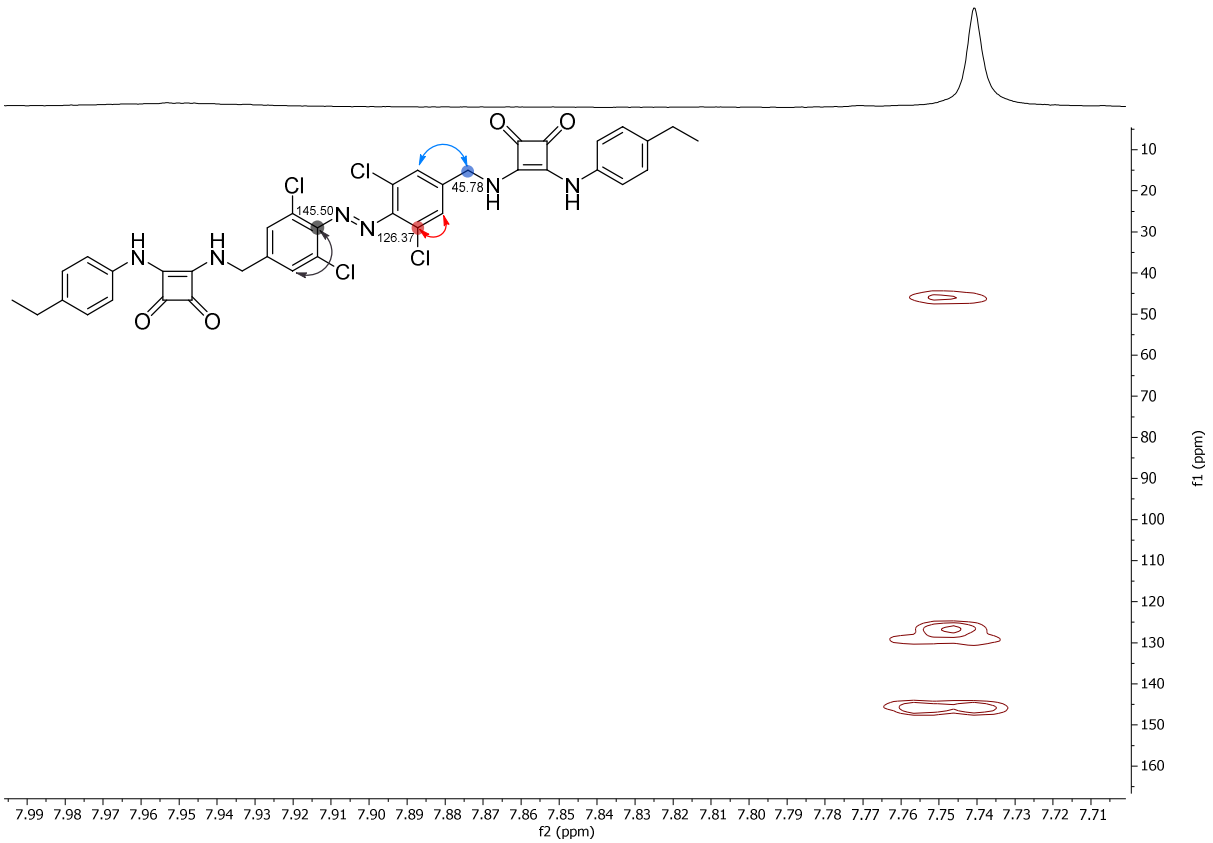

Figure S17. HMBC of **1b**. Key azobenzene $^{1}H–^{13}C$ correlations highlighted. (DMSO-d_6, 298 K).

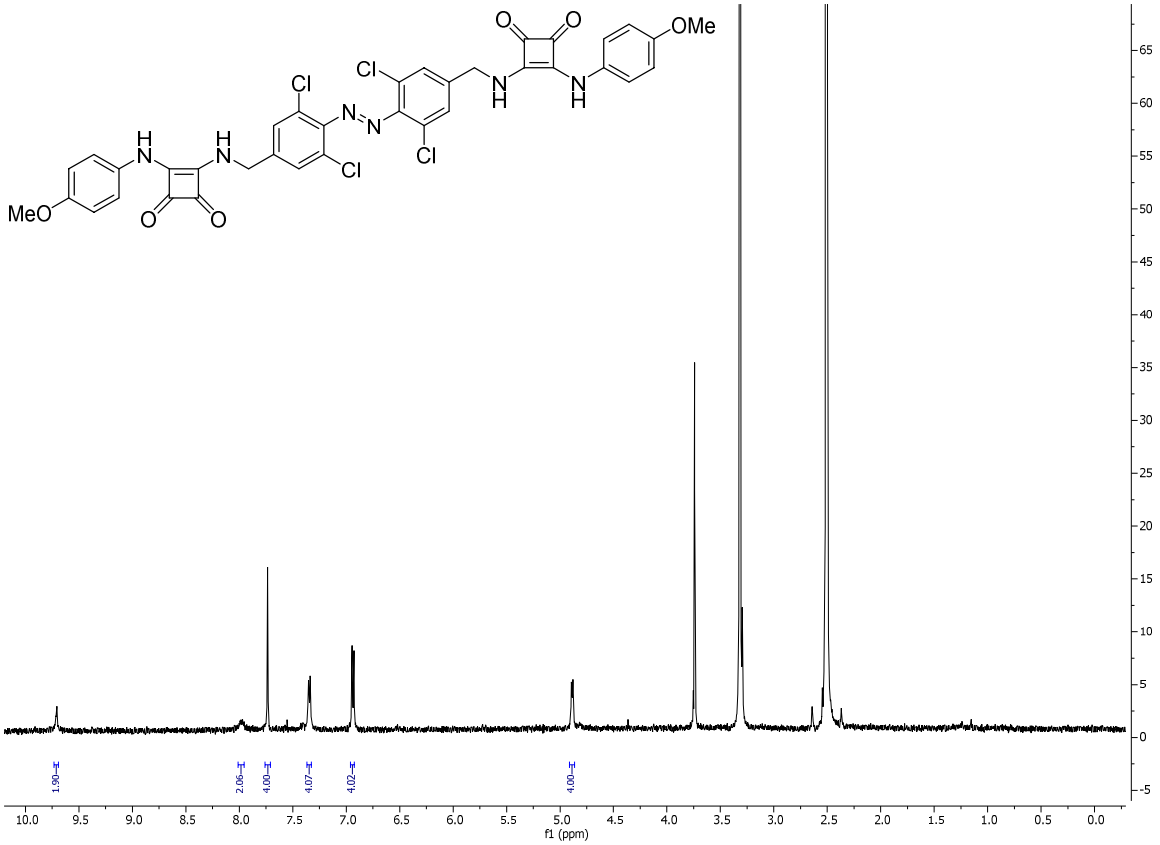

Figure S18. ^{1}H NMR Spectrum of ***E*-1c**. (DMSO-d_6, 298 K).

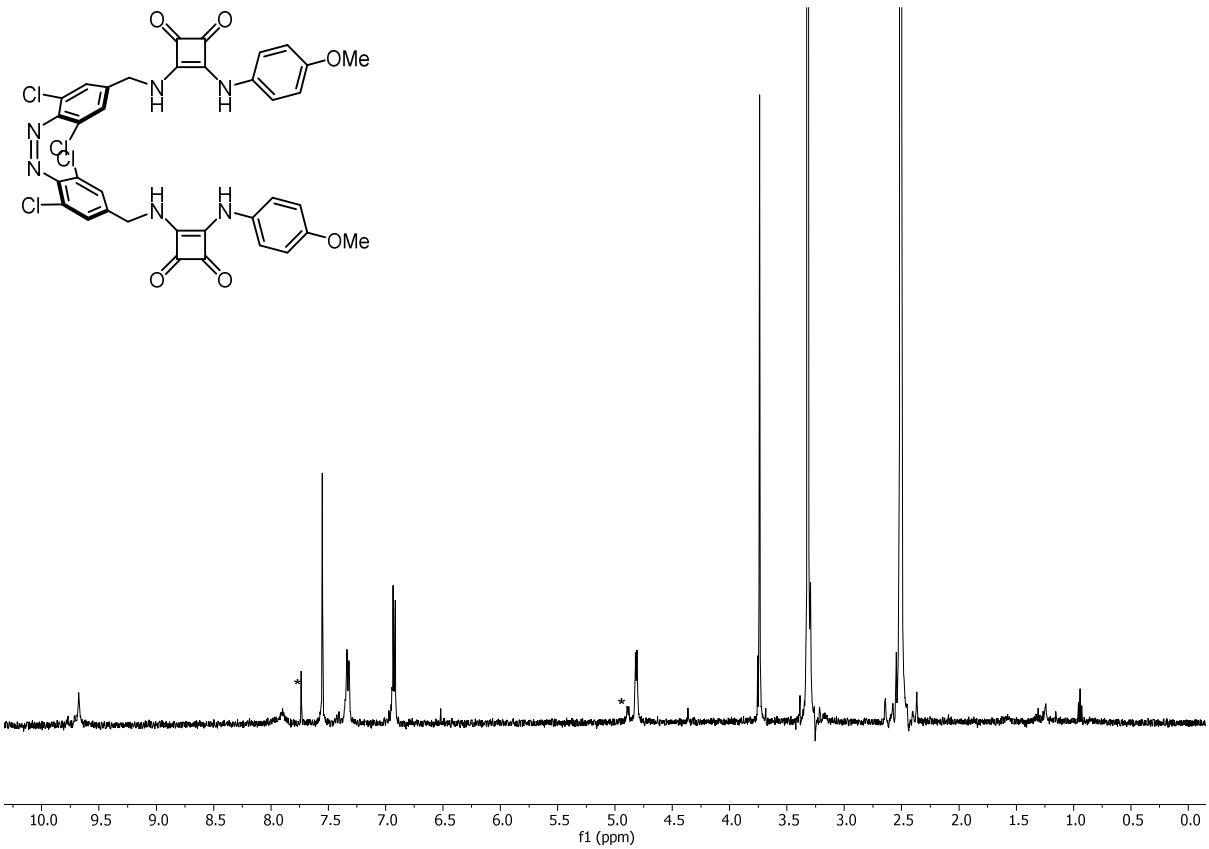

Figure S19. ^{1}H NMR Spectrum of ***Z*-1c** at photostationary state (77%). ***E*-1c** signals labelled as *. (DMSO-d_6, 298 K).

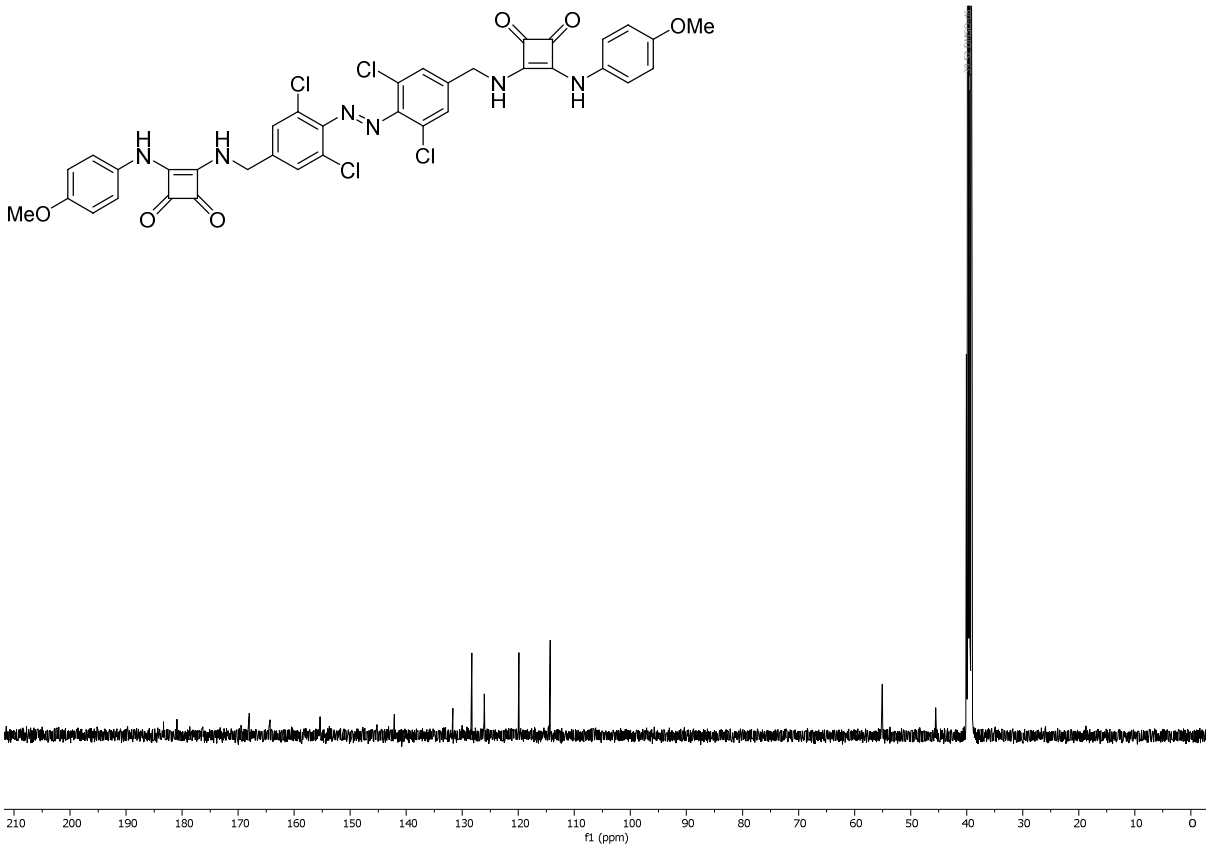

Figure S20. ^{13}C NMR Spectrum of ***E*-1c**. (DMSO-d_6, 378 K).

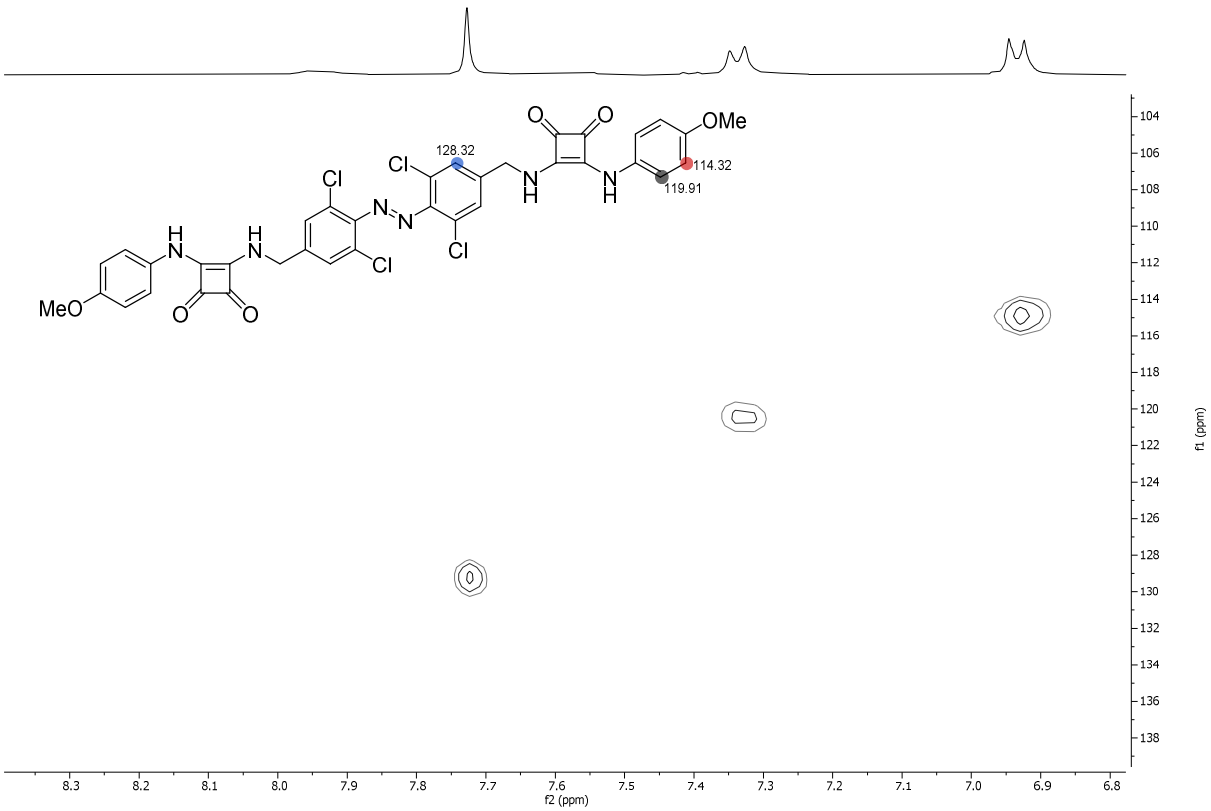

Figure S21. HSQC of **1c**. Key aromatic ^{1}H–^{13}C correlations highlighted. (DMSO-d_6, 298 K).

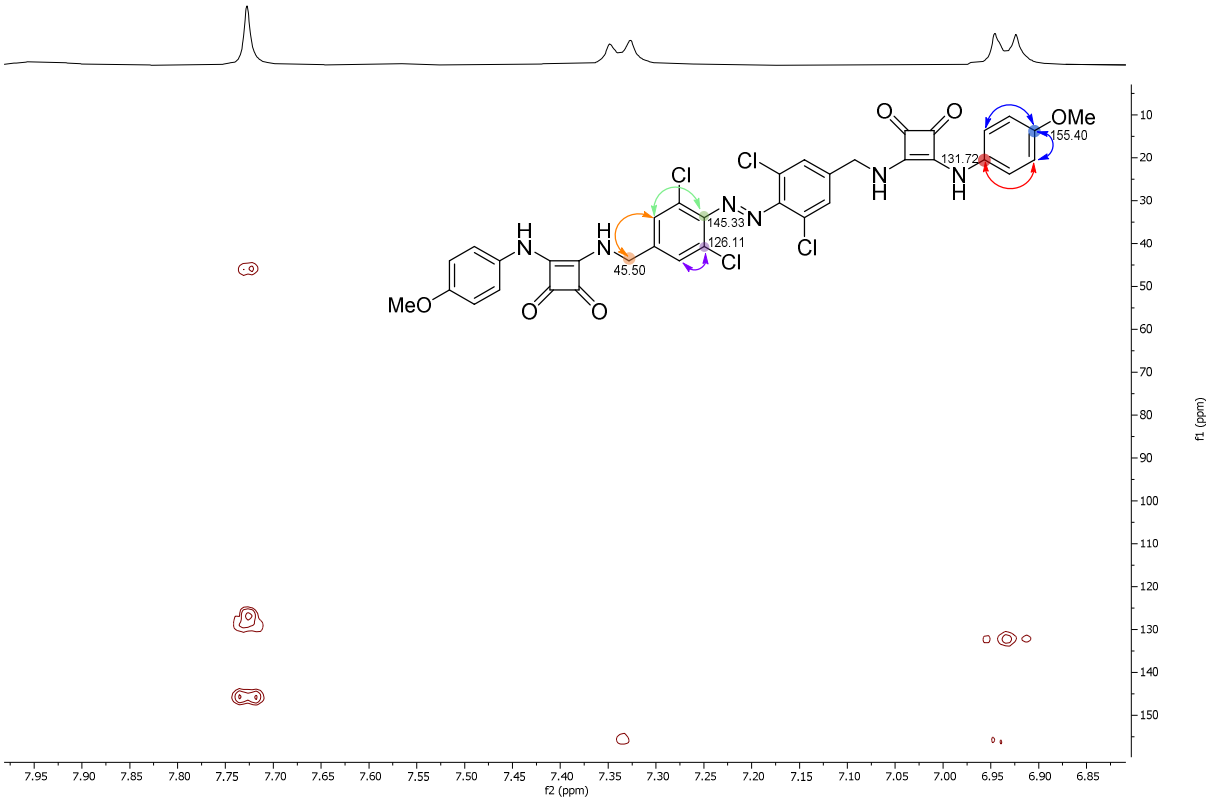

Figure S22. HMBC of **1c**. Key aromatic ^{1}H–^{13}C correlations highlighted. (DMSO-d_6, 298 K).

Figure S23. ^{1}H NMR Spectrum of ***E*-1d**. (DMSO-d_6, 298 K).

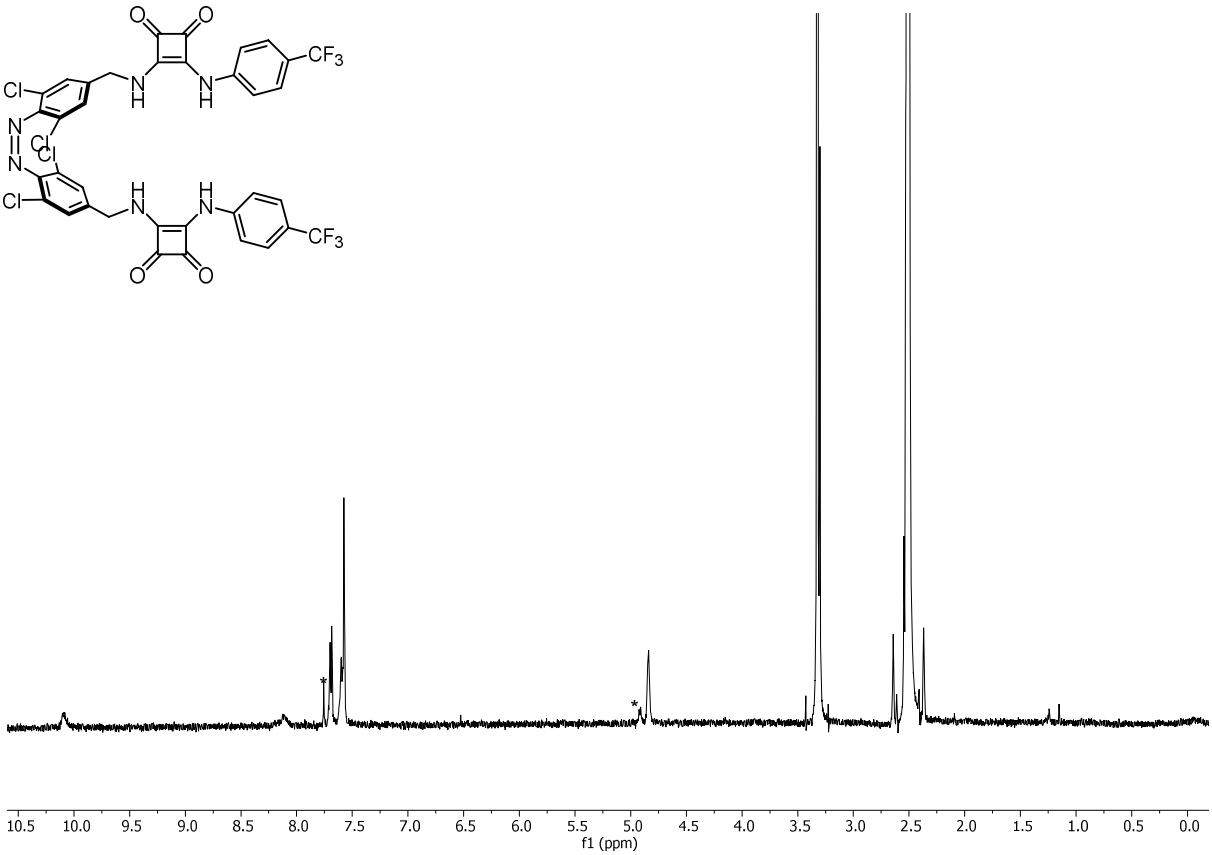

Figure S24. ^{1}H NMR Spectrum of ***Z*-1d** at photostationary state (77%). ***E*-1d** signals labelled as *. (DMSO-d_6, 298 K).

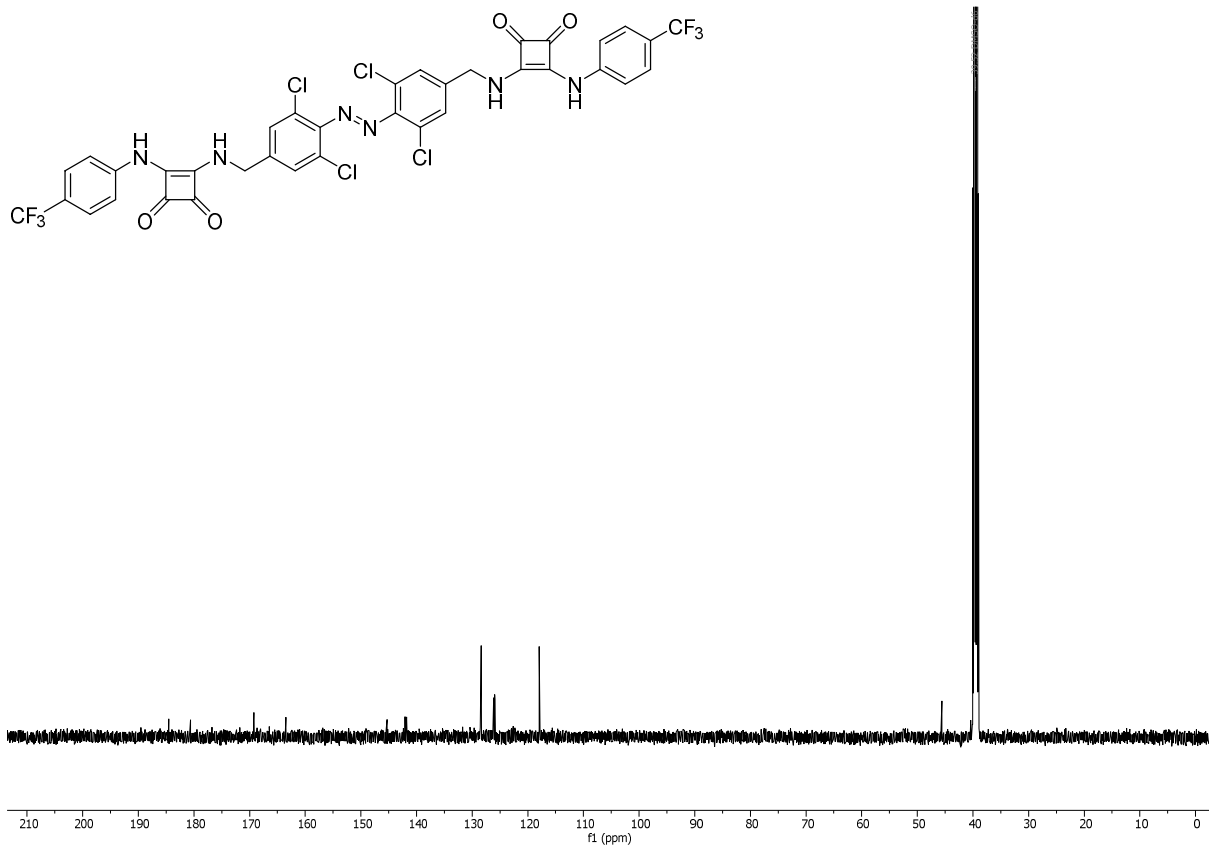

Figure S25. ^{13}C NMR Spectrum of ***E*-1d**. (DMSO-d_6, 378 K).

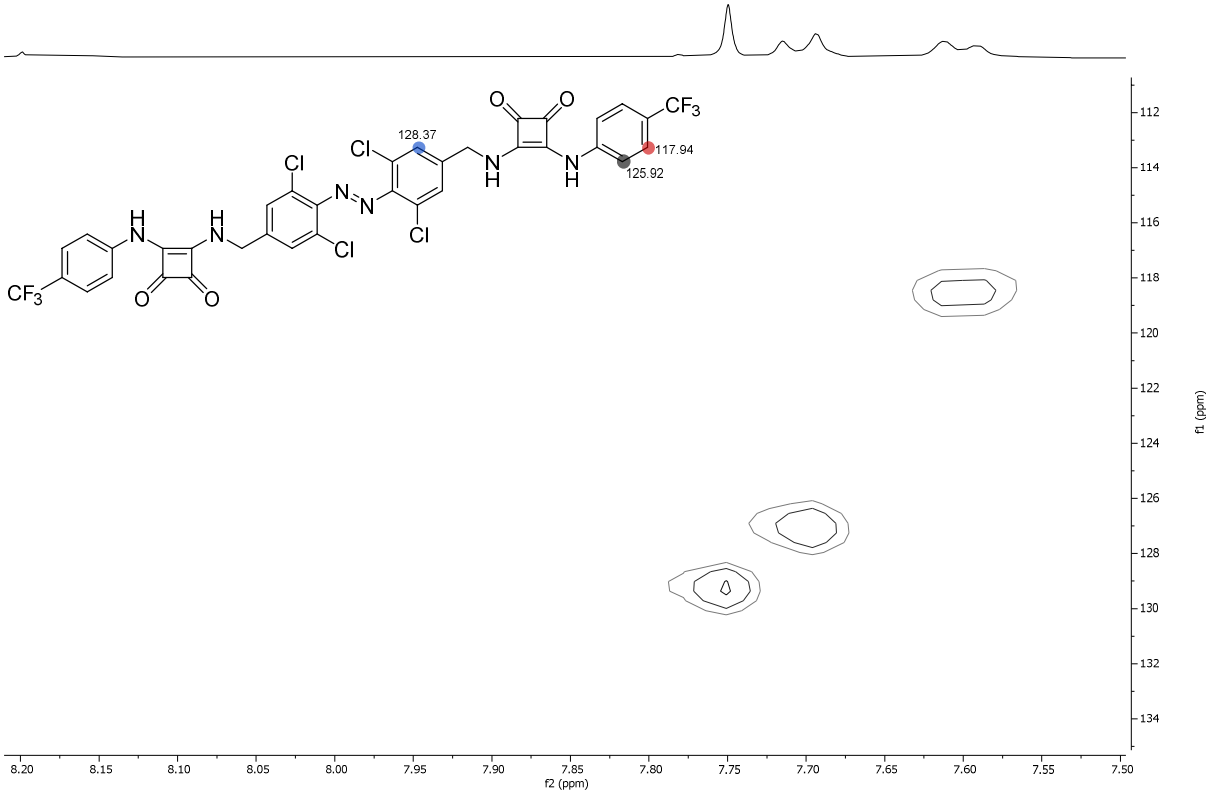

Figure S26. HSQC of **1d**. Key aromatic ^{1}H–^{13}C correlations highlighted. (DMSO-d_6, 298 K).

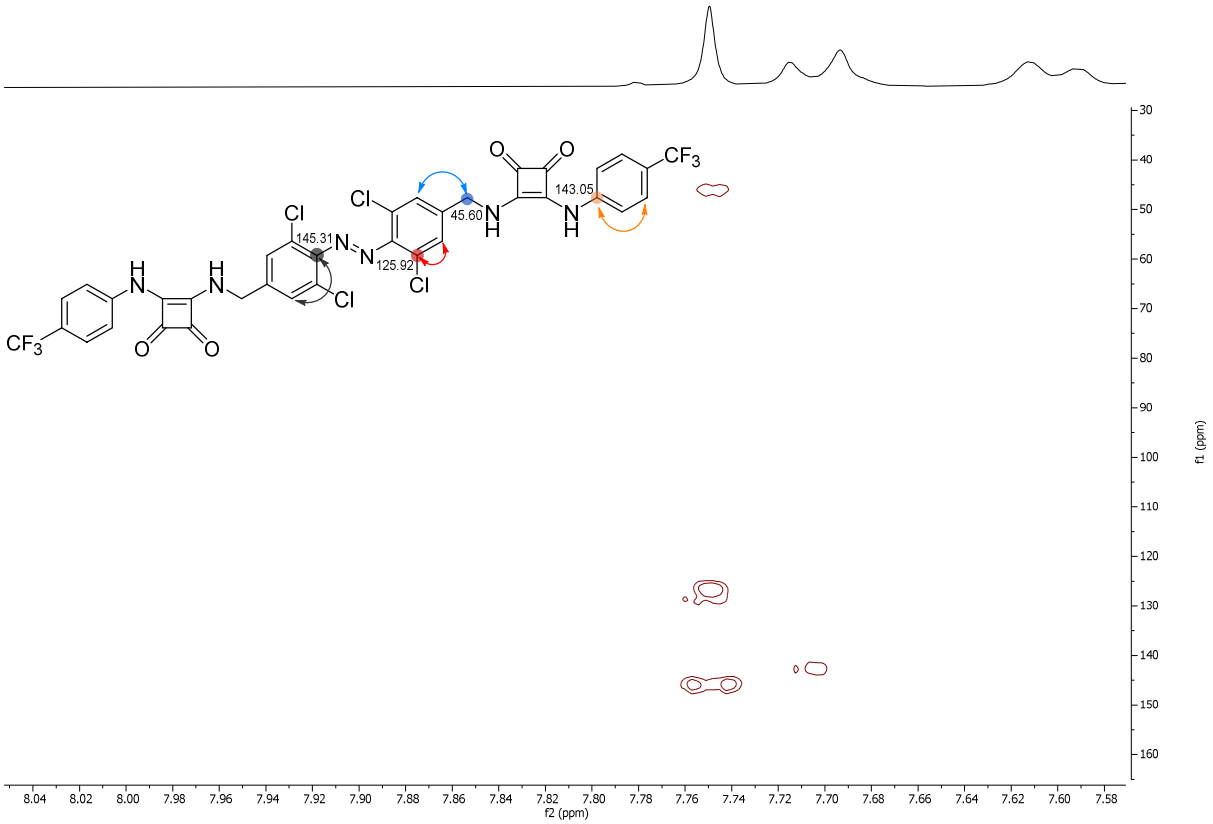

Figure S27. HMBC of **1d**. Key azobenzene aromatic ^{1}H–^{13}C correlations highlighted. (DMSO-d_6, 298 K).

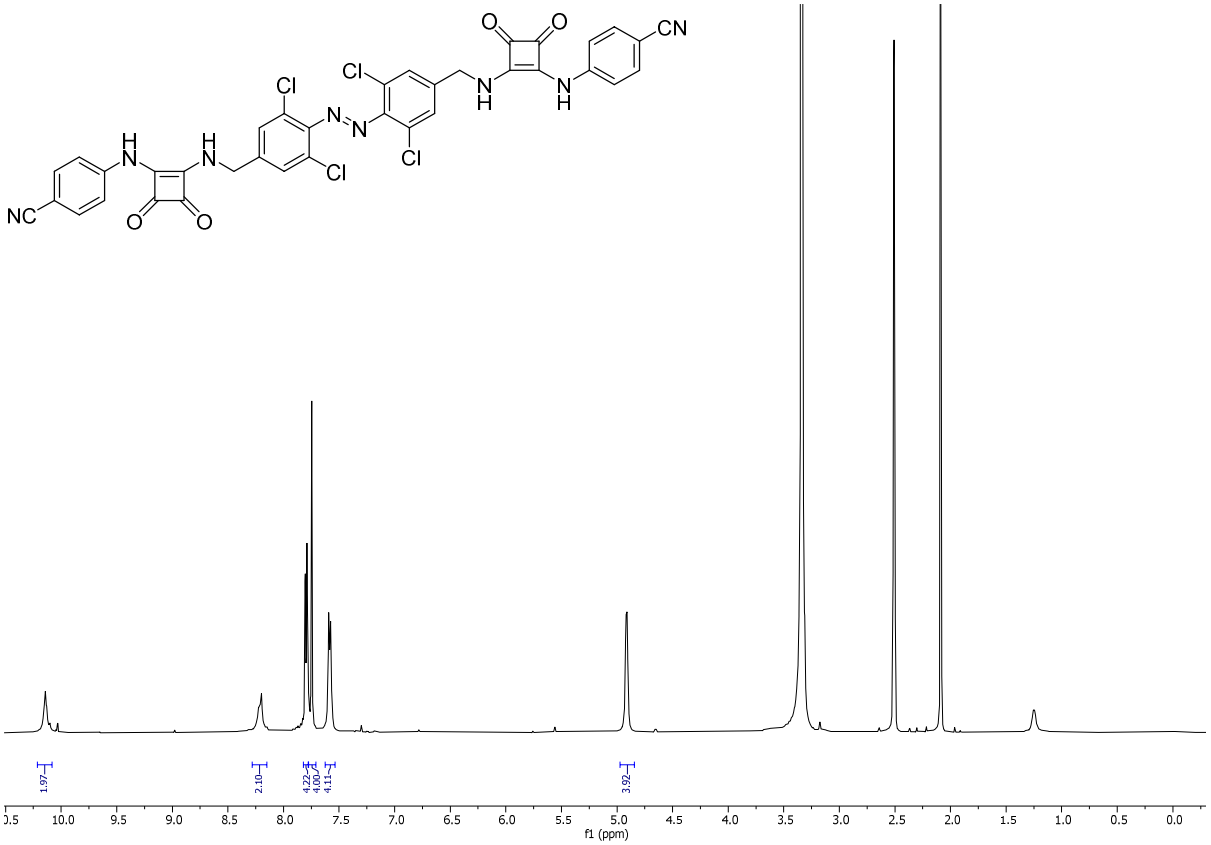

Figure S28. ^{1}H NMR Spectrum of ***E*-1e**. (DMSO-d_6, 298 K).

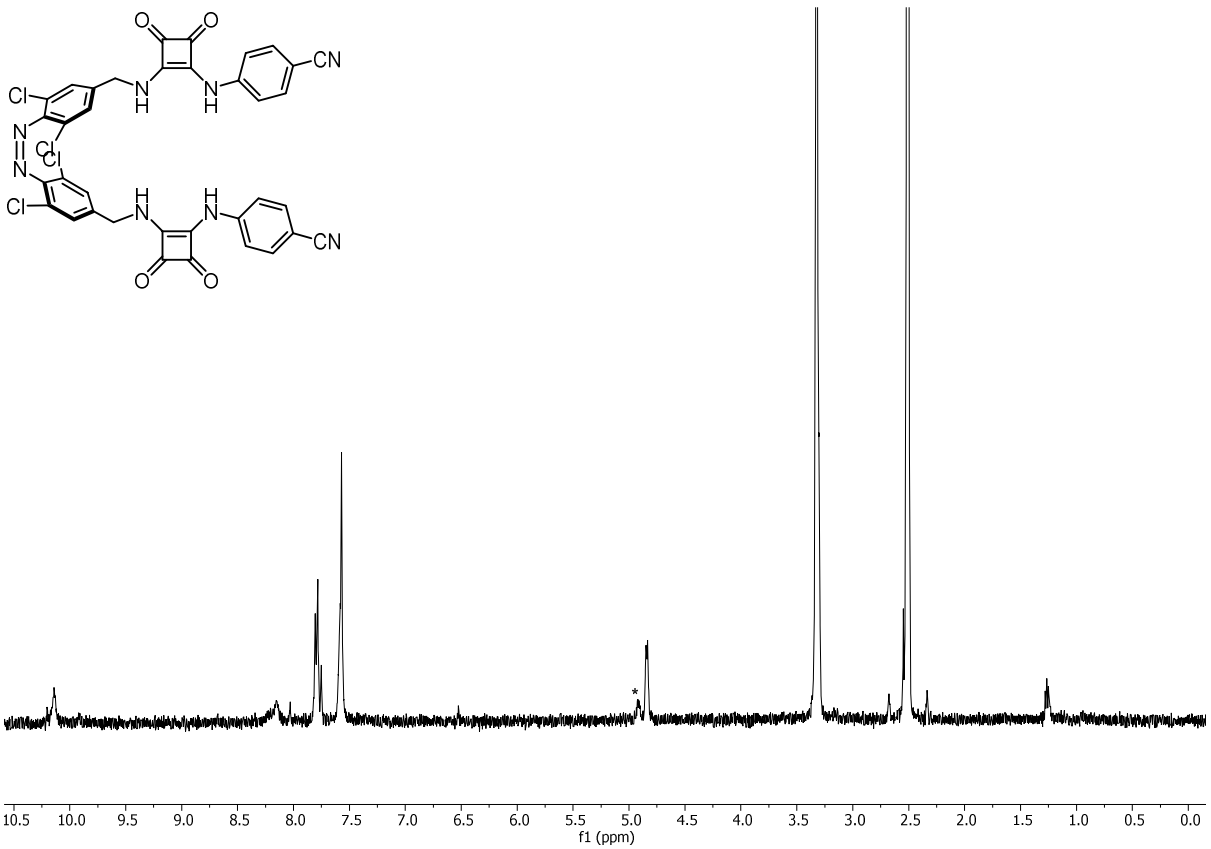

Figure S29. ^{1}H NMR Spectrum of ***Z*-1e** at photostationary state (77%). ***E*-1e** signals labelled as *. (DMSO-d_6, 298 K).

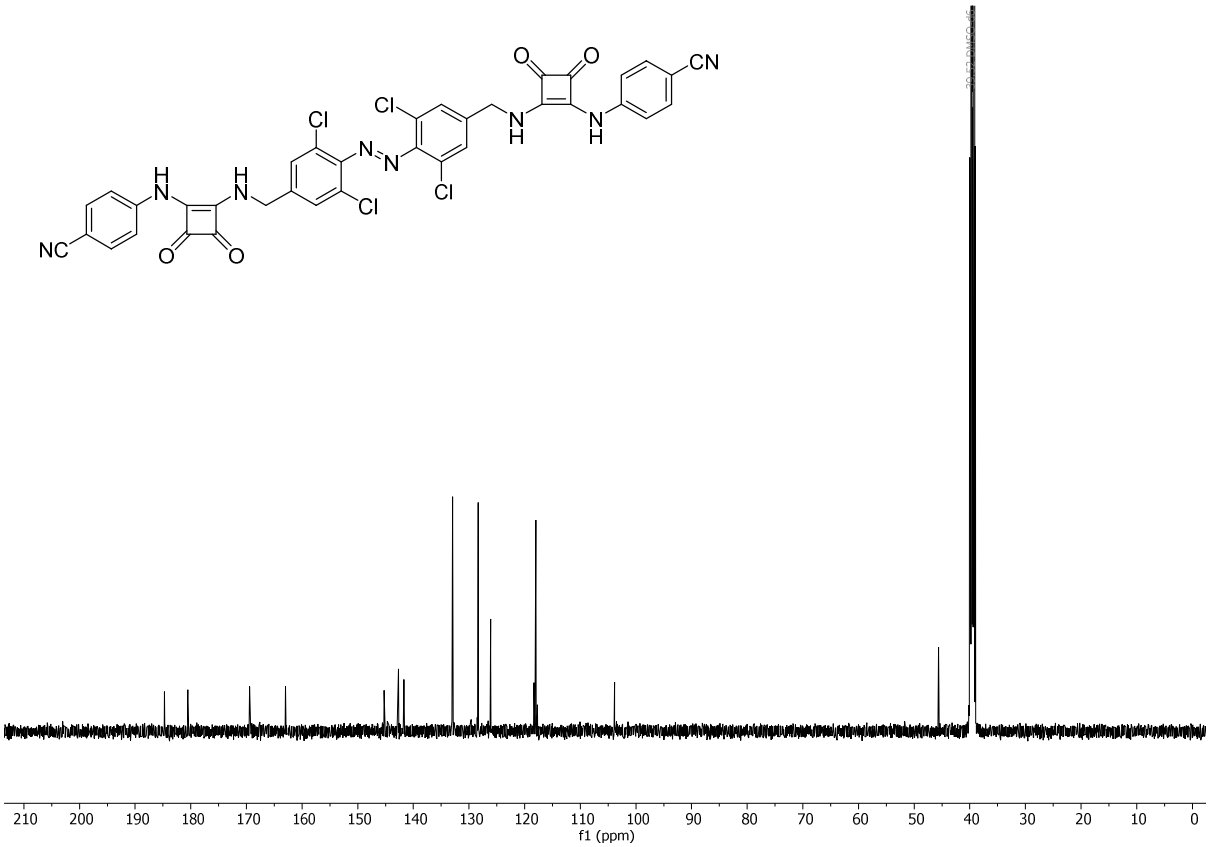

Figure S30. ^{13}C NMR Spectrum of ***E*-1e**. (DMSO-d_6, 378 K).

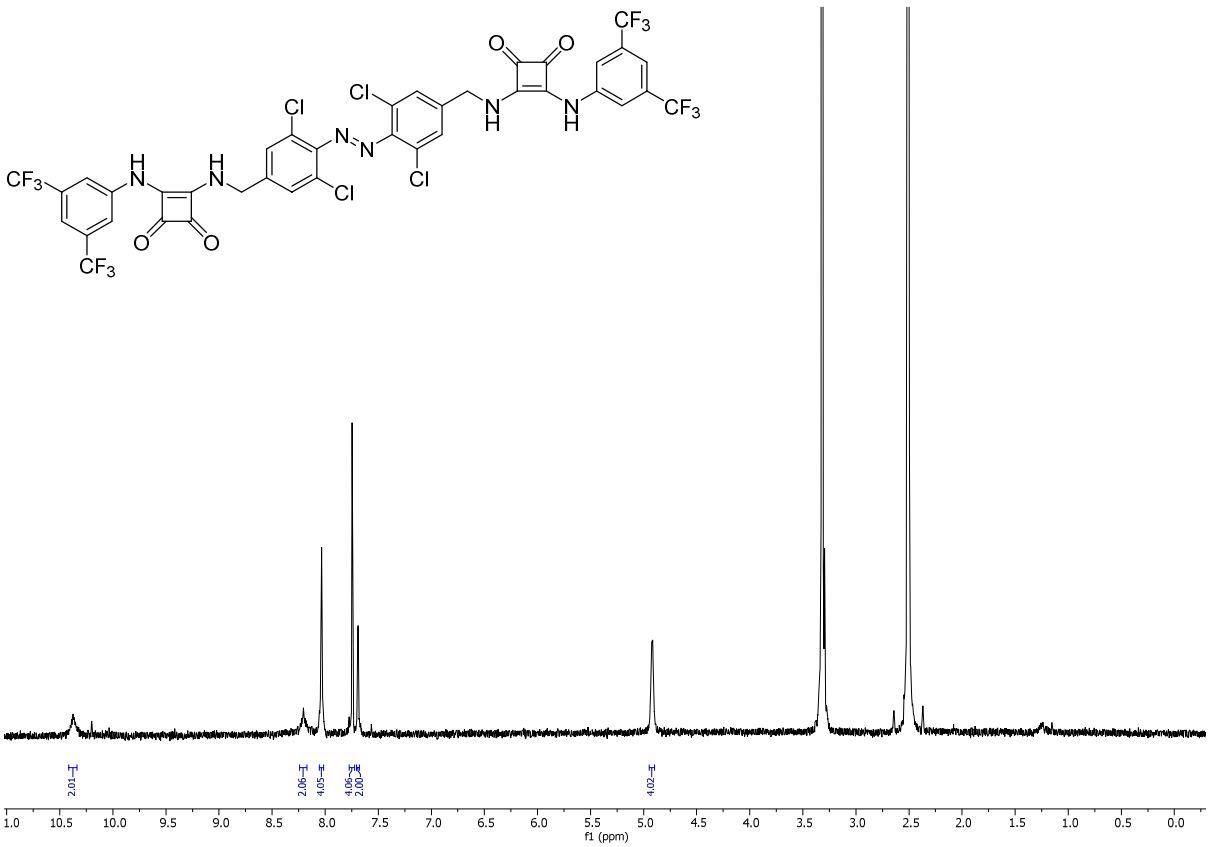

Figure S31. ^{1}H NMR Spectrum of ***E*-1f**. (DMSO-d_6, 298 K).

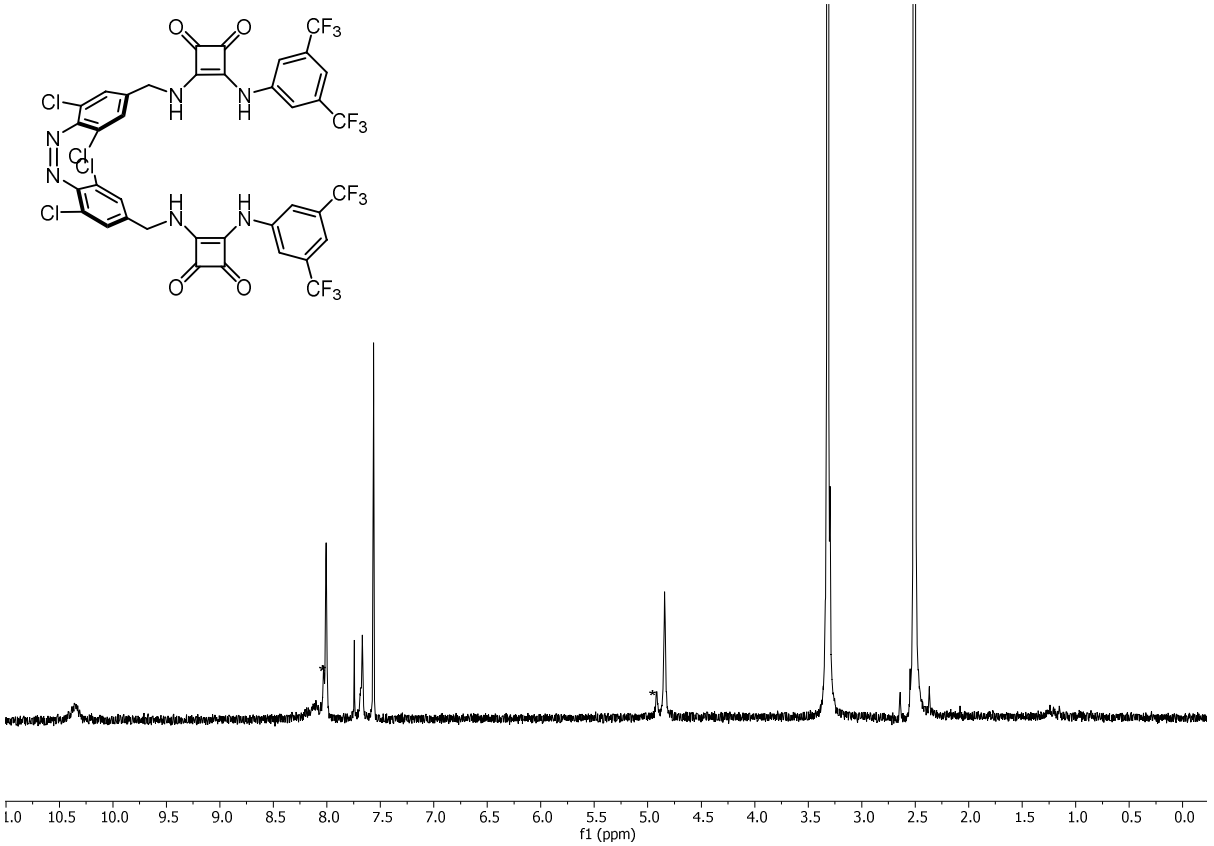

Figure S32. ^{1}H NMR Spectrum of ***Z*-1f** at photostationary state (77%). ***E*-1f** signals labelled as *. (DMSO-d_6, 298 K).

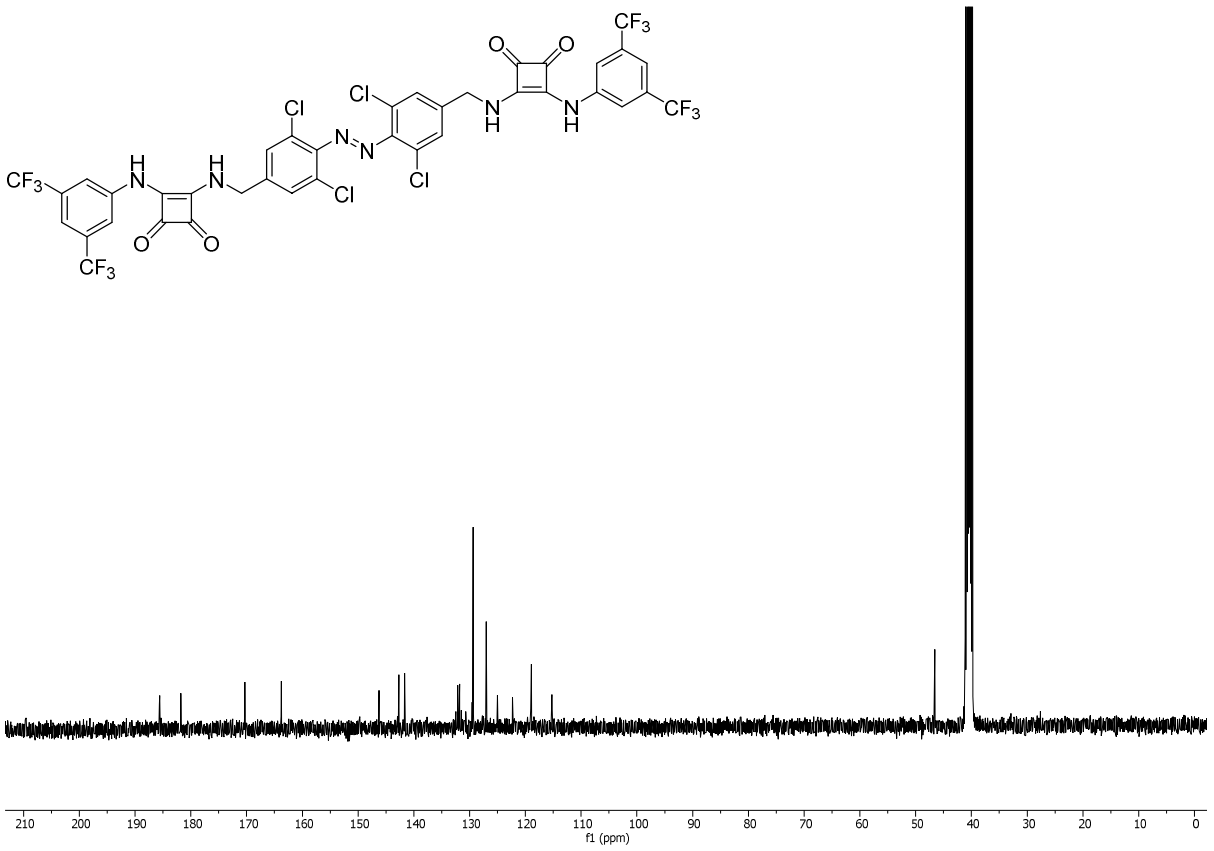

Figure S33. ^{13}C NMR Spectrum of ***E*-1f**. (DMSO-d_6, 358 K).

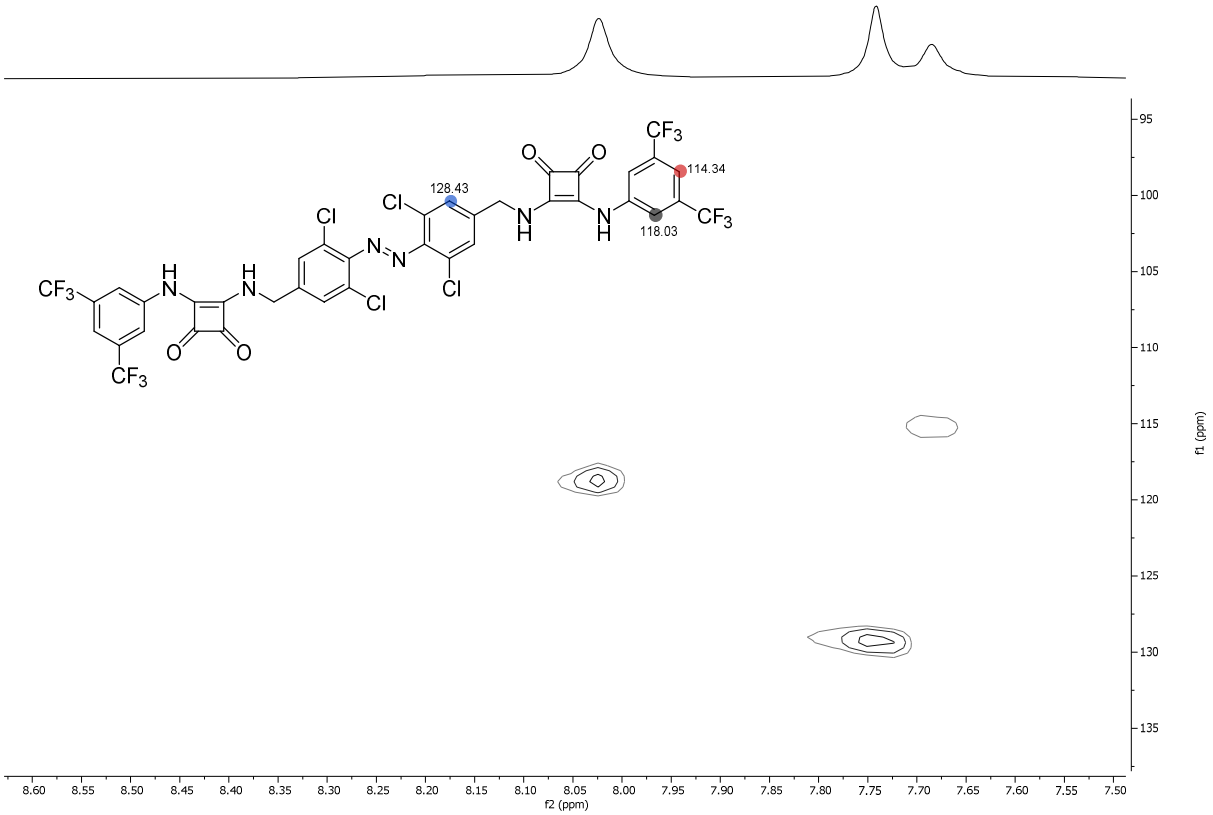

Figure S34. HSQC of **1f**. Key aromatic $^{1}H–^{13}C$ correlations highlighted. (DMSO-d_6, 298 K).

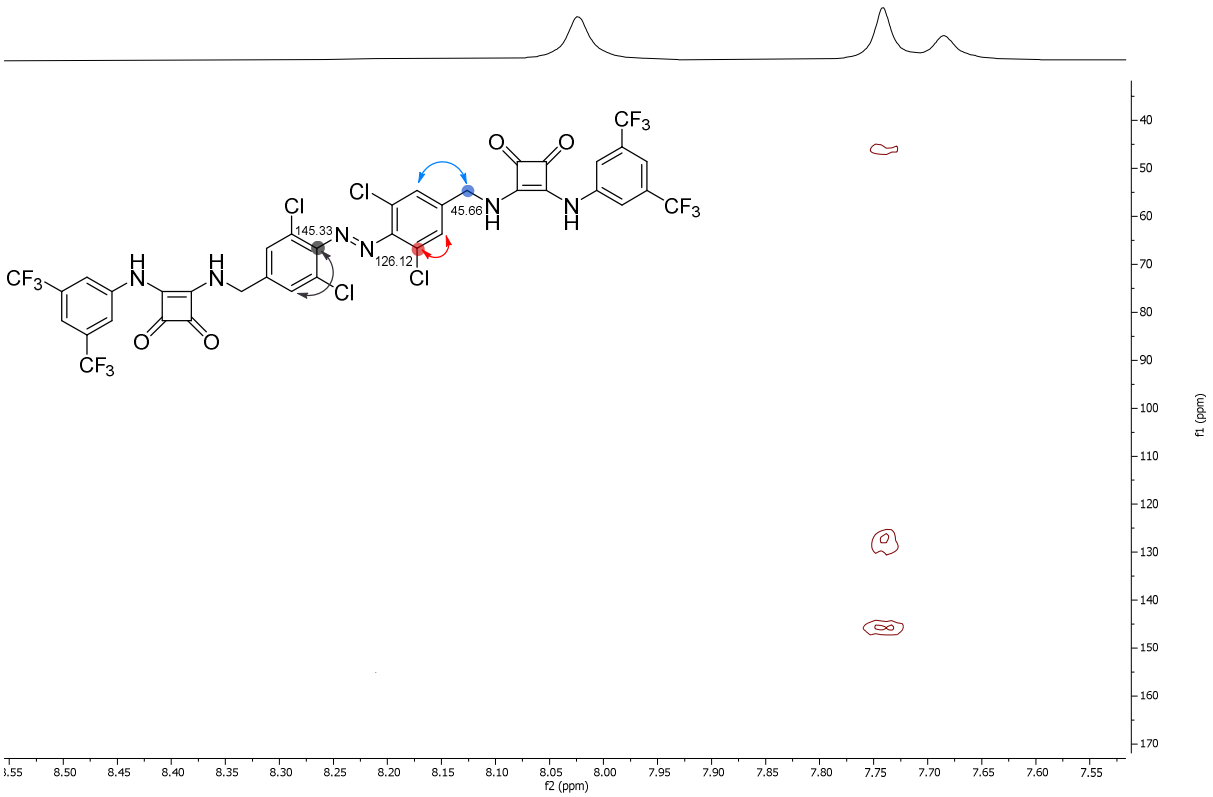

Figure S35. HMBC of **1f**. Key azobenzene aromatic $^{1}H–^{13}C$ correlations highlighted (DMSO-d_6, 298 K).

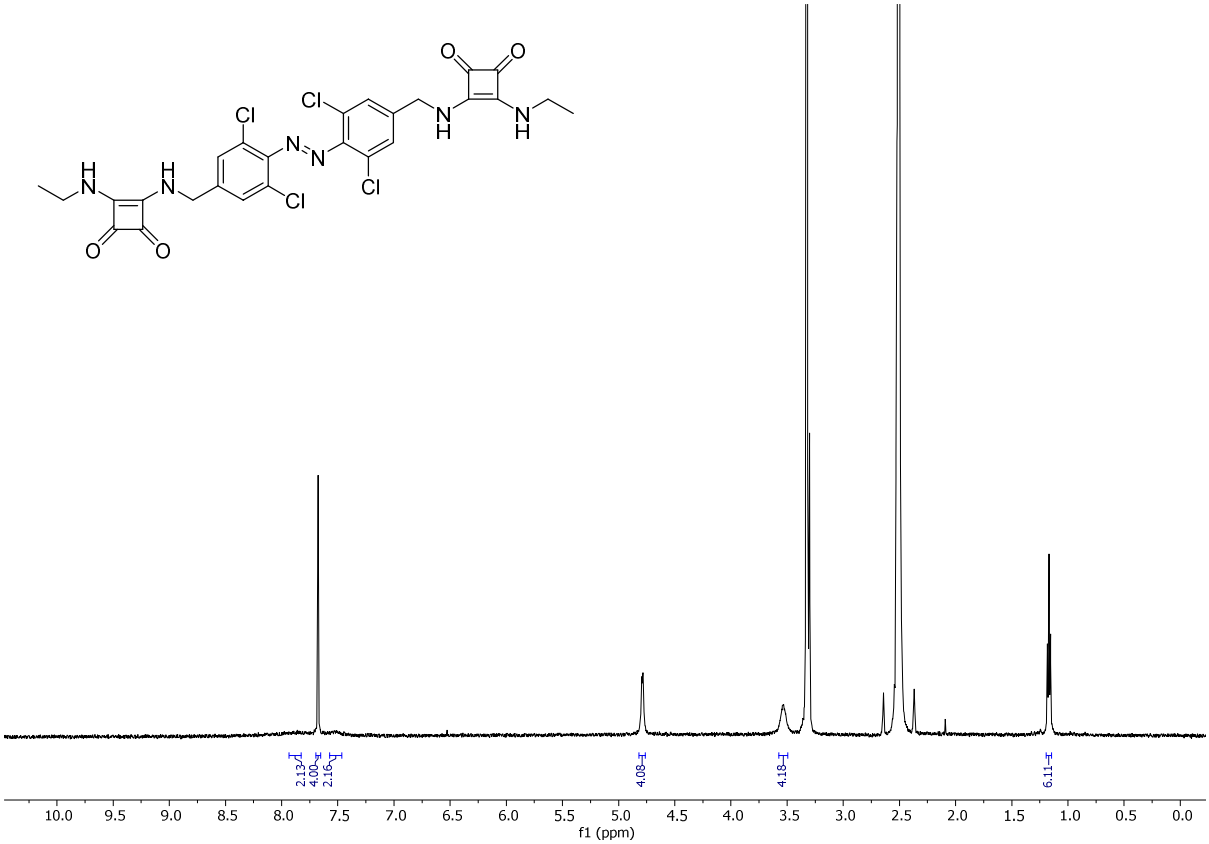

Figure S36. ^{1}H NMR Spectrum of ***E*-1g**. (DMSO-d_6, 298 K).

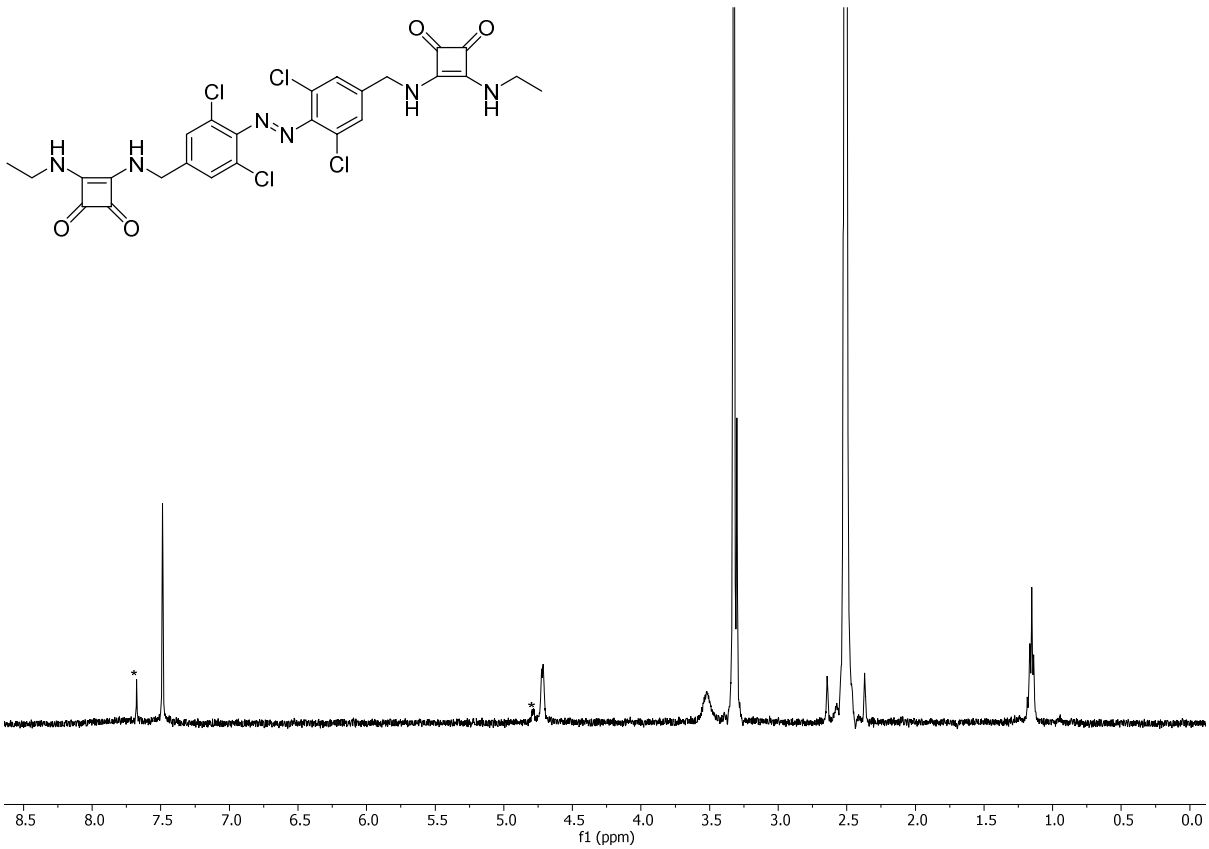

Figure S37. ^{1}H NMR Spectrum of ***Z*-1g** at photostationary state (77%). ***E*-1g** signals labelled as * (DMSO-d_6, 298 K).

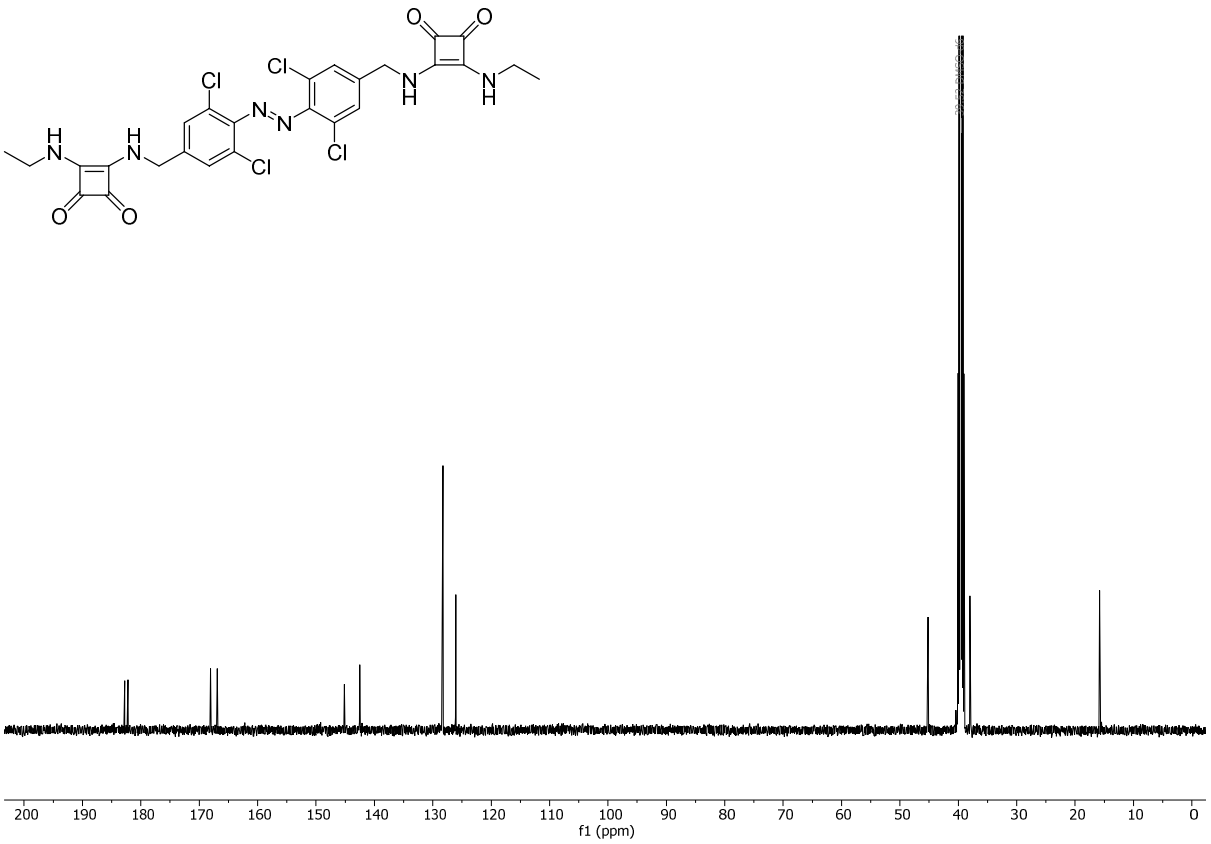

Figure S38. ^{13}C NMR Spectrum of ***E*-1g**. (DMSO-d_6, 378 K).

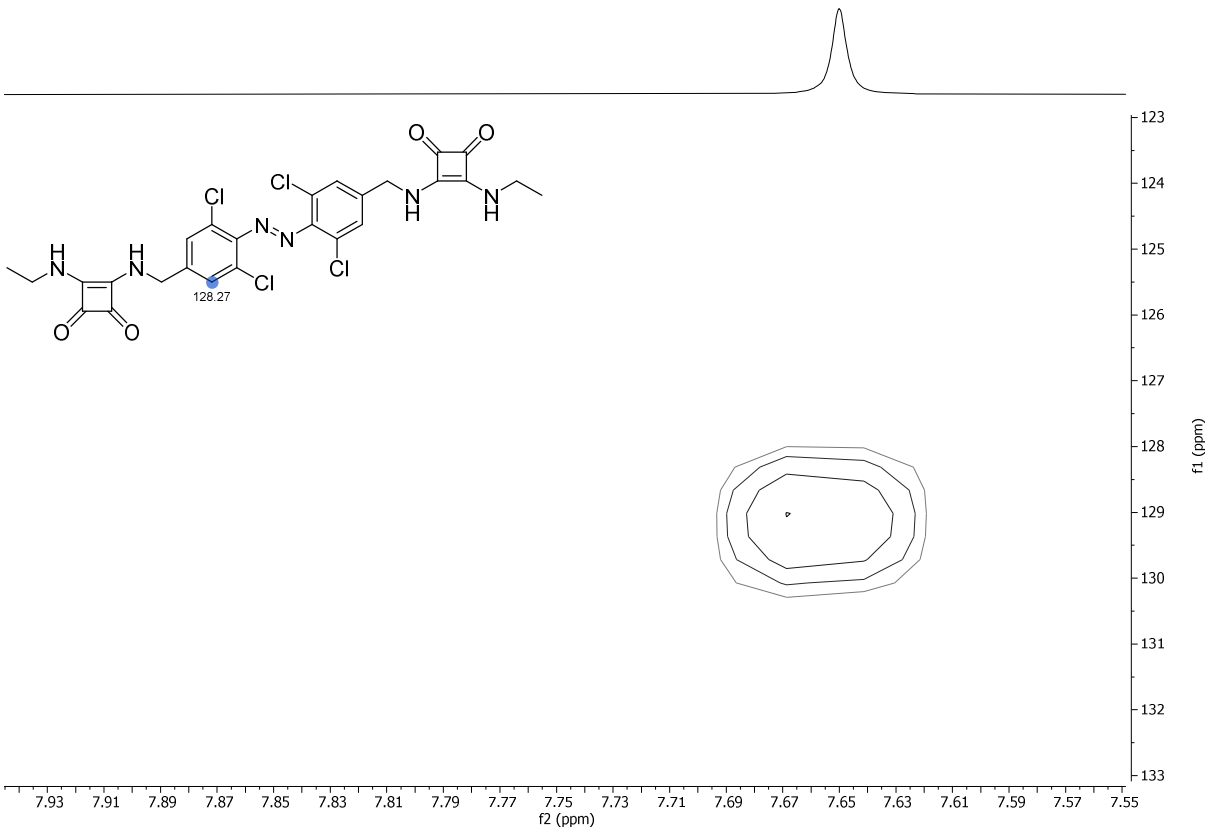

Figure S39. HSQC of **1g**. Key aromatic ^{1}H–^{13}C correlation highlighted (DMSO-d_6, 298 K).

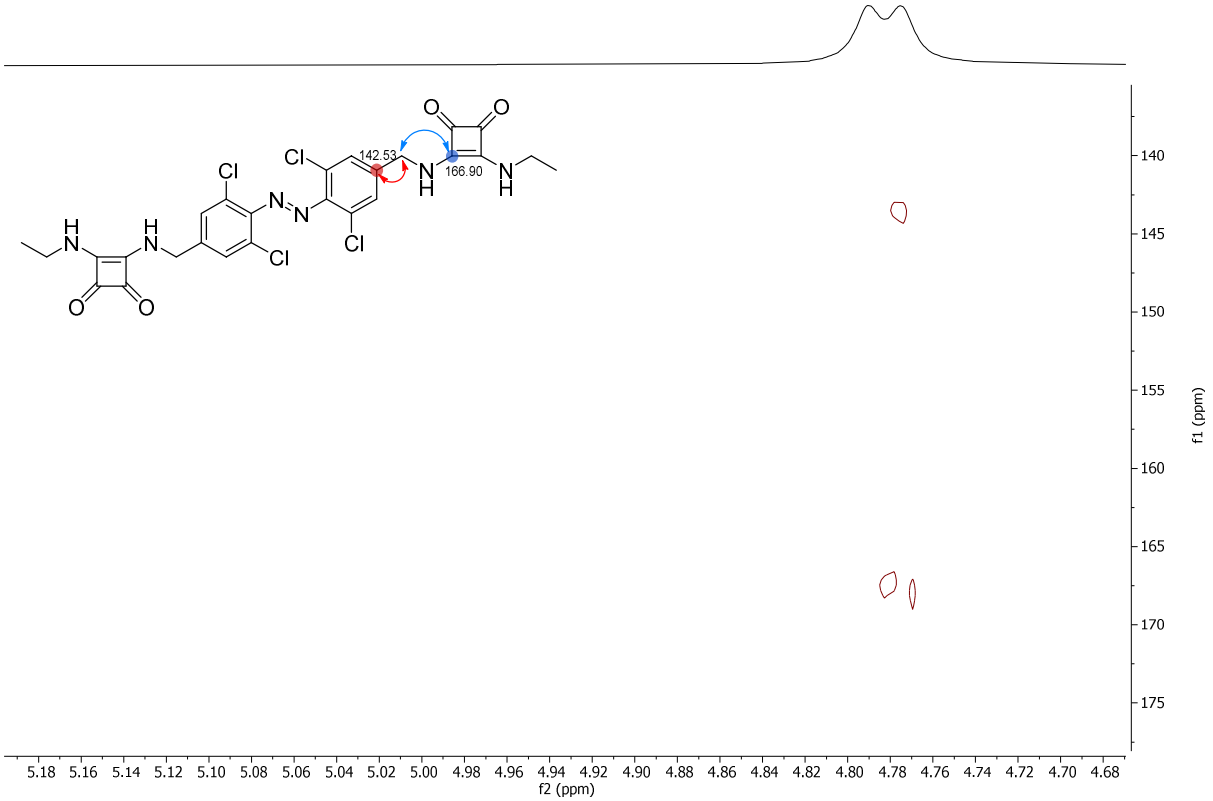

Figure S40. HMBC of **1g**. Key ^{1}H–^{13}C correlations to benzyl proton highlighted (DMSO-d_6, 298 K).

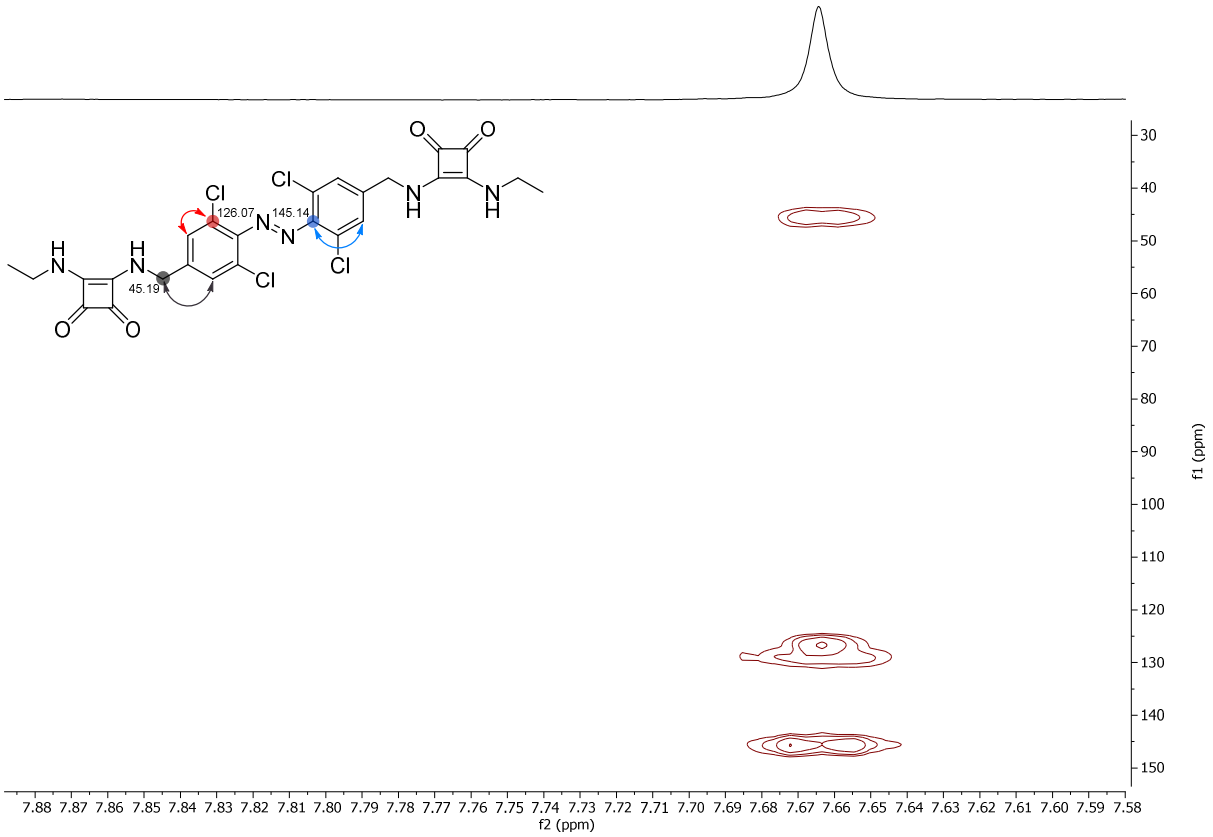

Figure S41. HMBC of **1g**. Key ^{1}H–^{13}C correlations to azobenzene proton highlighted (DMSO-d_6, 298 K).

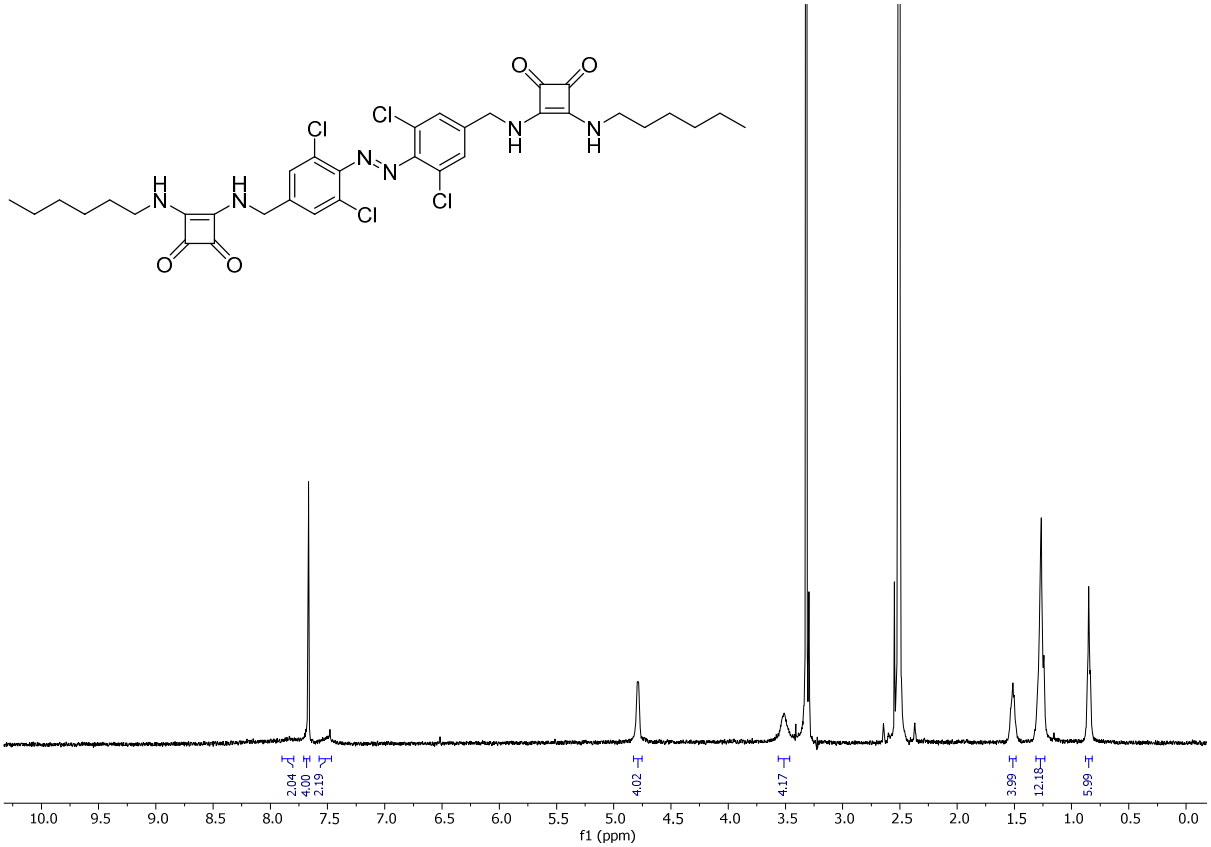

Figure S42. ^{1}H NMR Spectrum of ***E*-1h**. (DMSO-d_6, 298 K).

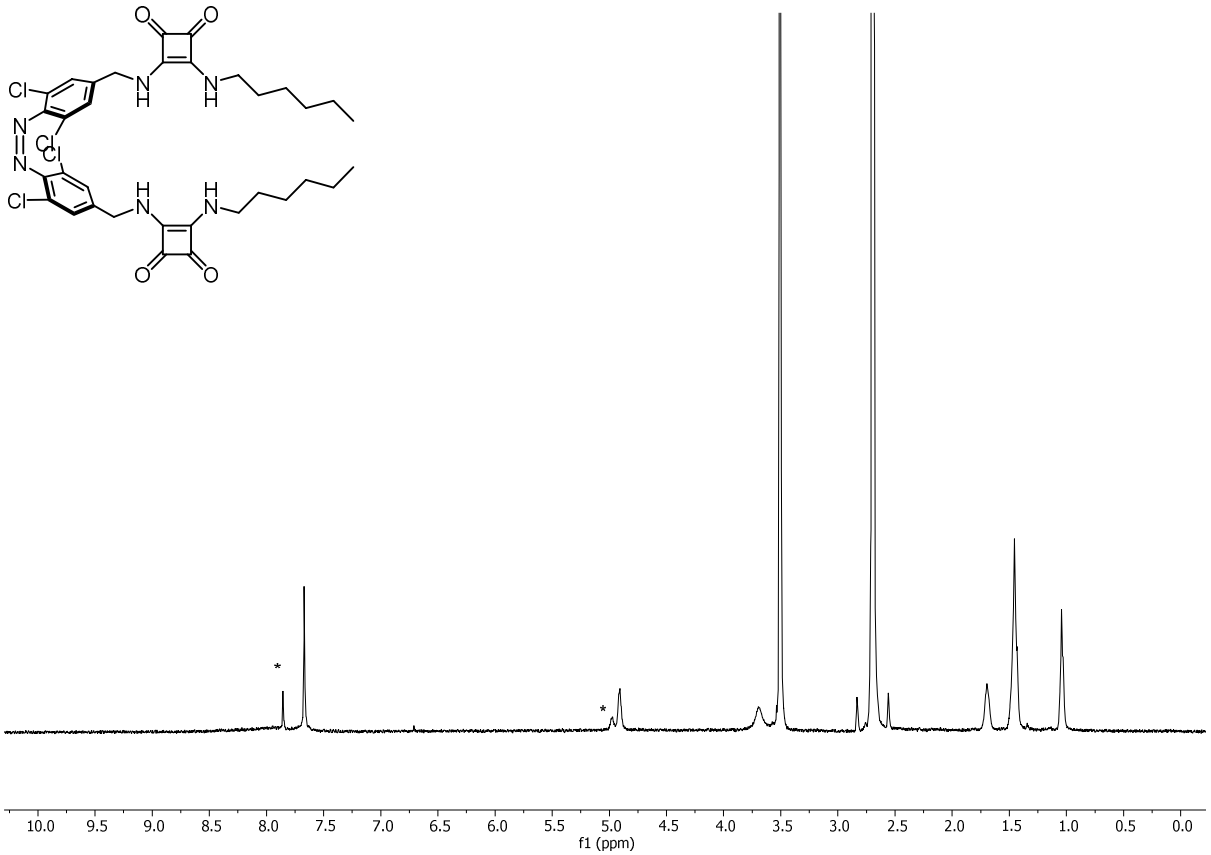

Figure S43. ^{1}H NMR Spectrum of ***Z*-1h** at photostationary state (77%). ***E*-1h** signals labelled as * (DMSO-d_6, 298 K).

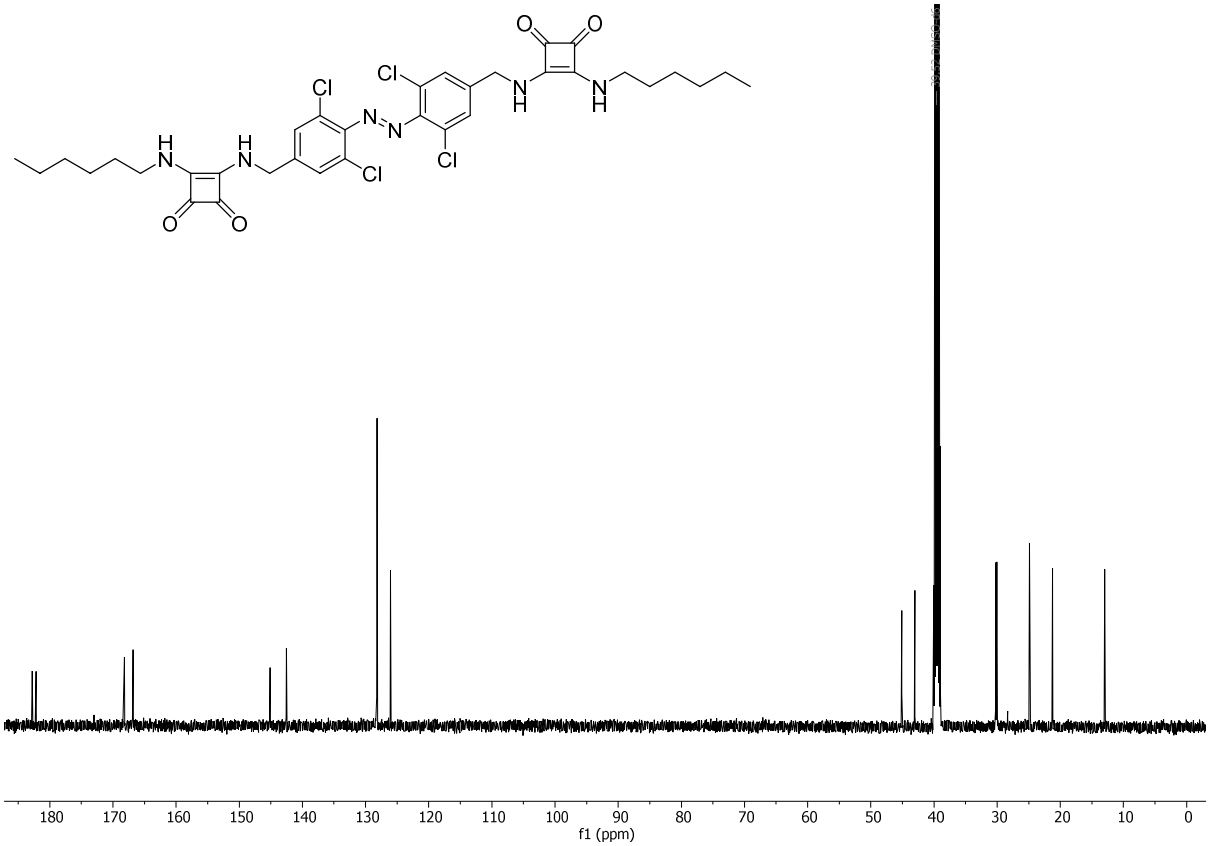

Figure S44. ^{13}C NMR Spectrum of ***E*-1h**. (DMSO-d_6, 378 K).

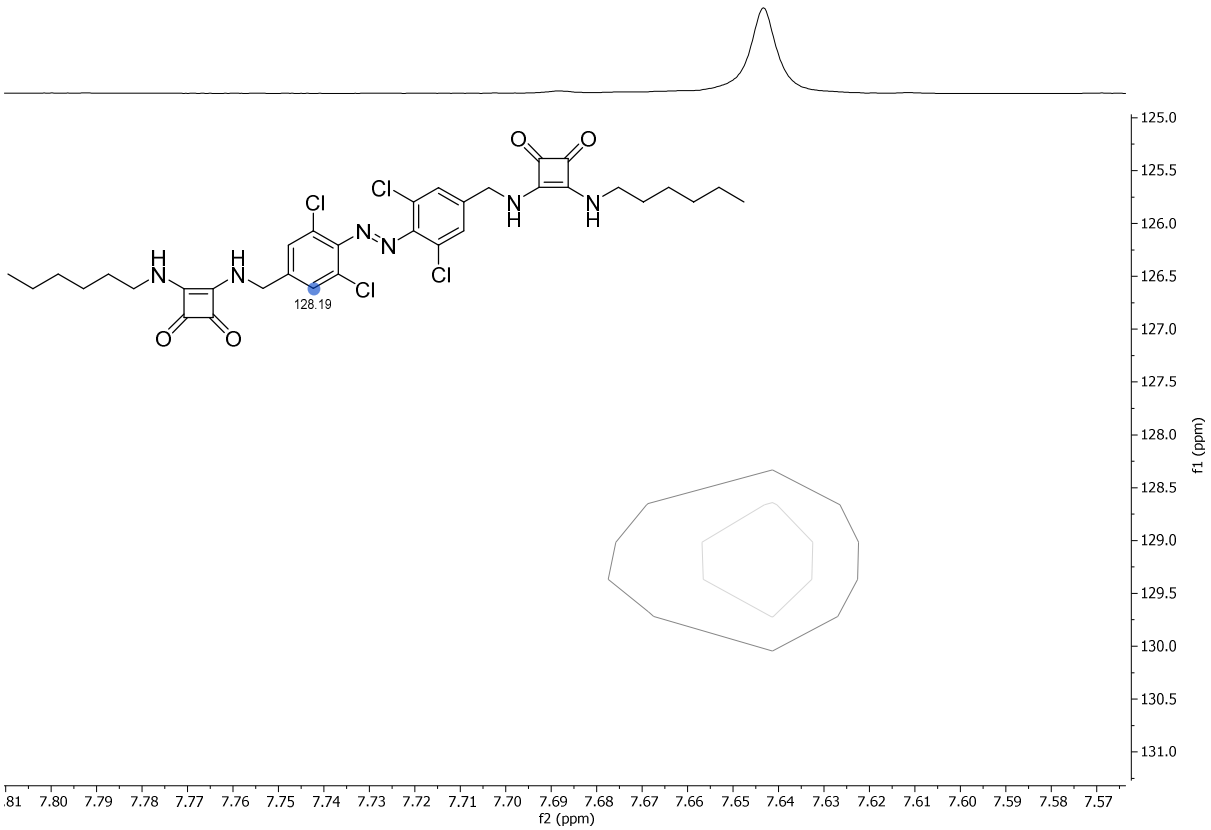

Figure S45. HSQC of **1h**. Key aromatic ^{1}H–^{13}C correlation highlighted (DMSO-d_6, 298 K).

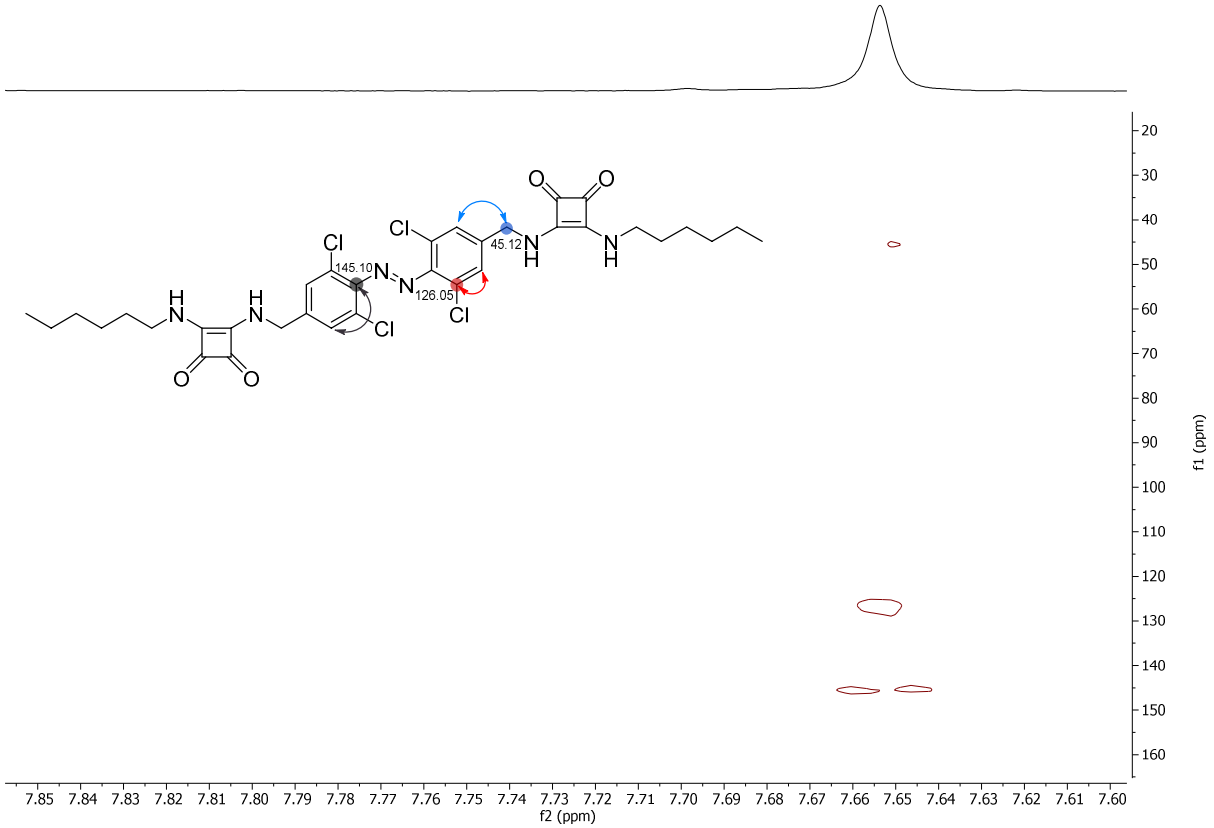

Figure S46. HMBC of **1h**. Key ^{1}H–^{13}C azobenzene proton correlations highlighted (DMSO-d_6, 298 K).

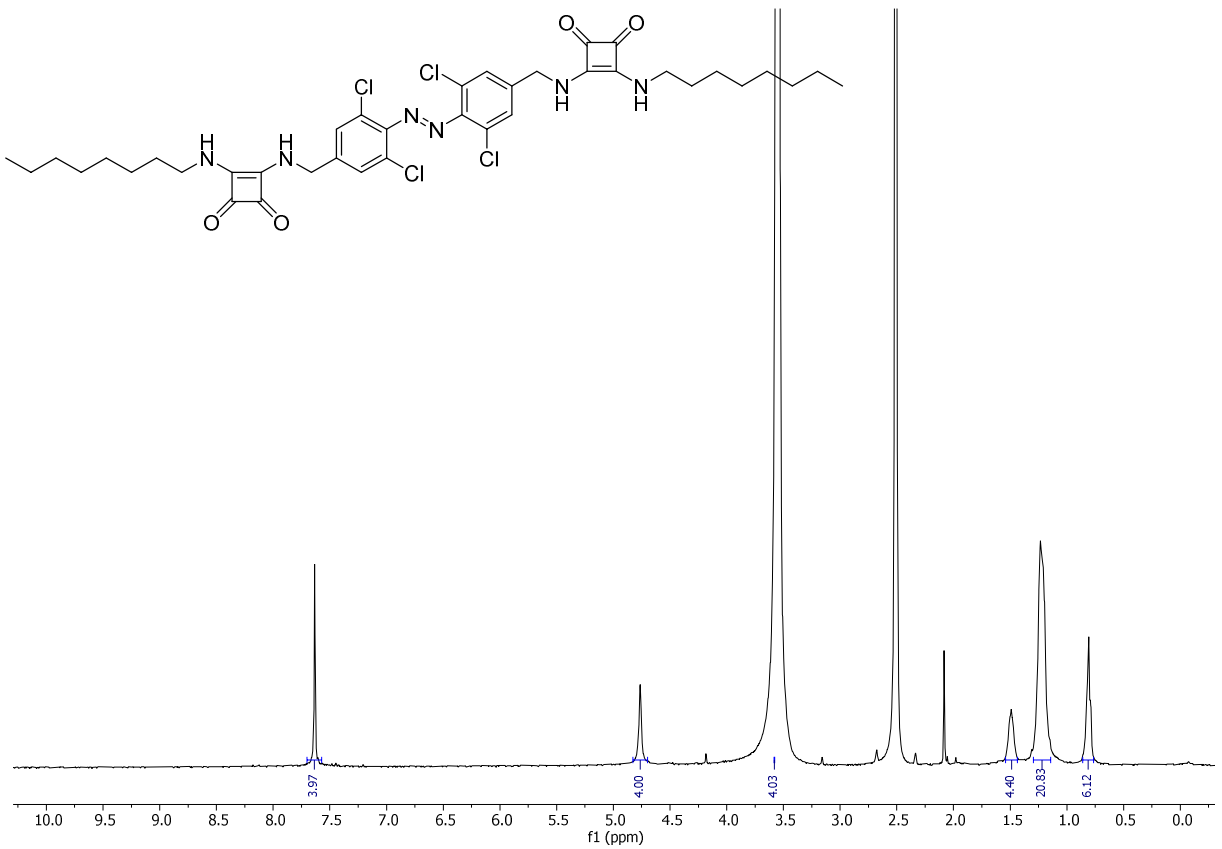

Figure S47. ^{1}H NMR Spectrum of ***E*-1a**. (DMSO-d_6, 298 K).

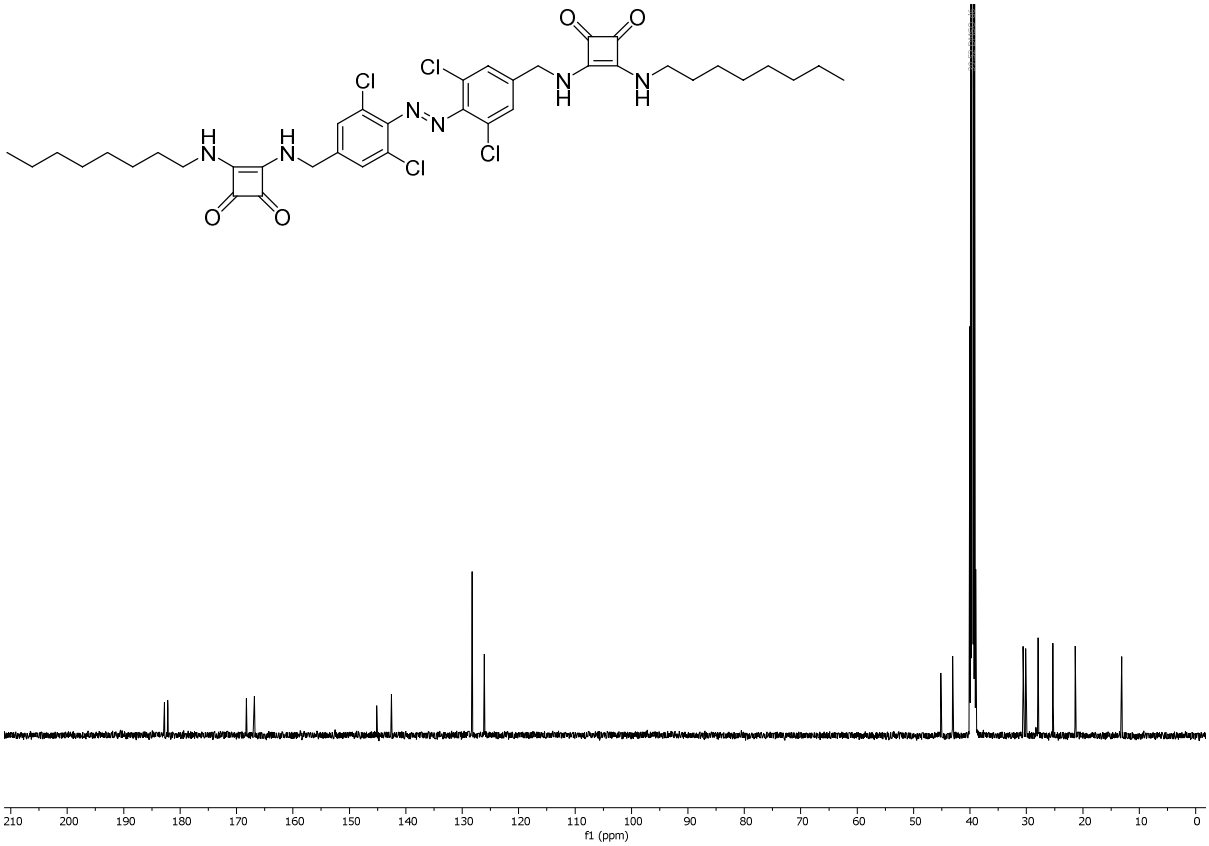

Figure S48. ^{13}C NMR Spectrum of ***E*-1i**. (DMSO-d_6, 378 K).

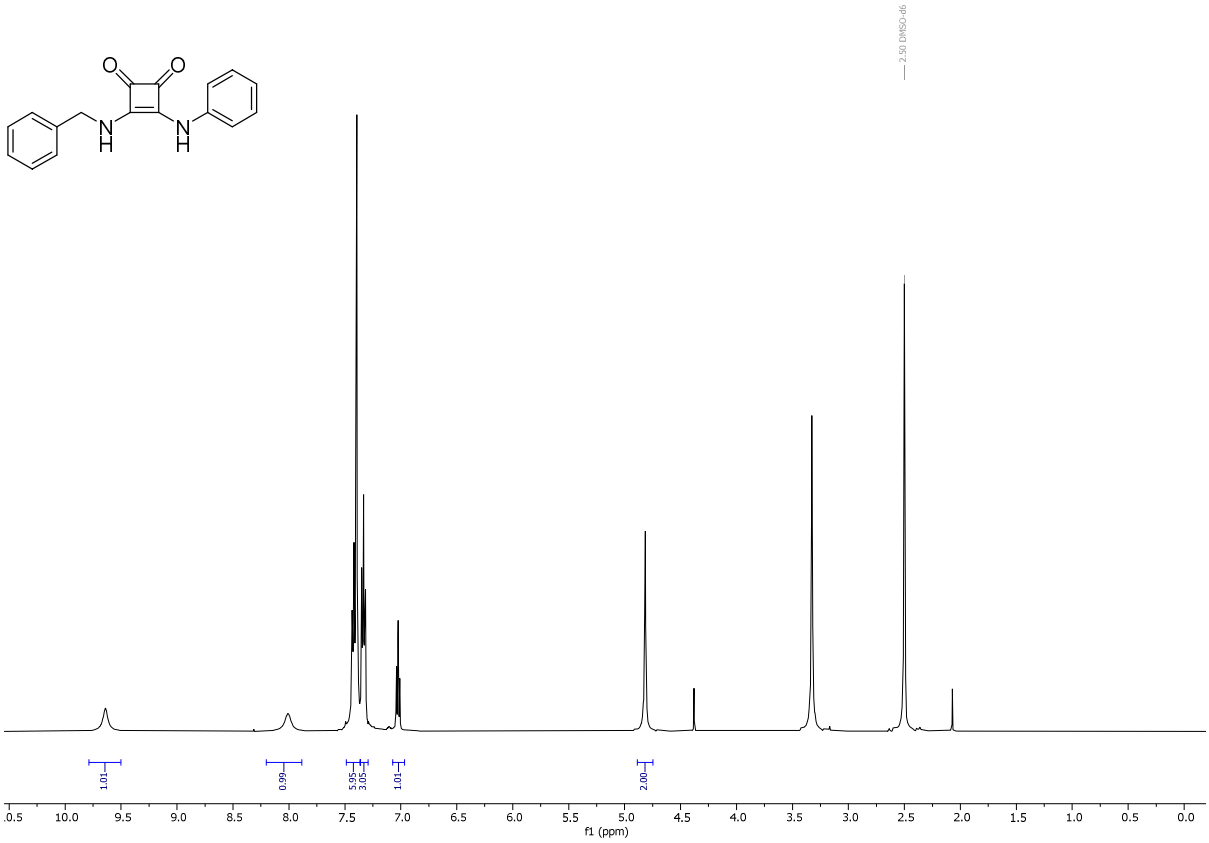

Figure S49. ^{1}H NMR Spectrum of S**1** (DMSO-d_6, 298 K).

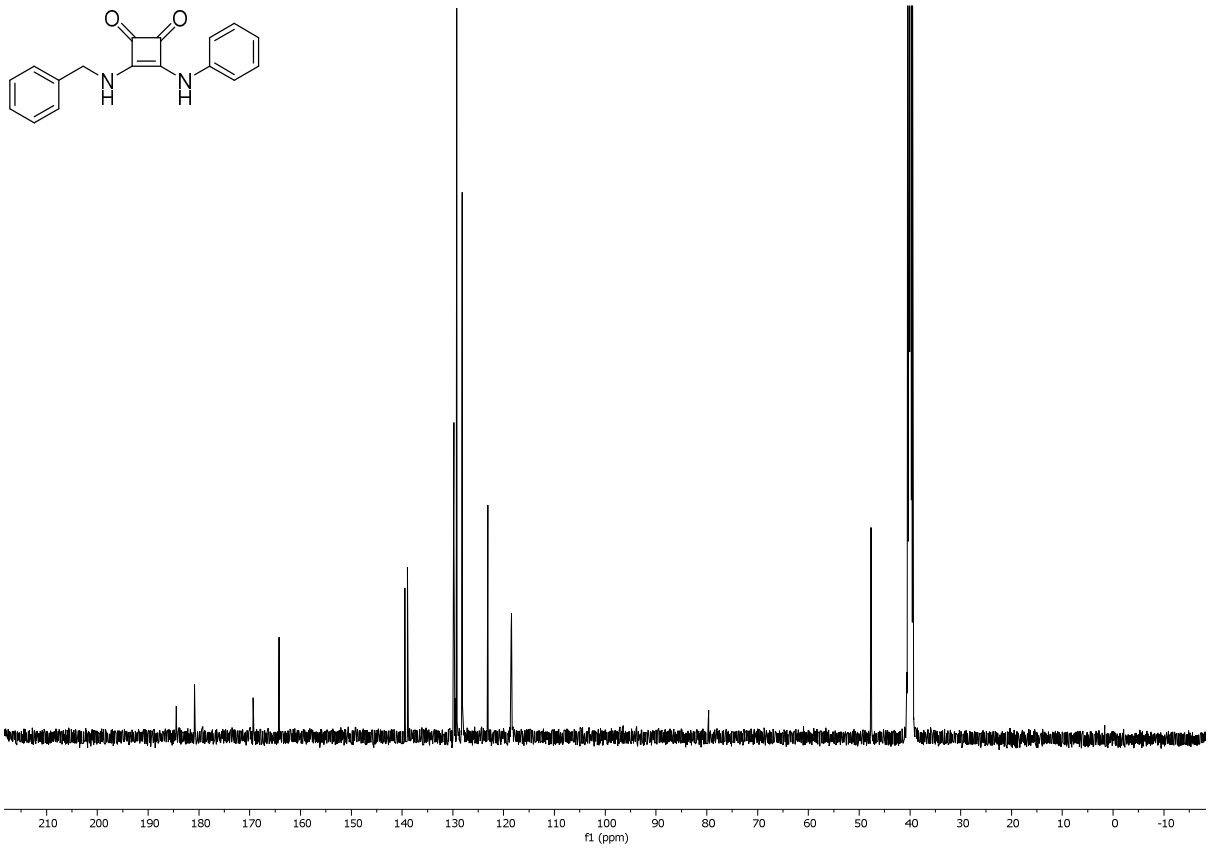

Figure S50. ^{13}C NMR Spectrum of **S1** (DMSO-d_6, 298 K).

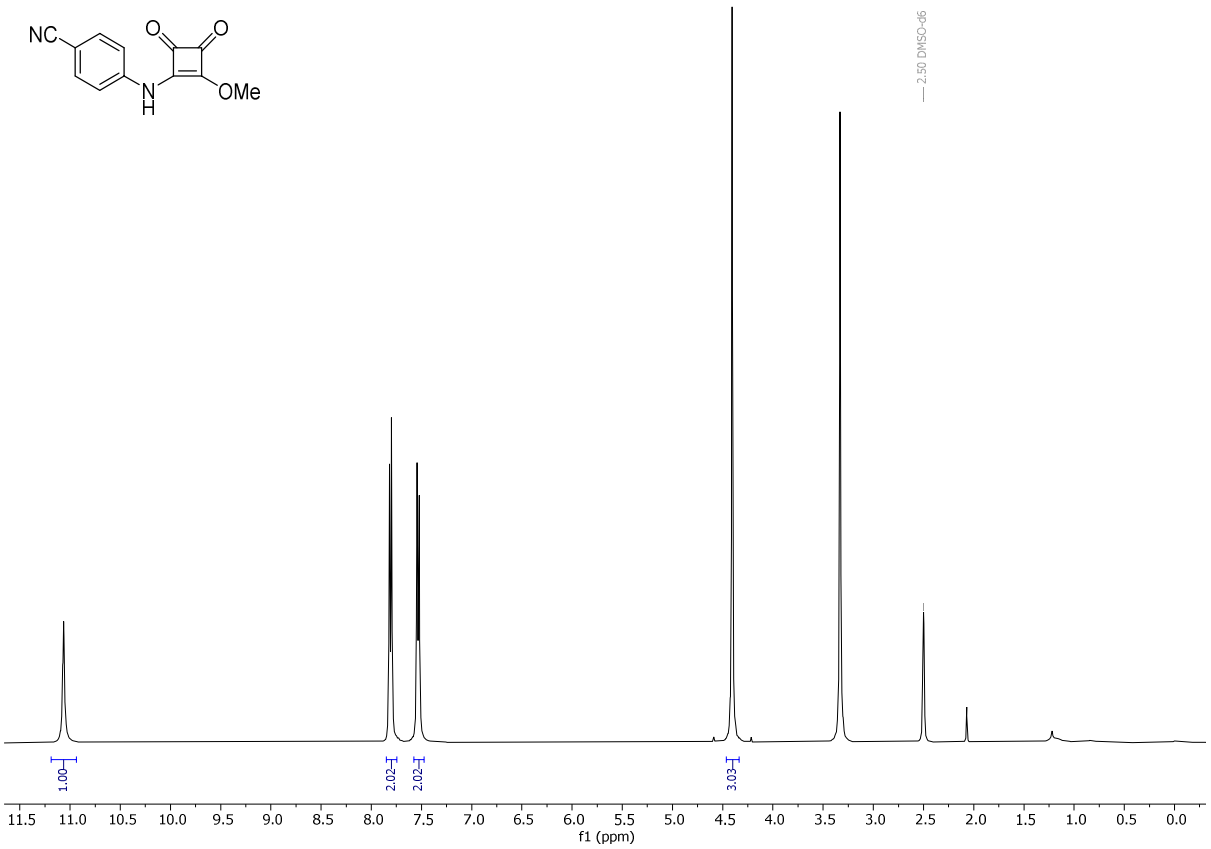

Figure S51. ^{1}H NMR Spectrum of **6e** (DMSO-d_6, 298 K).

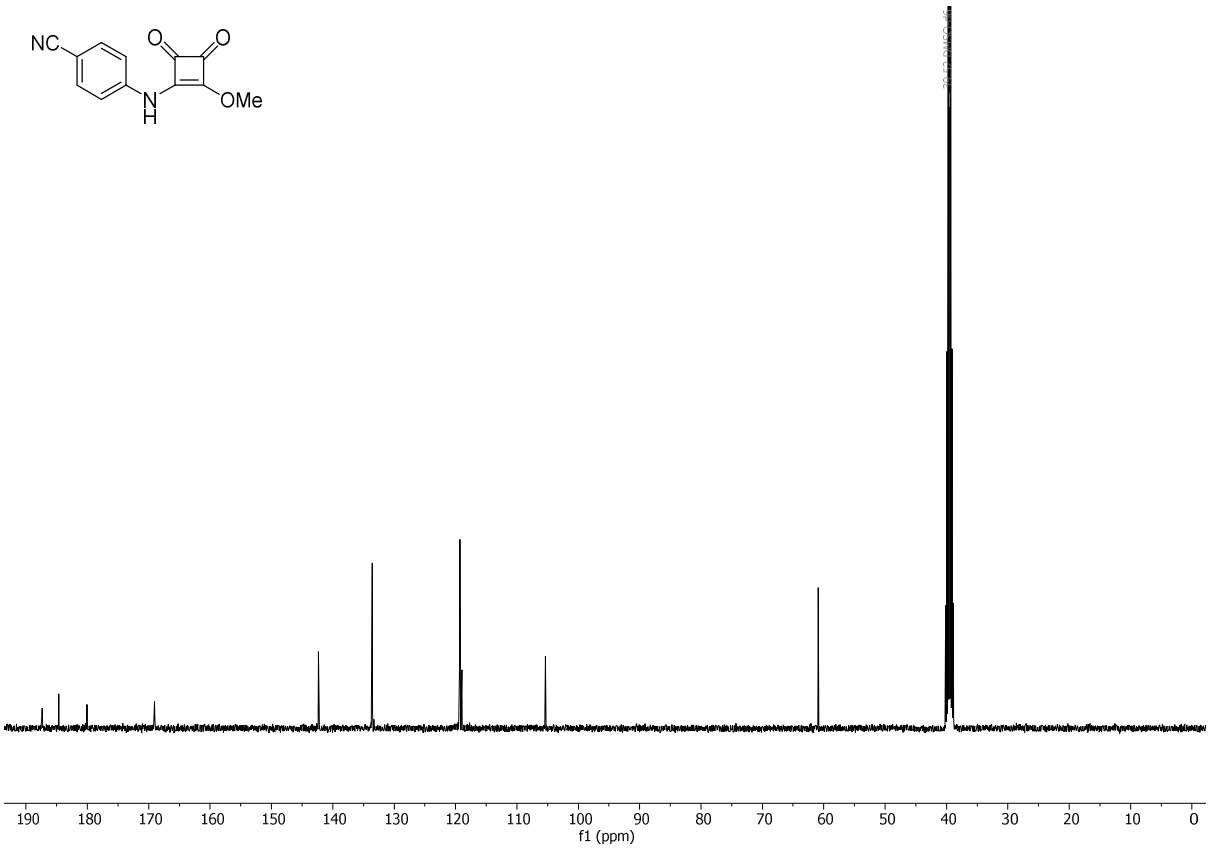

Figure S52. ^{13}C NMR Spectrum of **6e** (DMSO-d_6, 298 K).

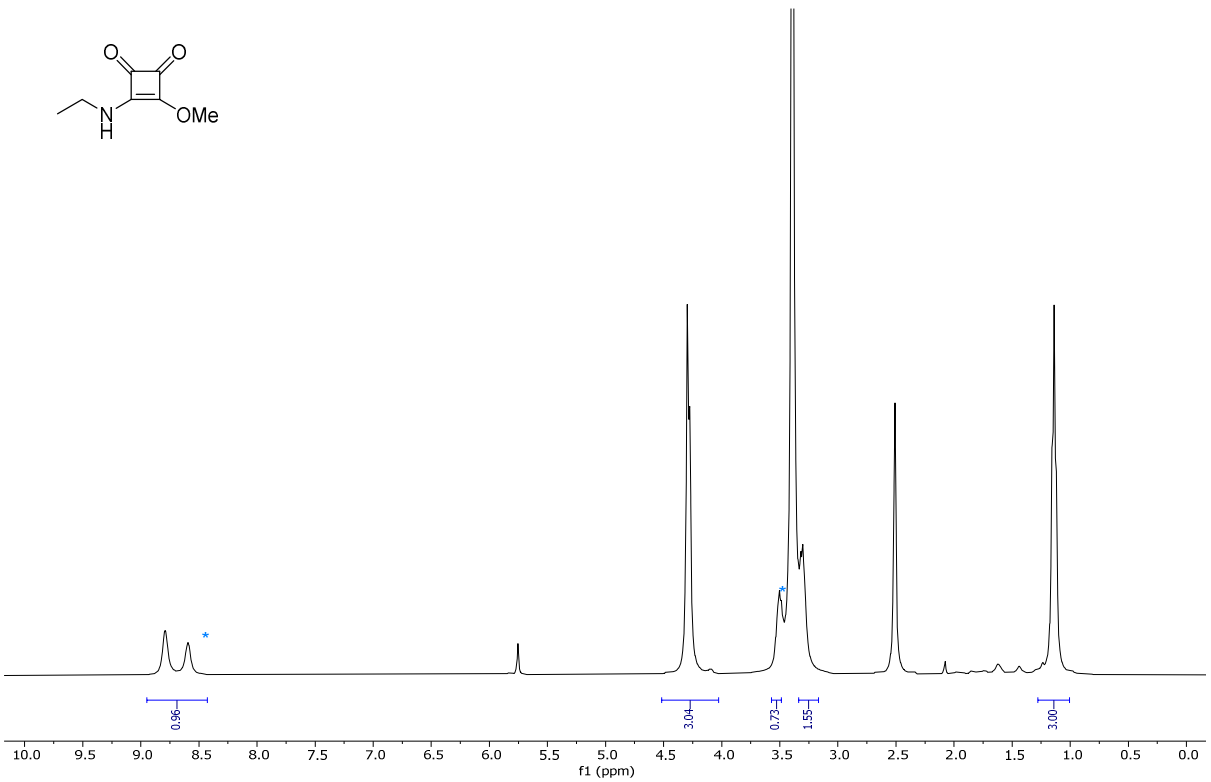

Figure S53. ^{1}H NMR spectrum of **6g**. Compound exists as rotamers (2:1) Minor signals labelled as * (DMSO-d_6, 298 K).

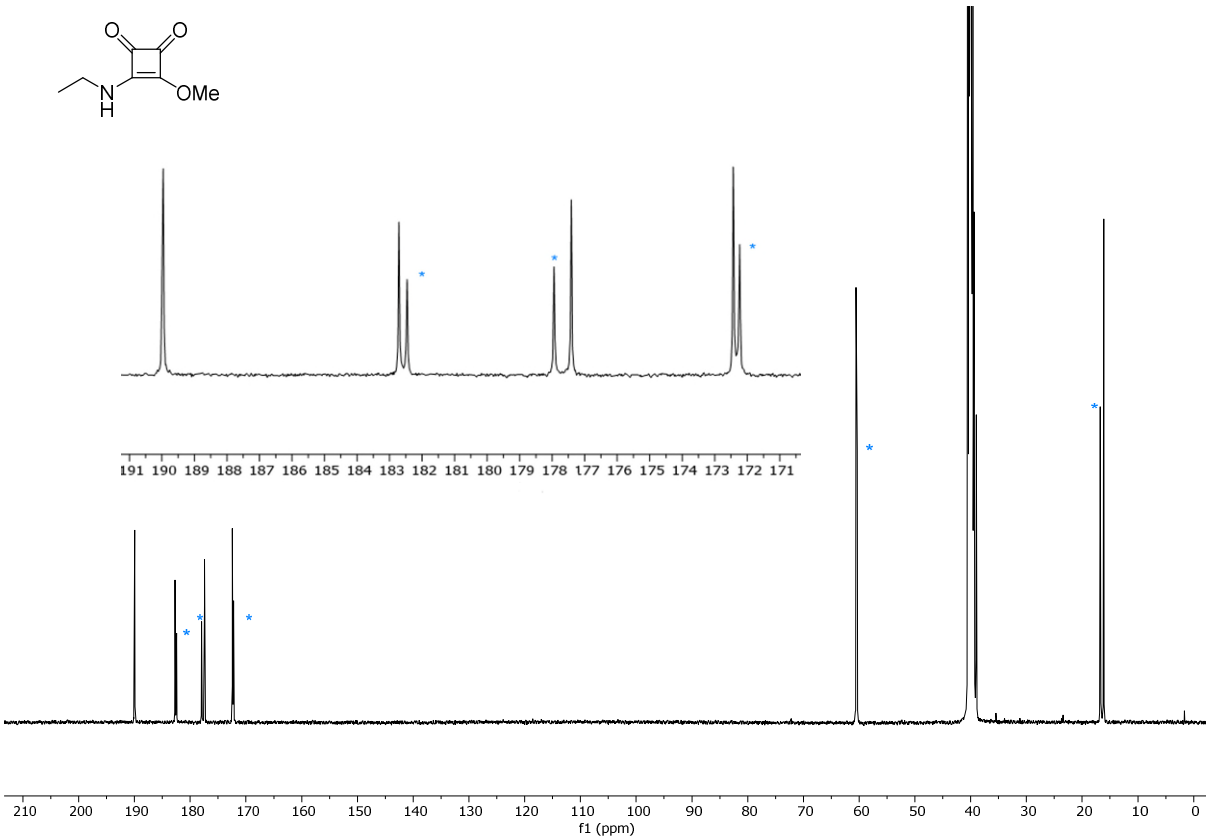

Figure S54. ^{13}C NMR spectrum of **6g**. Compound exists as rotamers (2:1) Minor signals labelled as * (DMSO-d_6, 298 K).

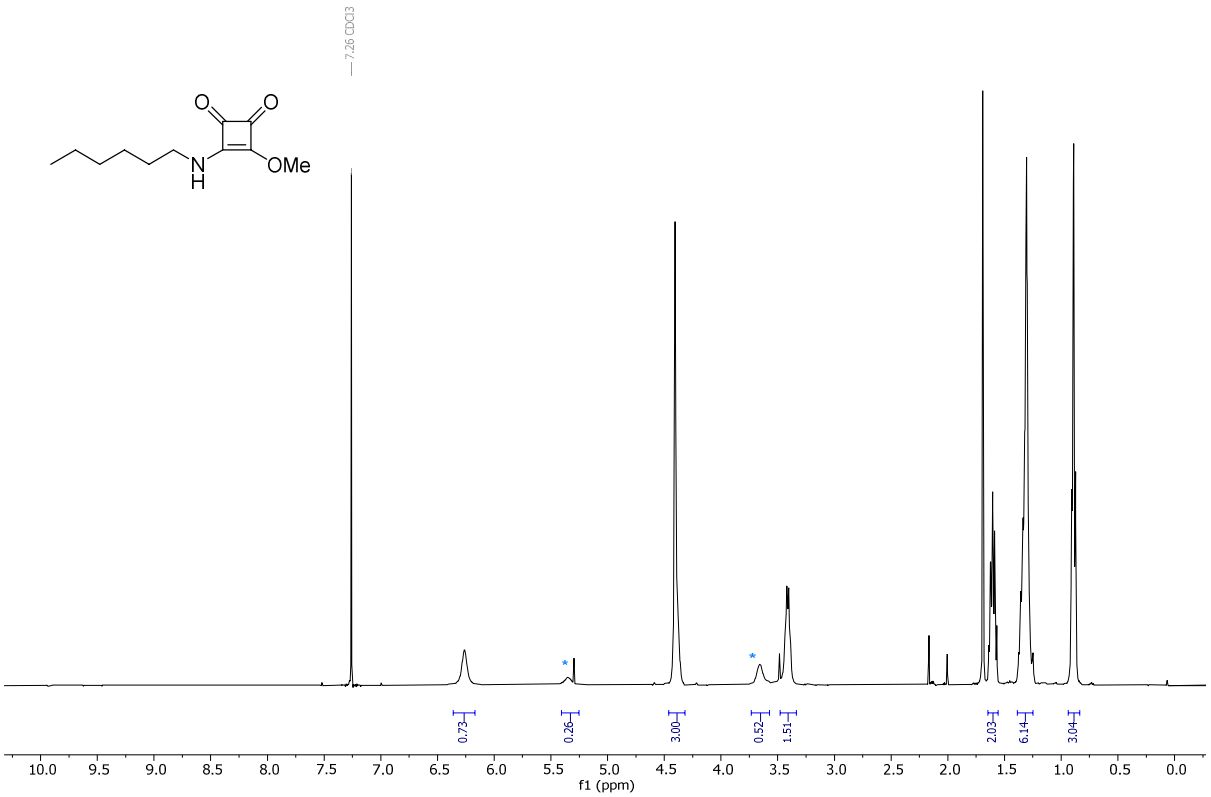

Figure S55. ^{1}H NMR spectrum of **6h**. Compound exists as rotamers (3:1) Minor signals labelled as * (Chloroform-*d*, 298 K).

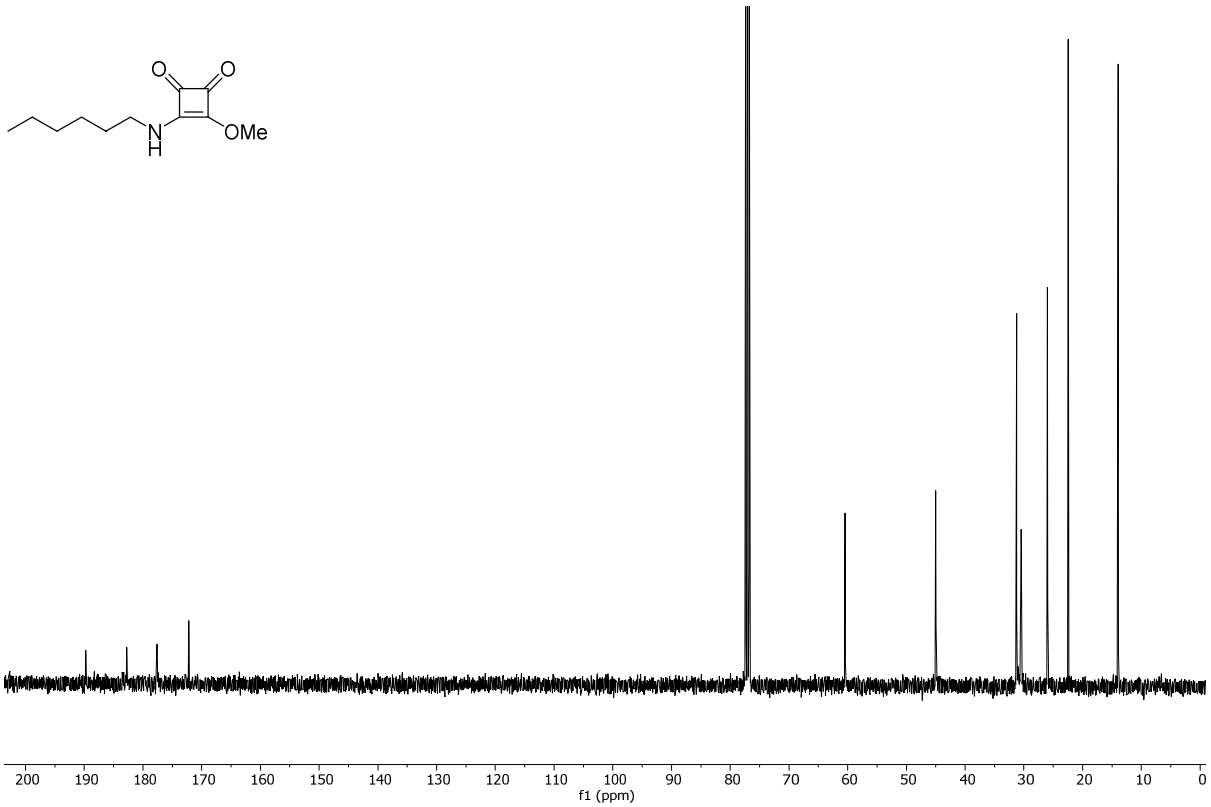

Figure S56. ^{13}C NMR spectrum of **6h**. (Chloroform-*d*, 298 K).

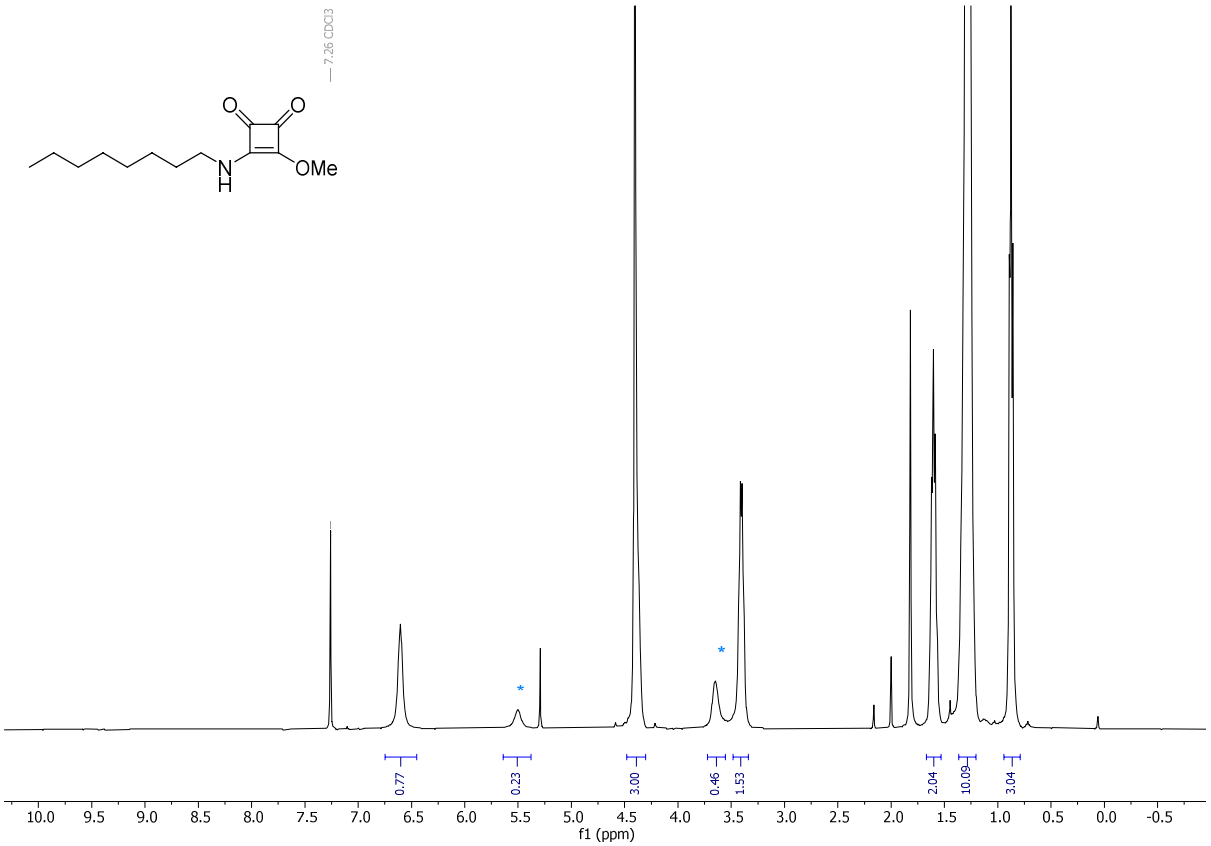

Figure S57. ^{1}H NMR spectrum of **6g**. Compound exists as rotamers (4:1) Minor signals labelled as * (Chloroform-*d*, 298 K).

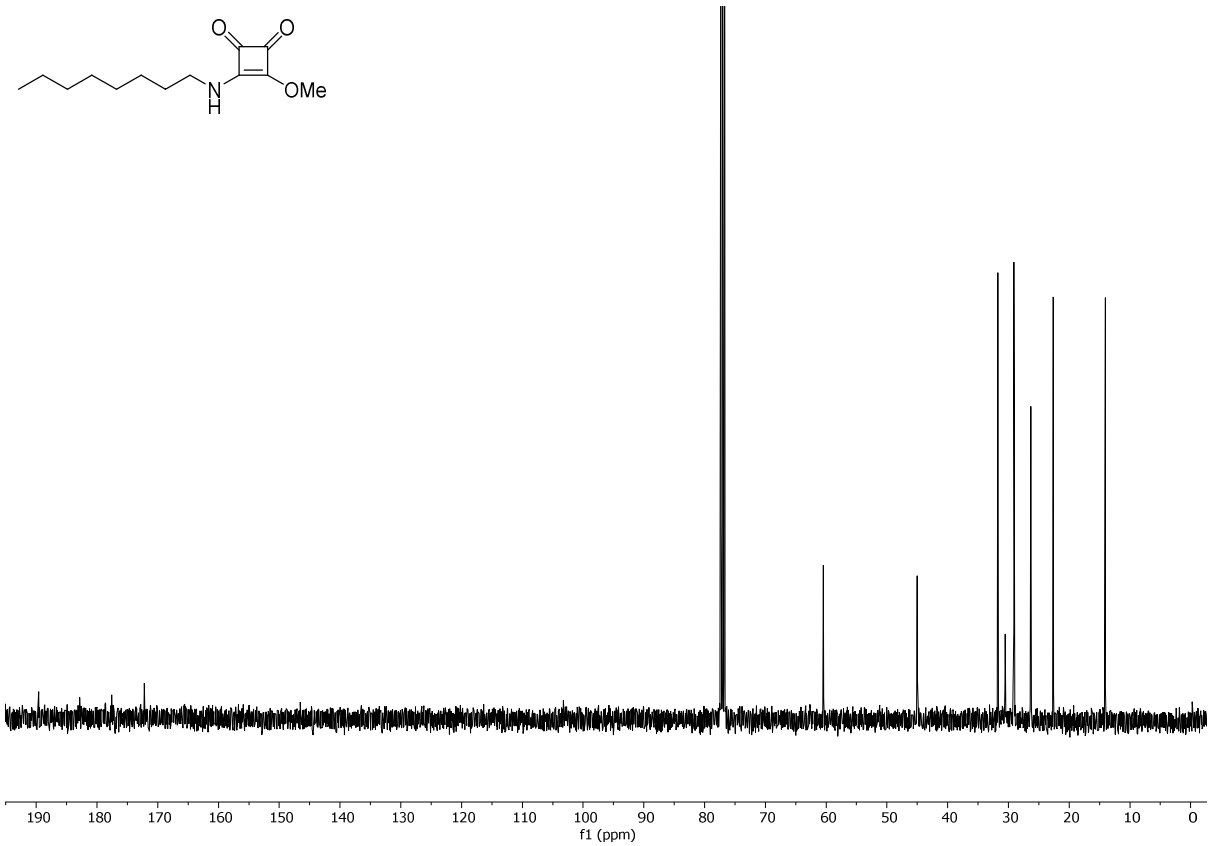

Figure S58. ^{13}C NMR spectrum of **6g**. (Chloroform-*d*, 298 K).

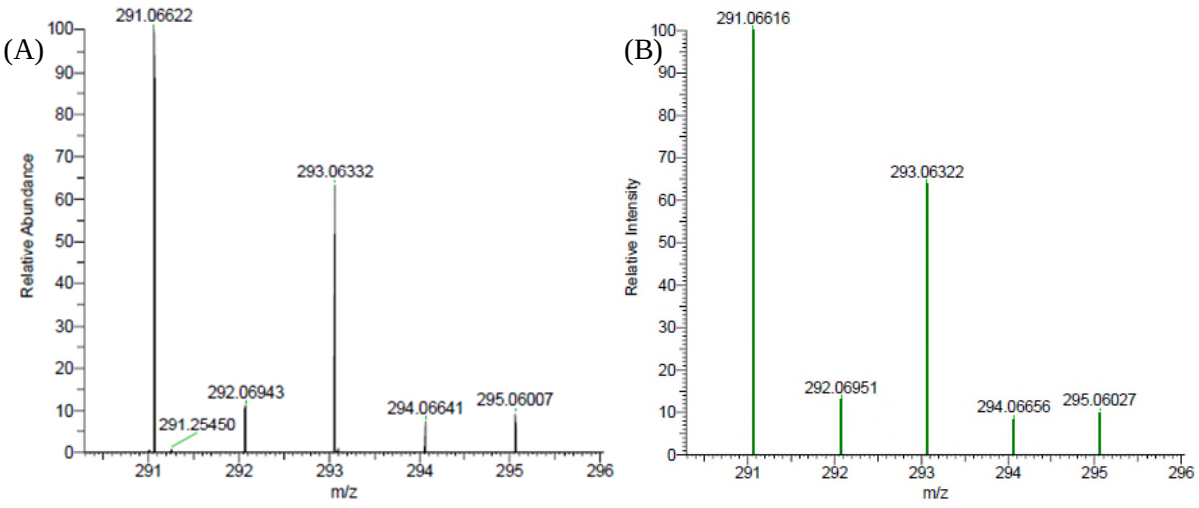

Figure S59. (A) HRMS spectrum of **3**. (B) Theoretical spectrum of **3**.

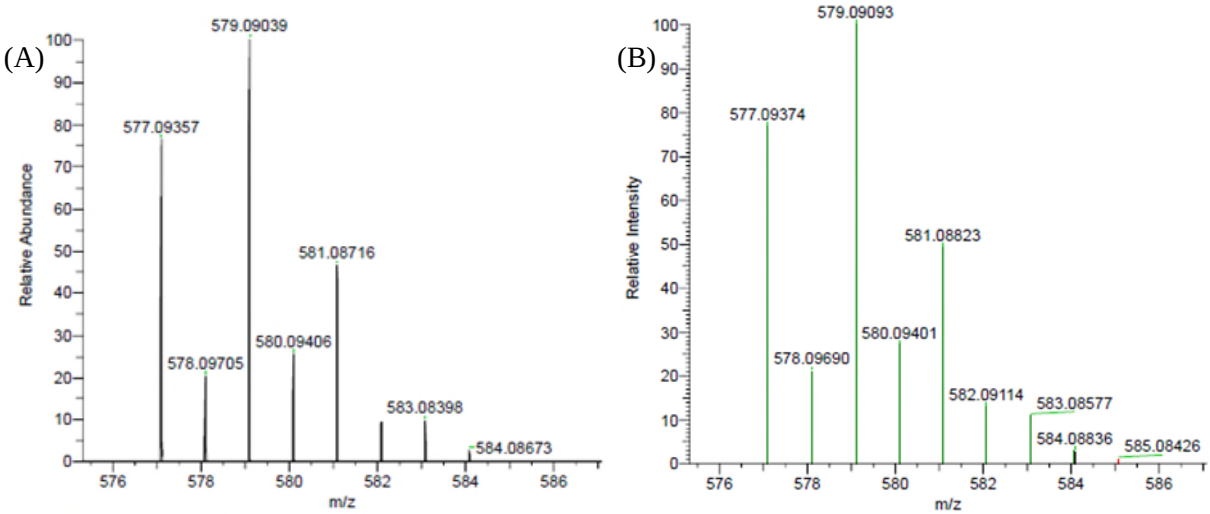

Figure S60. (A) HRMS spectrum of **4**. (B) Theoretical spectrum of **4**.

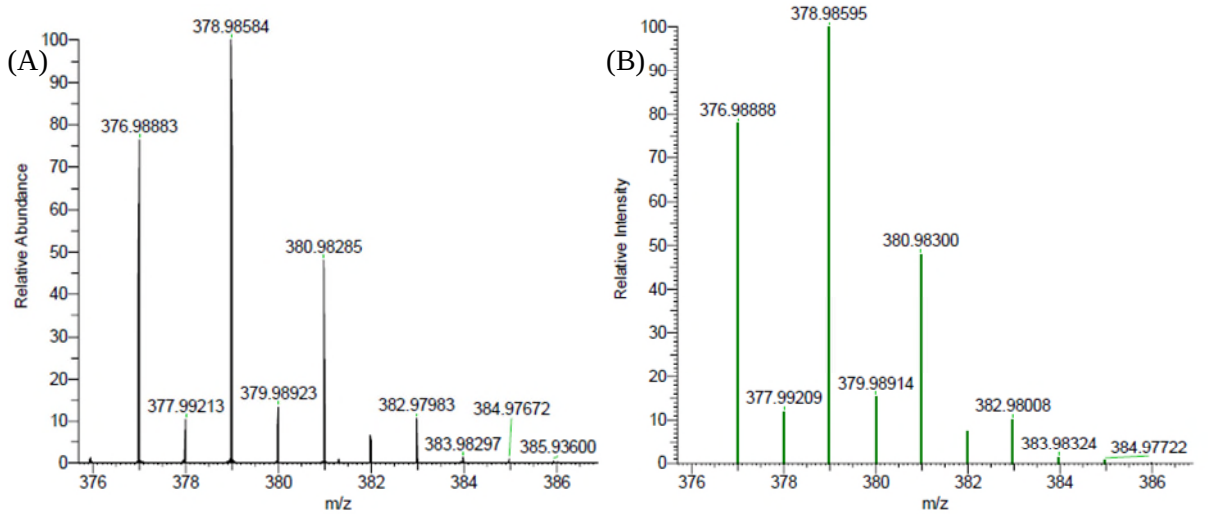

Figure S61. (A) HRMS spectrum of **5**. (B) Theoretical spectrum of **5**.

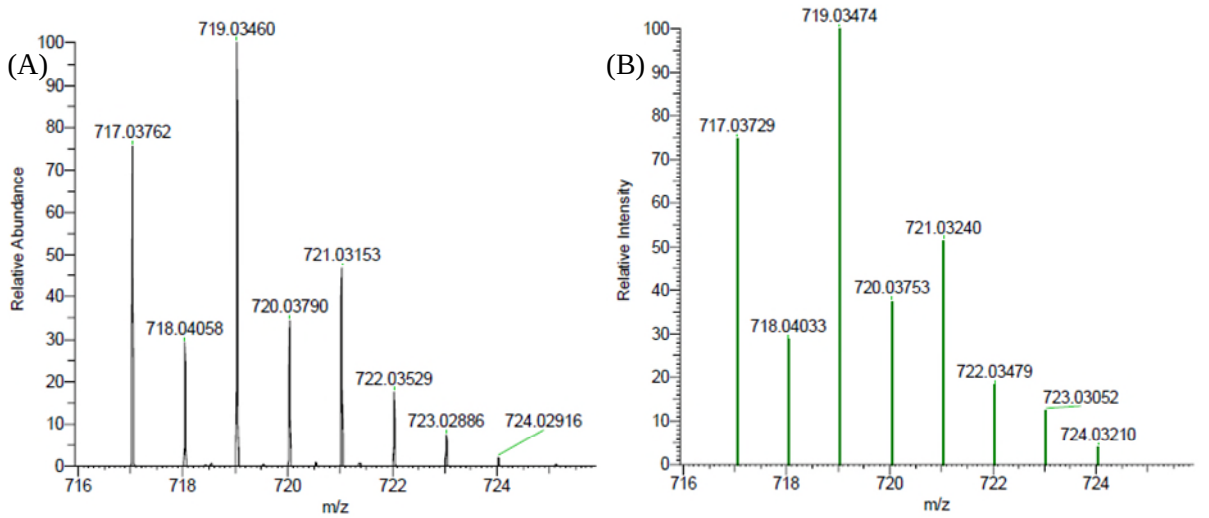

Figure S62. (A) HRMS spectrum of **1a**. (B) Theoretical spectrum of **1a**.

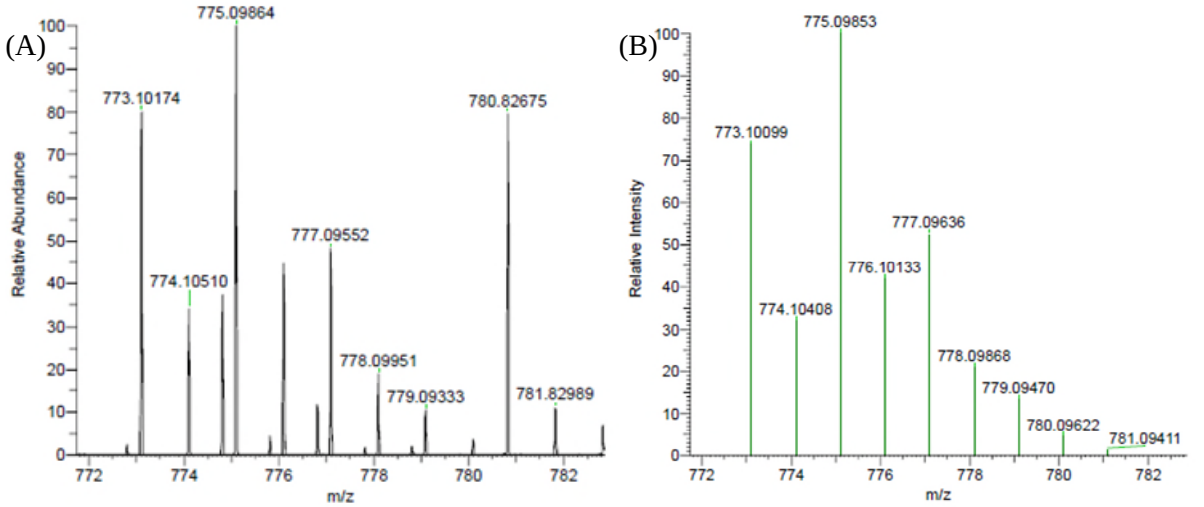

Figure S63. (A) HRMS spectrum of **1b**. (B) Theoretical spectrum of **1b**.

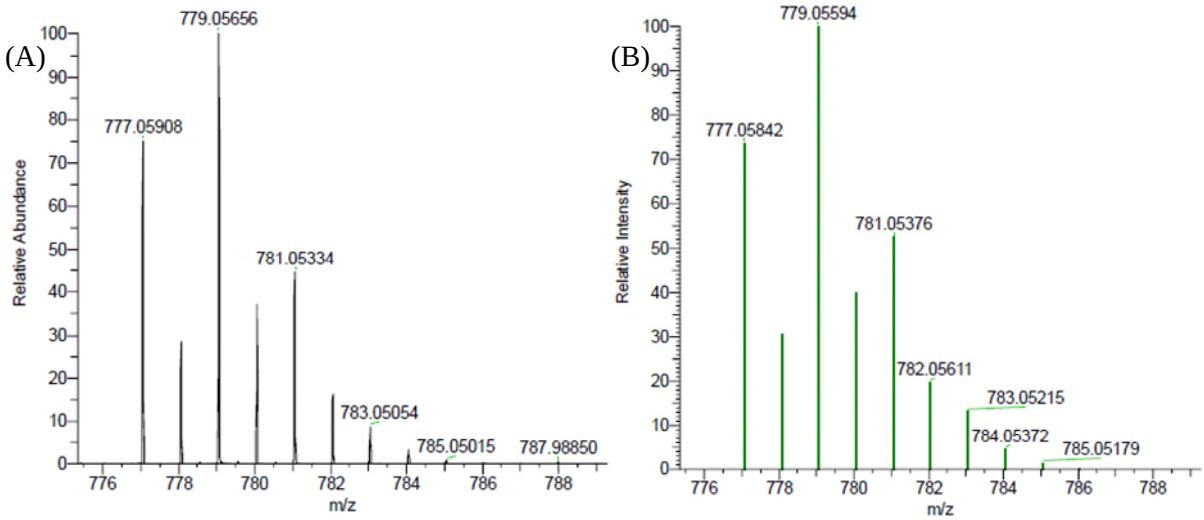

Figure S64. (A) HRMS spectrum of **1c**. (B) Theoretical spectrum of **1c**.

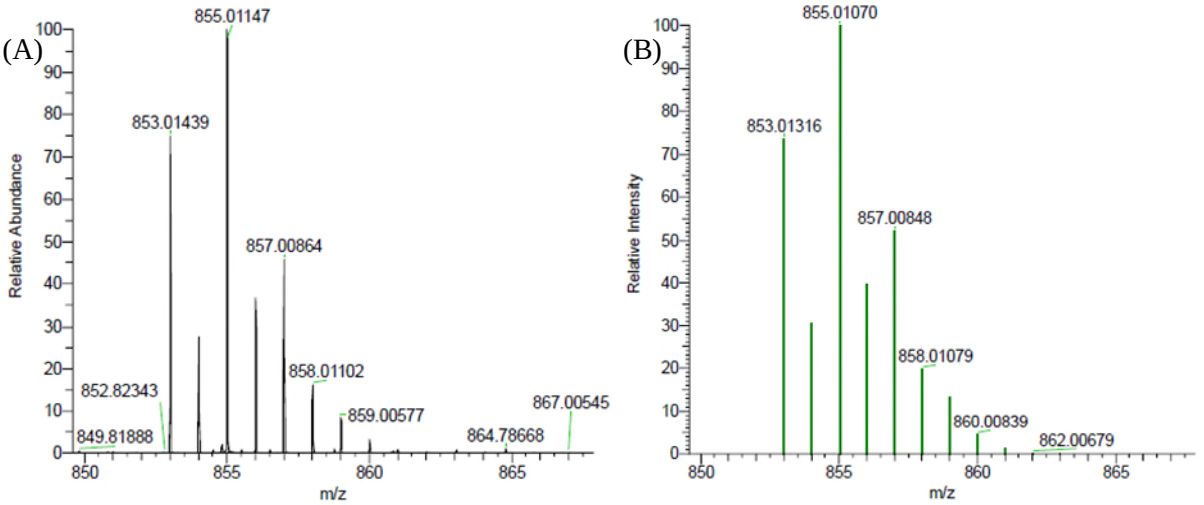

Figure S65. (A) HRMS spectrum of **1d**. (B) Theoretical spectrum of **1d**.

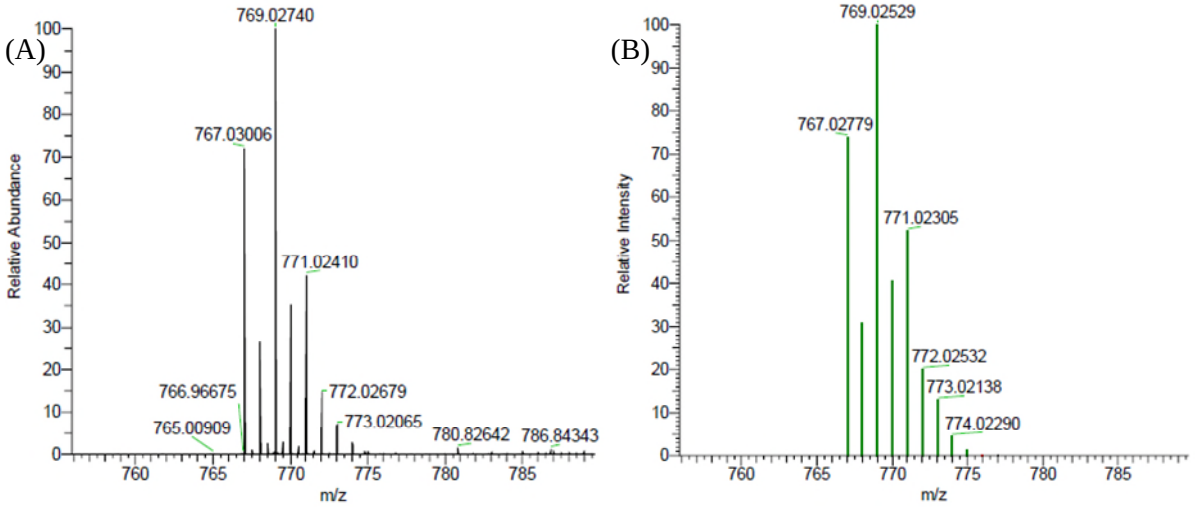

Figure S66. (A) HRMS spectrum of **1e**. (B) Theoretical spectrum of **1e**.

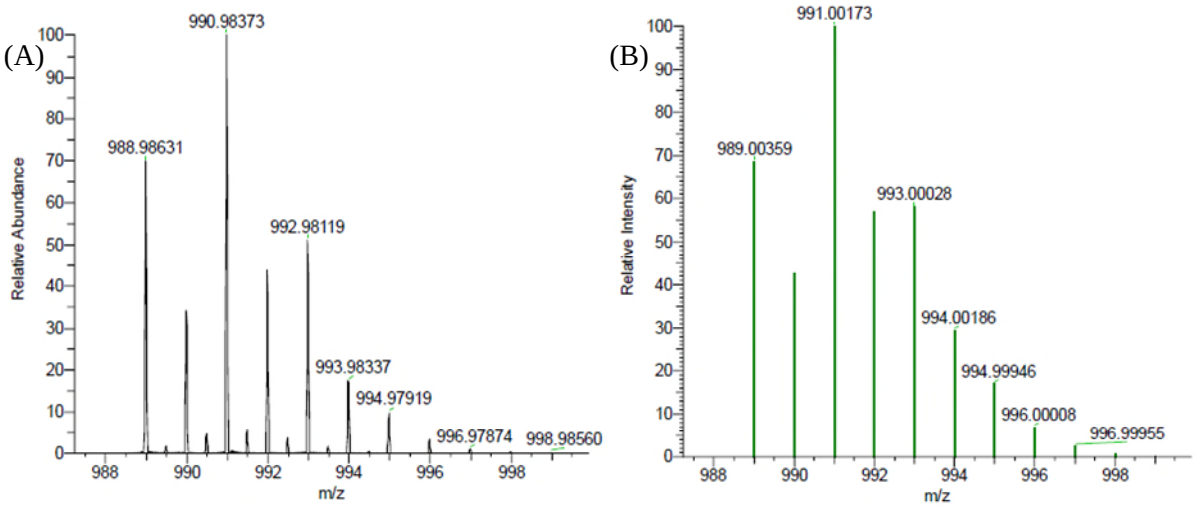

Figure S67. (A) HRMS spectrum of **1f**. (B) Theoretical spectrum of **1f**.

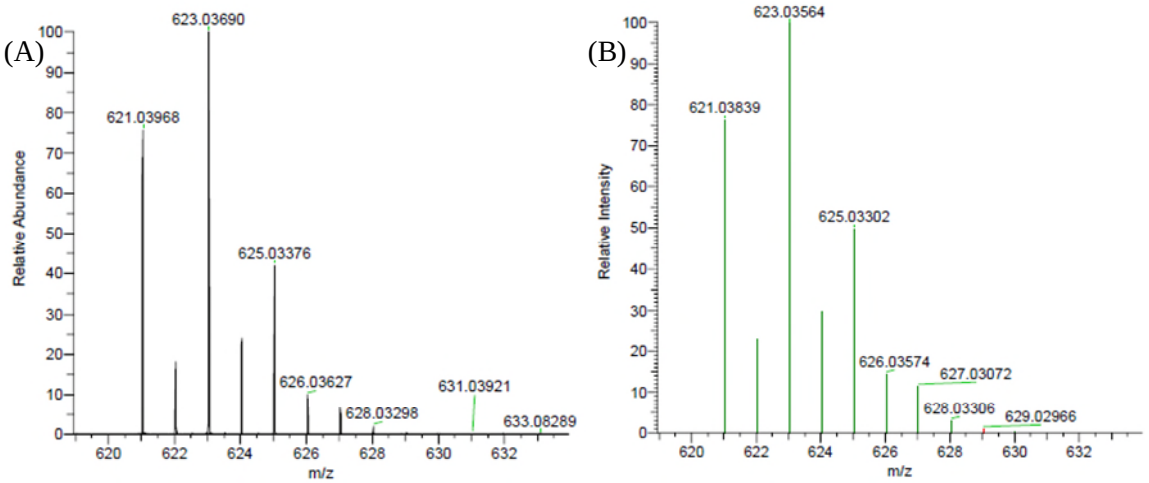

Figure S68. (A) HRMS spectrum of **1g**. (B) Theoretical spectrum of **1g**.

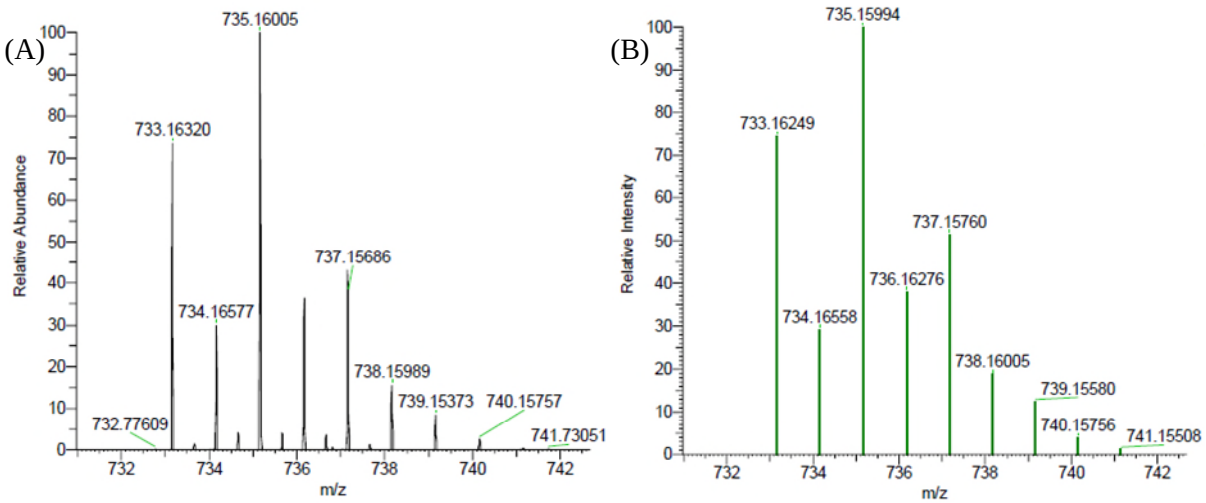

Figure S69. (A) HRMS spectrum of **1h**. (B) Theoretical spectrum of **1h**.

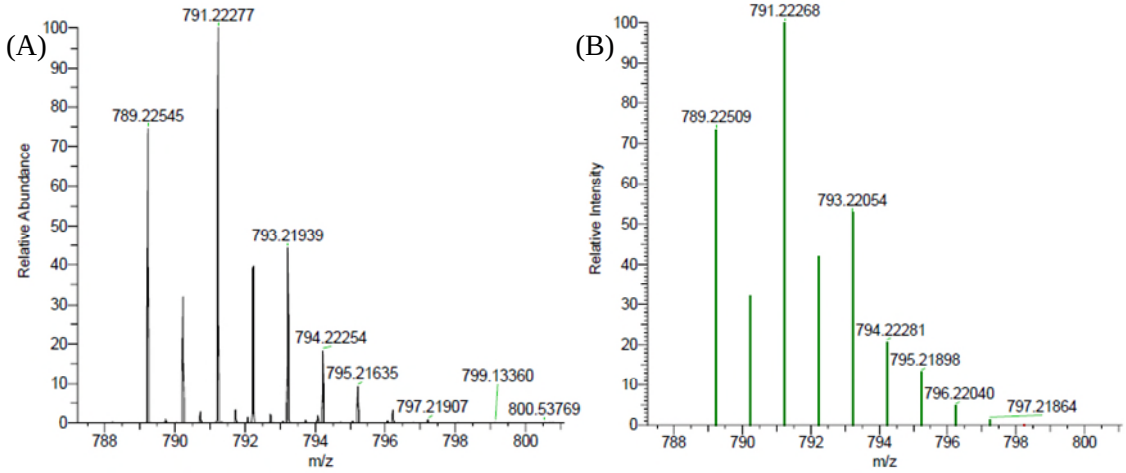

Figure S70. (A) HRMS spectrum of **1i**. (B) Theoretical spectrum of **1i**.

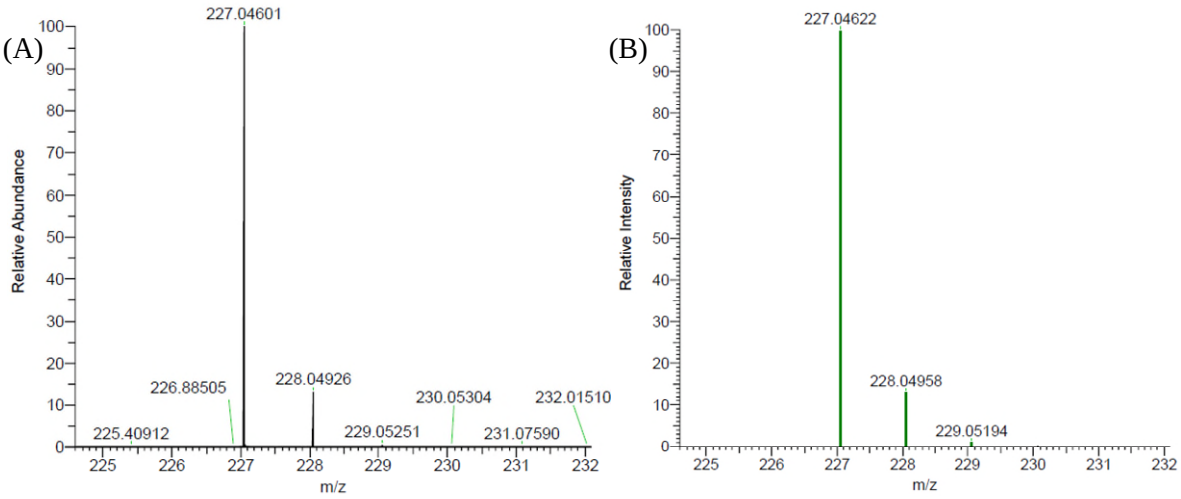

Figure S71. (A) HRMS spectrum of **6e.** (B) Theoretical spectrum of **6e**.

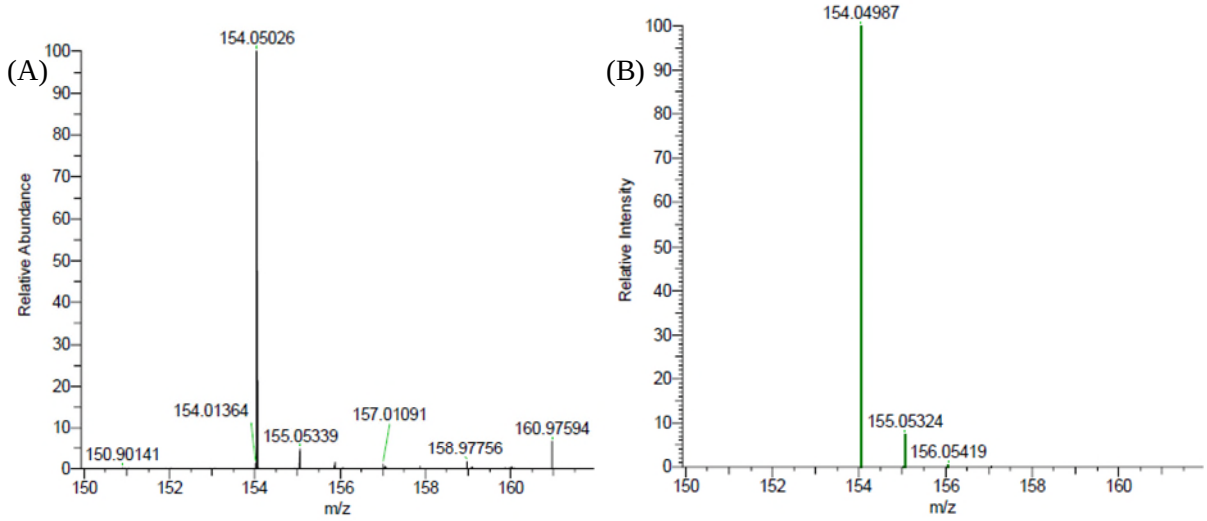

Figure S72. (A) HRMS spectrum of **6g.** (B) Theoretical spectrum of **6g**.

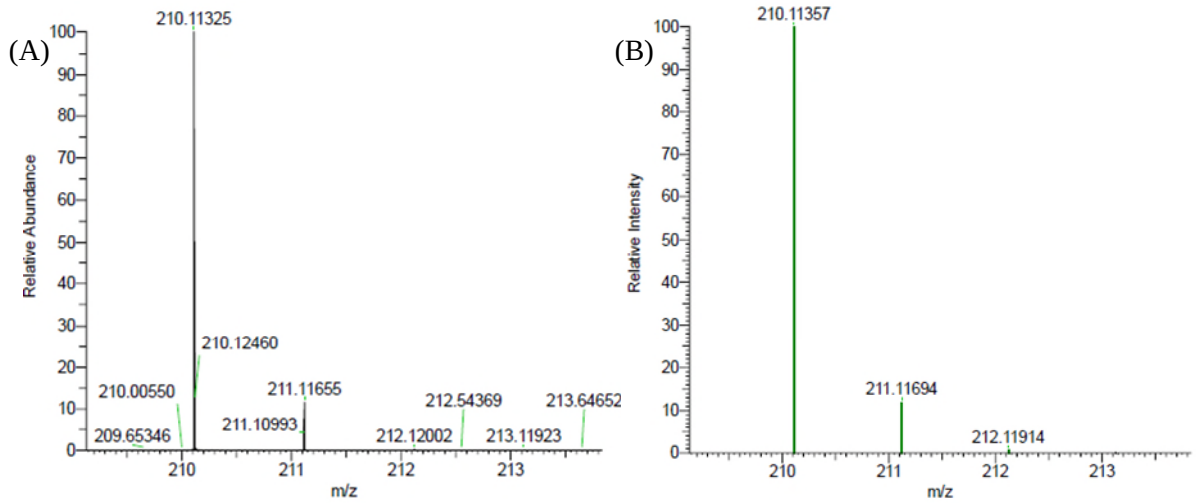

Figure S73. (A) HRMS spectrum of **6h.** (B) Theoretical spectrum of **6h**.

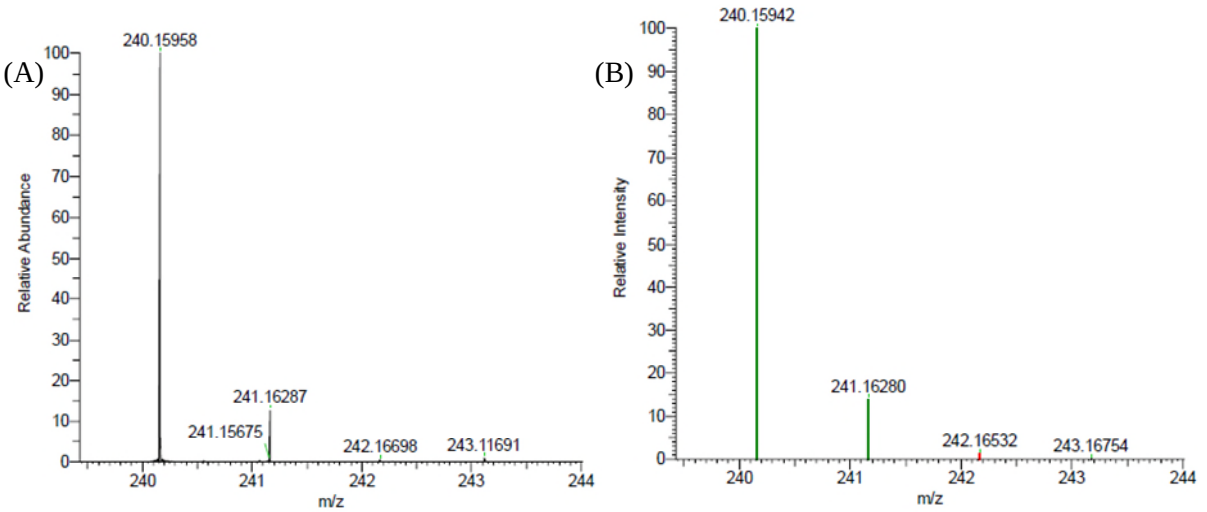

Figure S74. (A) HRMS spectrum of **6i.** (B) Theoretical spectrum of **6i**.

3 Photo-switching experiments using high powered LEDs.

Photo-irradiation of liquid samples was carried out using Thorlabs high-power mounted LEDs (models M625L4 and M455L4) in in-house custom built set-ups using optical components supplied by Thorlabs (see Fig S75).

For irradiating small vials of samples, NMR tubes and cuvettes, a Thorlabs cuvette holder (CVH100/M) equipped with mounted LEDs was used. Mirrors opposite to the LED was used to increase the intensity in the sample compartment. A 1A current was supplied to the LED, controlled by a Thorlabs T-Cube LED Driver (LEDD1B). Samples were irradiated for sufficient time to reach the photo-stationary state, as confirmed by NMR or UV-vis experiments. *In-situ* anion transport experiments were conducted on similar apparatus with a larger sample chamber, sufficient to accommodate a 17 mm vial, with perpendicular mounting of an ion selective electrode (ISE). The entire set-up was mounted on a magnetic stirrer to facilitate gentle stirring of the sample (Fig S76)

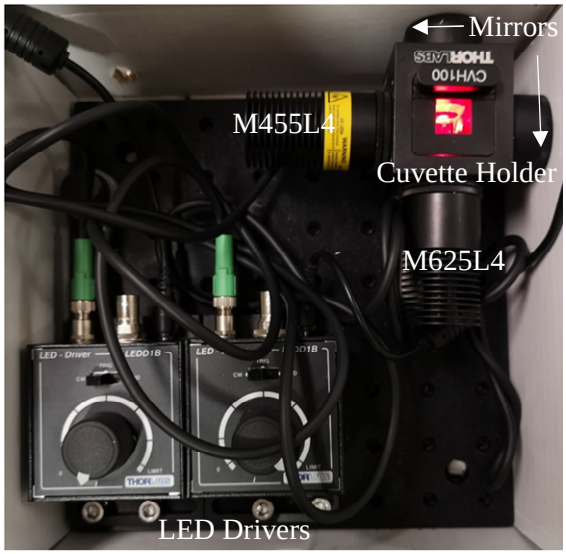

Figure S75. Apparatus for photo-irradiating small liquid samples

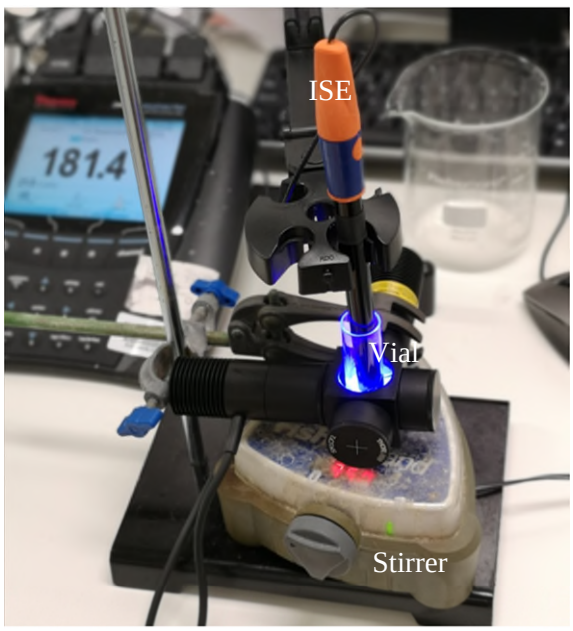

Figure S76. (B) Apparatus for photo-triggered ion transport experiments

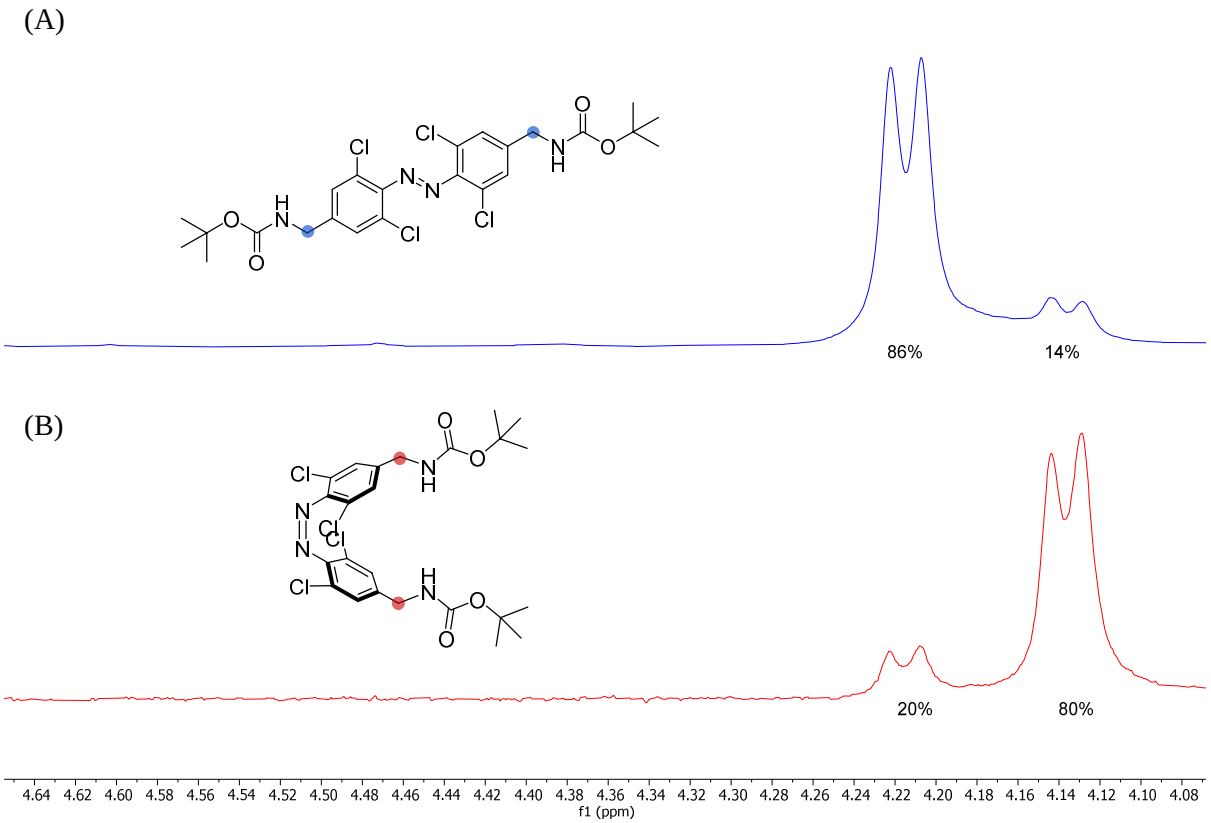

Figure S77. Photostationary states for (A) ***E*-4** (B) ***Z*-4** (^{1}H NMR spectra in d_6-DMSO)

Compound **4** PSS contained 80% *Z* isomer, all squaramide derivatives the PSS contained 77% *Z* isomer, by ^{1}H NMR integration.

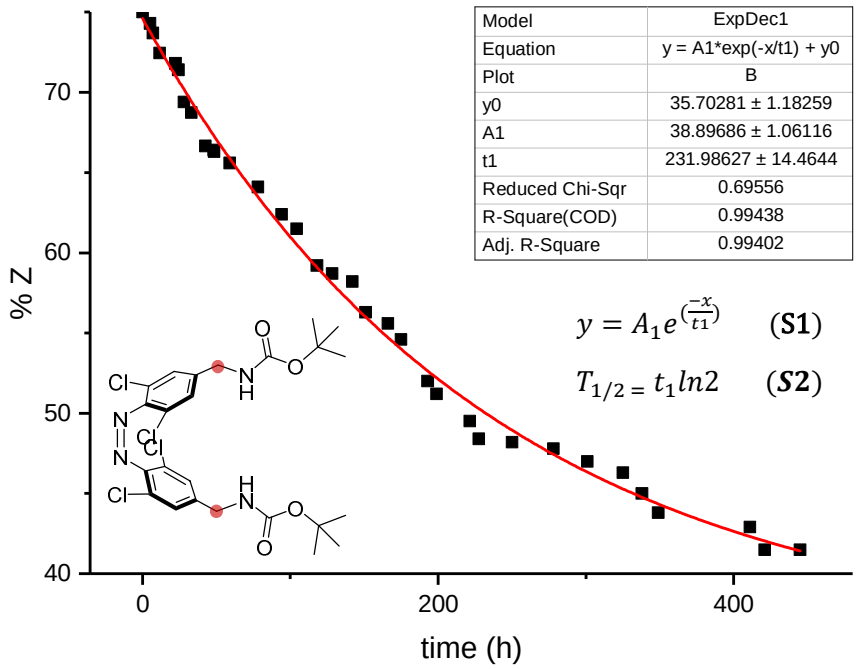

Model	ExpDec1
Equation	y = A1*exp(-x/t1) + y0
Plot	B
y0	35.70281 ± 1.18259
A1	38.89686 ± 1.06116
t1	231.98627 ± 14.4644
Reduced Chi-Sqr	0.69556
R-Square(COD)	0.99438
Adj. R-Square	0.99402

Figure S78. Lifetime plot of ***Z*-4** based on ^{1}H NMR integration of benzylic protons over time at room temperature in d_6-DMSO. Data was fitted using Origin Pro using an exponential decay model to determine t_1 (Equation S1). Half-life ($t_{1/2}$) was determined using Equation S2.

4 UV-Visible absorption spectra.

All UV-vis spectra were determined in DMSO solution. Extinction coefficients were determined by recording a UV-vis spectra for the *E* isomer at 10, 20, 30, 40 μM in DMSO respectively. The absorbance at the maximum of the π - π* transition of the *E*-isomers was plotted against concentration (Beer-Lambert plot) to determine the molar extinction coefficient ε. For each compound, the *E* isomer sample at 40 μM was irradiated with red light to generate the photostationary state, and another spectrum was run. This spectrum was normalised to units of ε and overlaid with the dark (100% *E* isomer) spectrum.

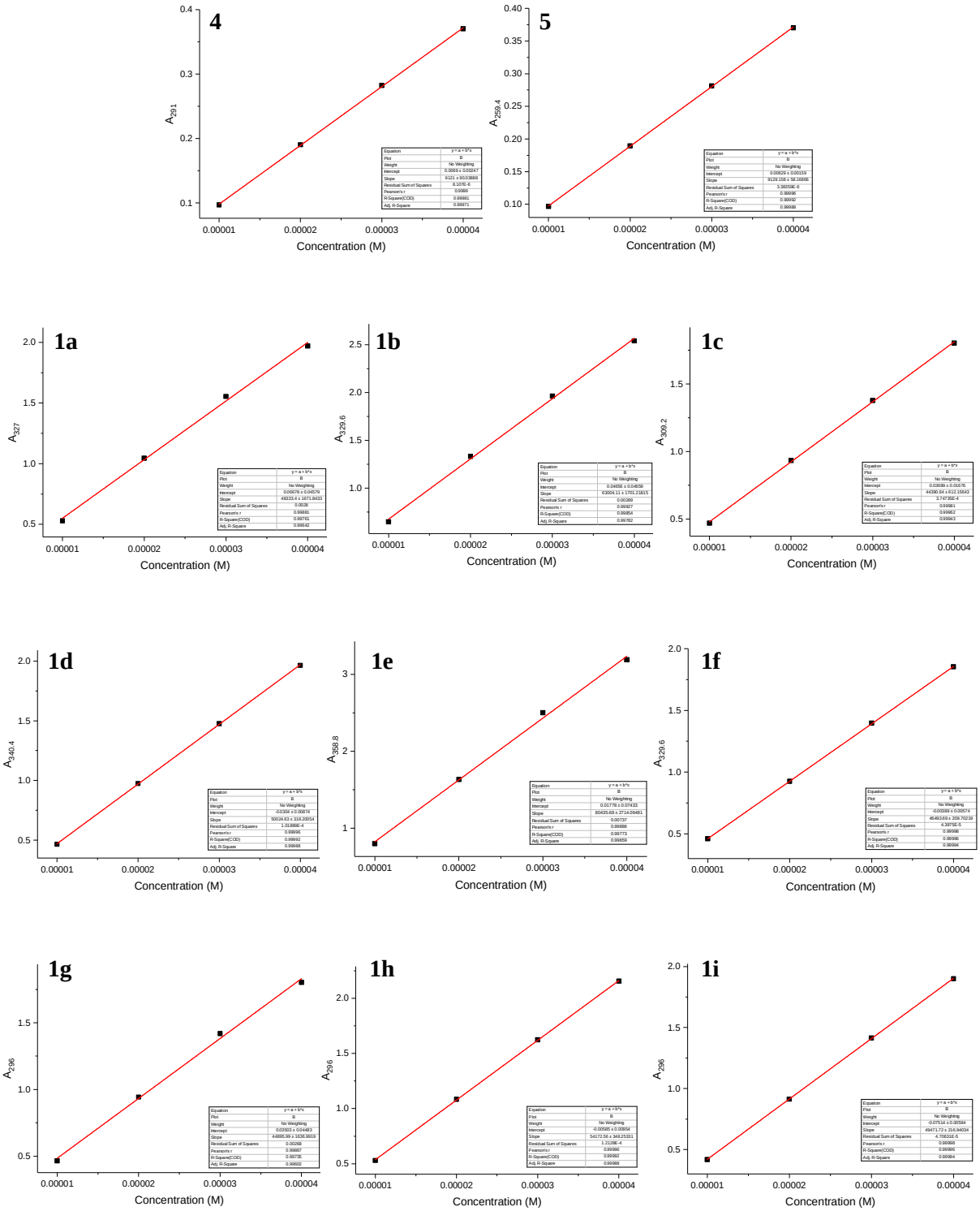

Figure S79. Beer-Lambert plots for azobenzene derivatives **4, 5, 1a-i**

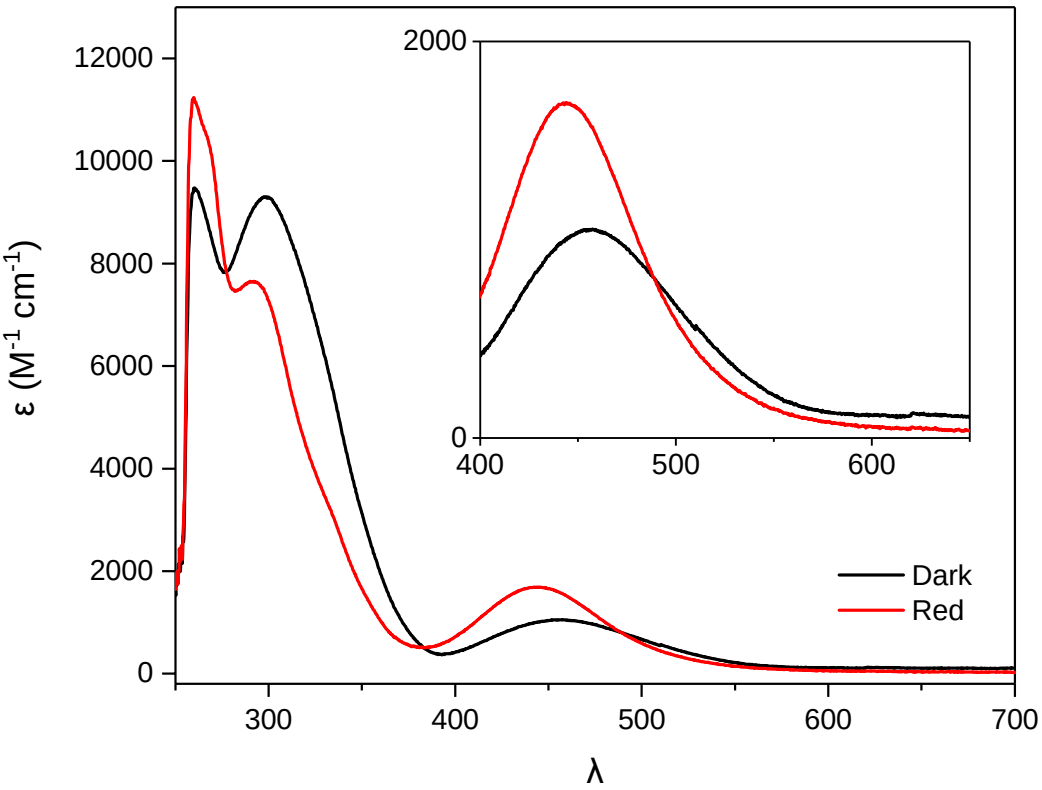

Figure S80. Spectrum of **4** in the dark (100% trans) and red (80% cis) state.

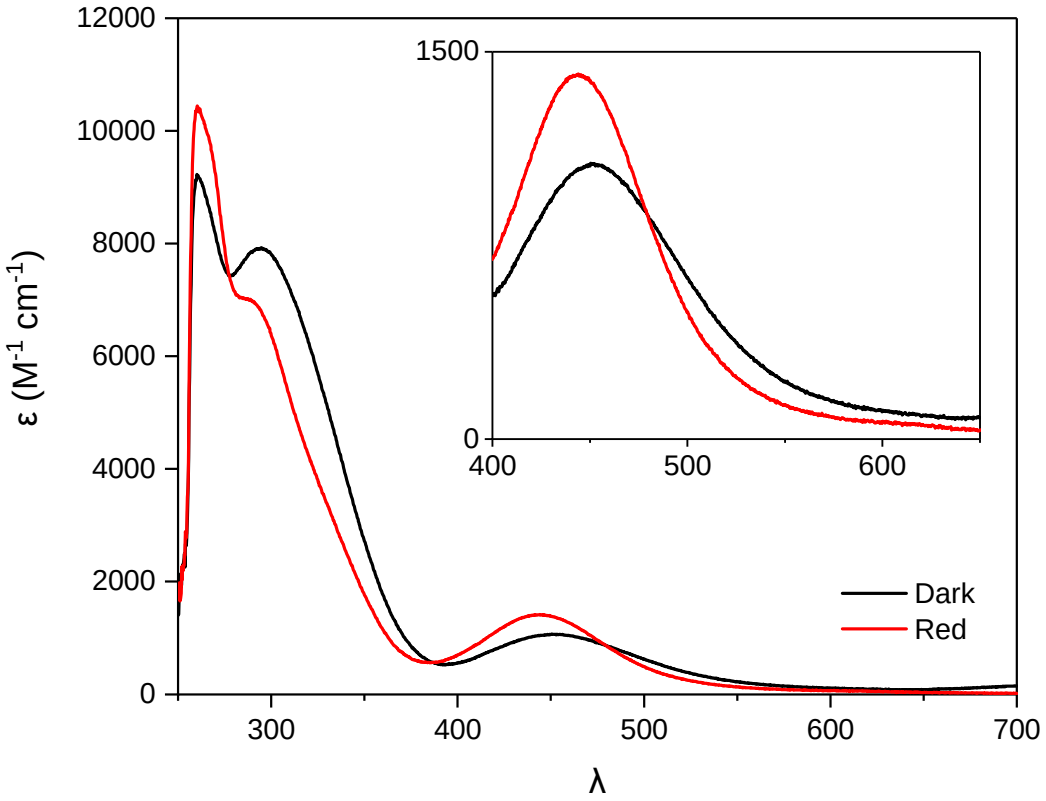

Figure S81. Spectrum of **5** in the dark (100% trans) and red (80% cis) state.

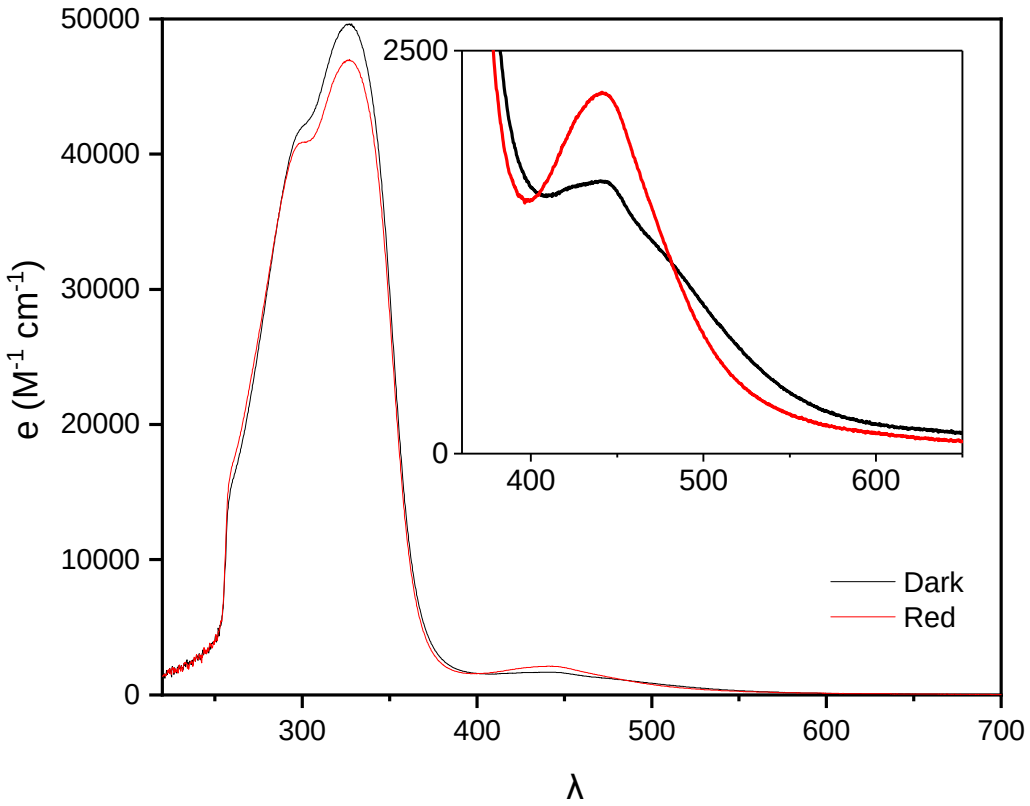

Figure S82. Spectrum of **1a** in the dark (100% trans) and red (77% cis) state.

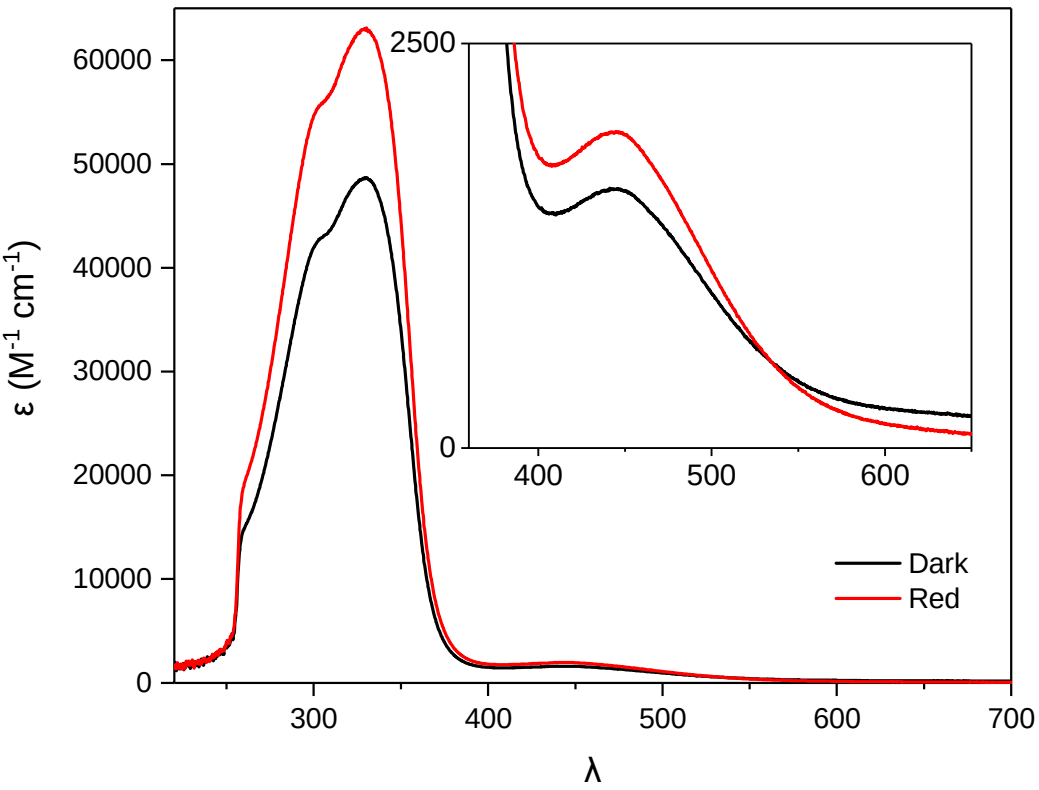

Figure S83. Spectrum of **1b** in the dark (100% trans) and red (77% cis) state.

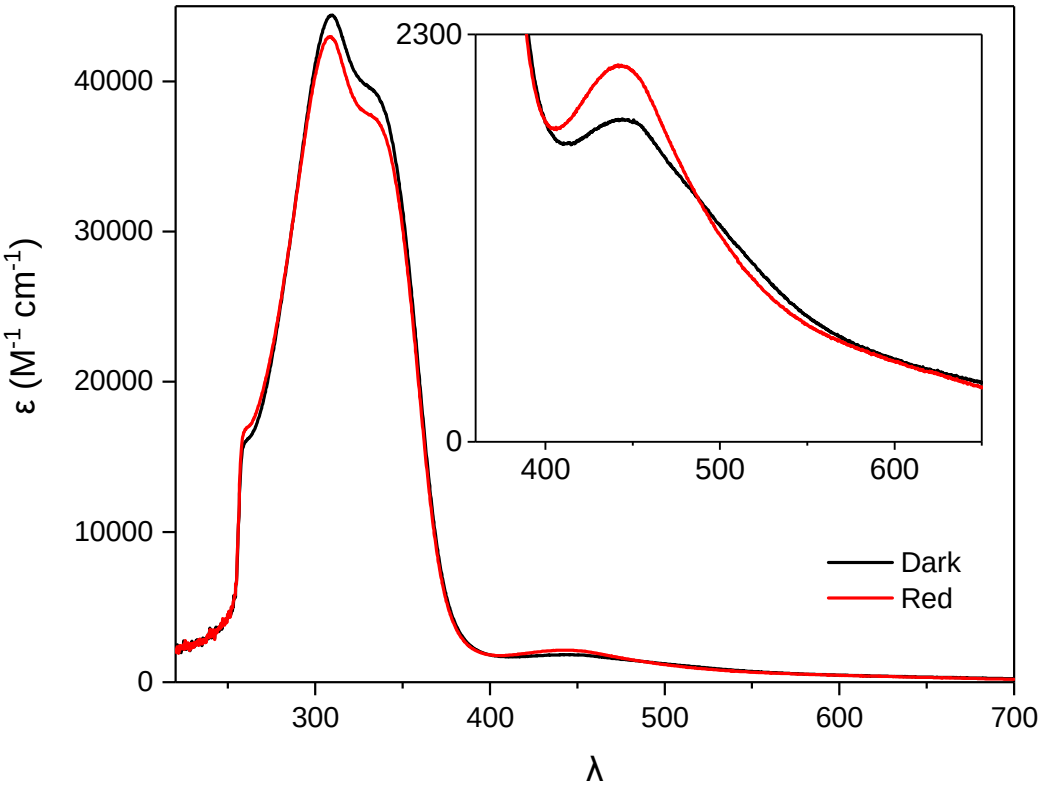

Figure S84. Spectrum of **1c** in the dark (100% trans) and red (77% cis) state.

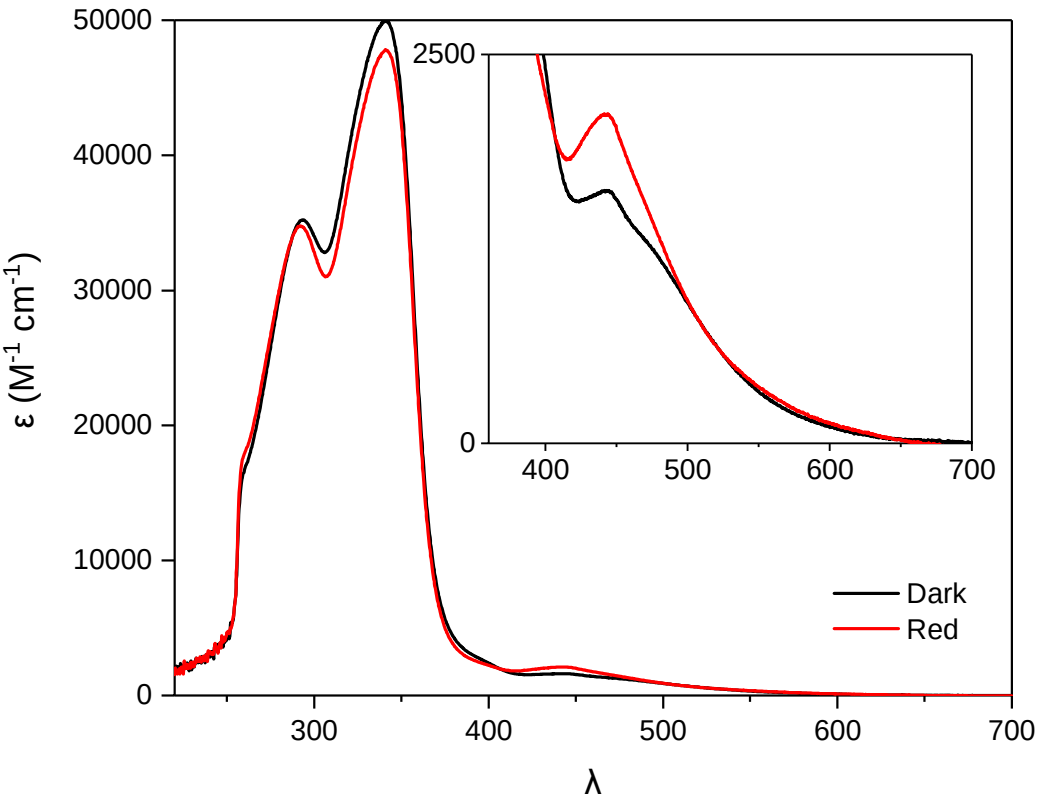

Figure S85. Spectrum of **1d** in the dark (100% trans) and red (77% cis) state.

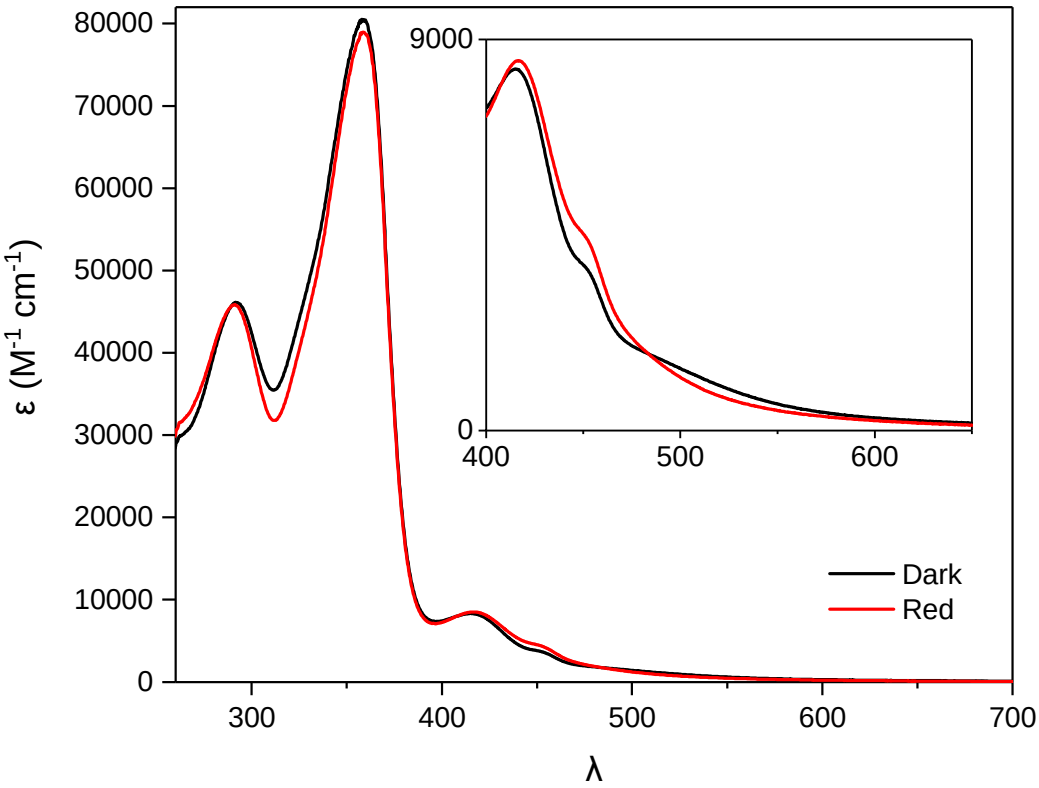

Figure S86. Spectrum of **1e** in the dark (100% trans) and red (77% cis) state.

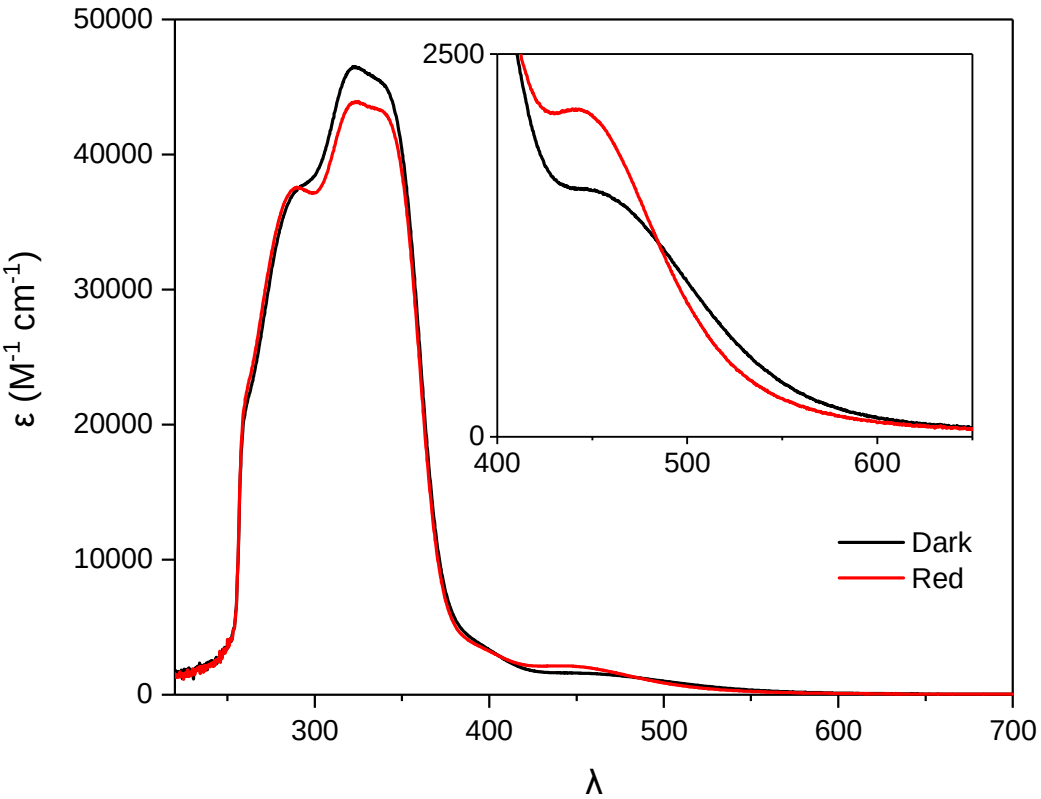

Figure S87. Spectrum of **1f** in the dark (100% trans) and red (77% cis) state.

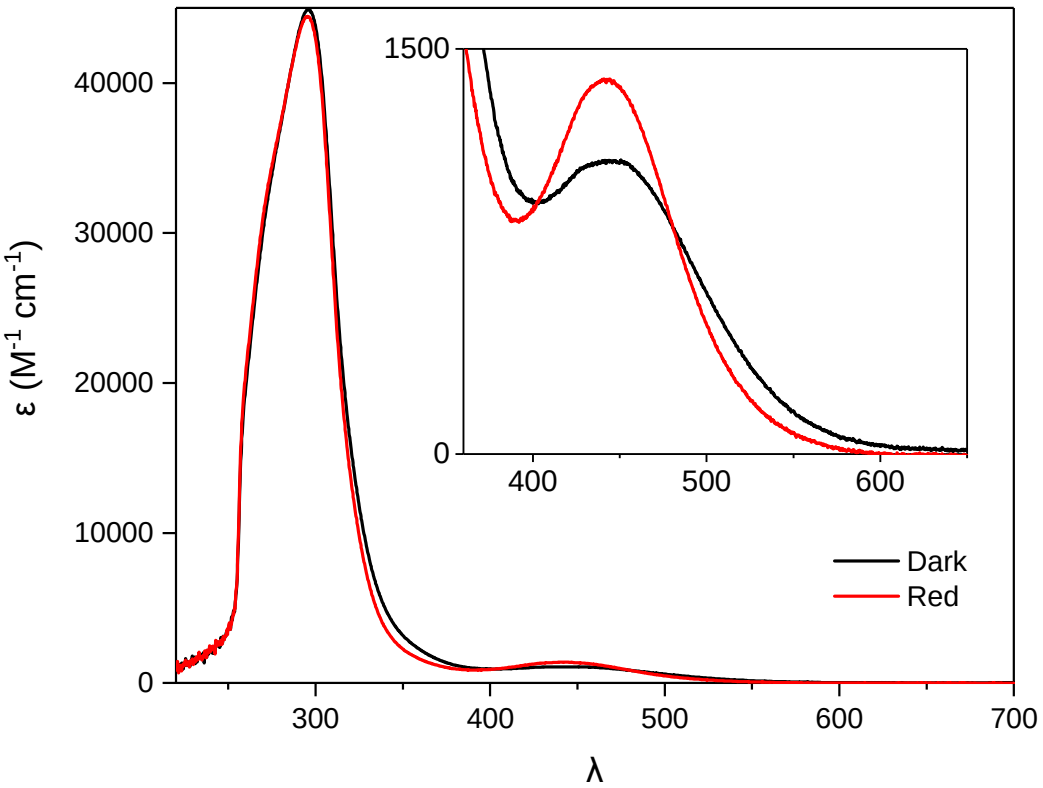

Figure S88. Spectrum of **1g** in the dark (100% trans) and red (77% cis) state.

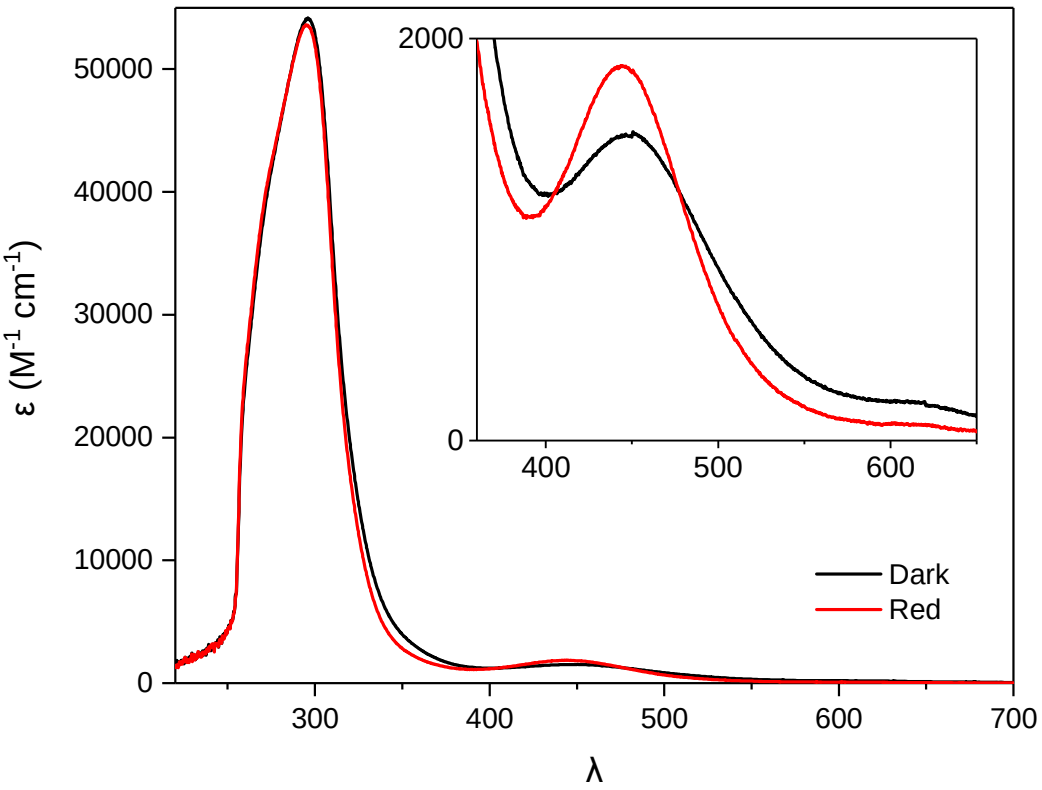

Figure S89. Spectrum of **1h** in the dark (100% trans) and red (77% cis) state.

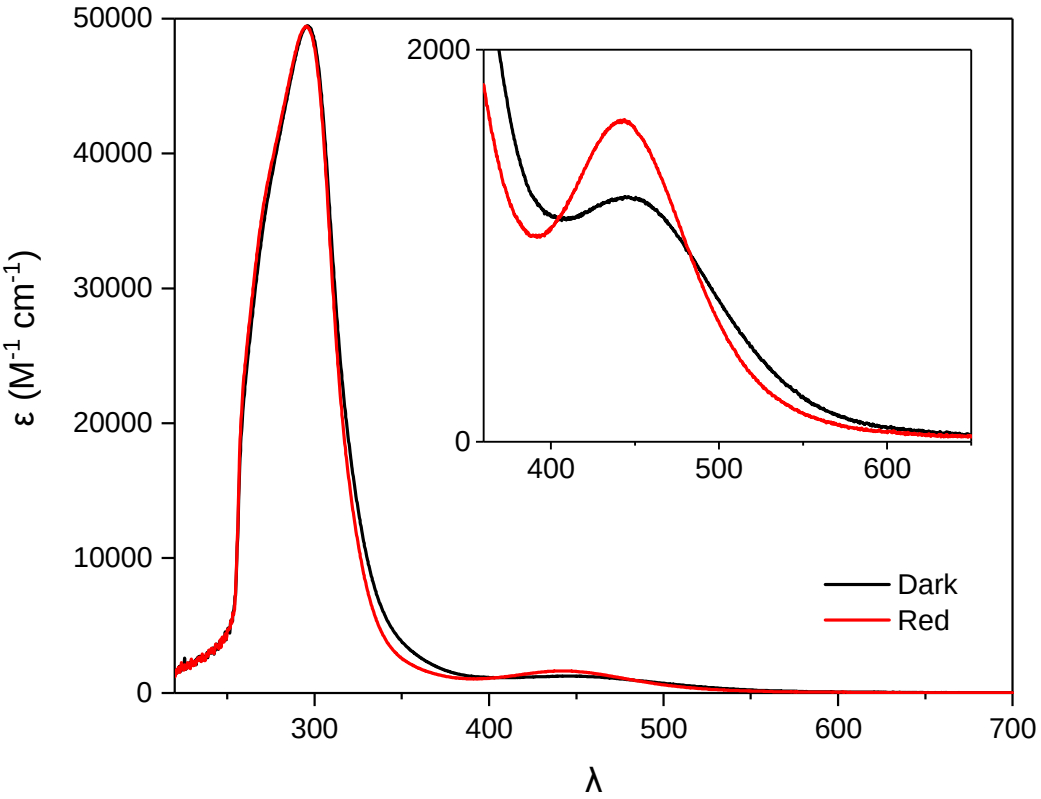

Figure S90. Spectrum of **1i** in the dark (100% trans) and red (77% cis) state.

5 NMR titration experiments

All binding constants were measured by ^{1}H NMR titrations in a Bruker AVIII 500 spectrometer at 500 MHz and 298 K. The host (squaramide azobenzene derivative) was dissolved in d_6-DMSO and added at 1 mM concentration and a known volume (0.5 mL) added to the NMR tube. Known volumes of guest (chloride, added as the TBA salt) in d_6-DMSO were added, and the spectra were recorded after each addition. The chemical shifts of the host spectra (squaramide NH, and Aryl CH protons, where resolved, see Figures S92 and S94 for representative data set for compound **1a**) were monitored as a function of guest concentration. The data was analysed using a global fit procedure for all three data sets simultaneously in the Dynafit software program,[3] using non-linear least squares analysis to obtain the best fit between observed and calculated chemical shifts, as described in further detail below. Errors were calculated as two times the standard deviation from the average value of two repeats (95% confidence limit). In all experiments the association of guest and host was fast on the NMR timescale.

***E* isomer:** Chloride binding to a dark adapted sample of **1** as the *E* isomer (>99% *E*) was determined by NMR titration analysis in d_6-DMSO as described above, fitting to a 1:1 binding model:

$$\mathbf{1}^{\boldsymbol{E}} + \mathrm{Cl}^- \overset{K_1{}^{E}{}_{\mathrm{obs}}}{\rightleftharpoons} \mathbf{1}^{\boldsymbol{E}}\cdot\mathrm{Cl}^-$$

In principle, 1:2 binding stoichiometry is possible due to the two identical squaramide receptors. However, in these titration experiments in DMSO, the overall association constants are weak ($K_1{}^{E}{}_{,\mathrm{obs}} \sim 10^2$), and binding of the second equivalent of anion was too weak to be detected, as inferred from the failure to fit the data to 1:2 binding models. This is presumably due to inter-anion repulsion in the 1:2 complex, leading to negligible association of the second anion in this competitive polar solvent. In contrast 1:1 binding models in our analysis gave excellent fits to the experimental data for all compounds studied.

The measured binding constant $K_1{}^{E}{}_{,\mathrm{obs},}$ is related to the actual binding constant for chloride binding to one squaramide motif, $K_1{}^{E}$, by the relation Equation S3, which accounts for the statistical factors.[4]

$$K_1{}^{E}{}_{\mathrm{obs}} = 2K_1{}^{E} \quad \textbf{(S3)}$$

Note, for a membrane embedded transporter with one binding site at the interface, the two anion binding sites are not identical (contrary to their form in bulk DMSO solution), and only one squaramide is likely to be available at the membrane interface to bind the incoming anion. It is therefore more appropriate to compare the statistically corrected $K_1{}^{E}$ value (= $K_1{}^{E}{}_{\mathrm{obs}}$ / 2) with observed $EC_{50}{}^{Z,PSS}$ values, rather than $K_1{}^{E}{}_{\mathrm{obs}}$ which assumes binding to either site is equally likely.

***Z* isomer:** A 1 mM sample of **1** in d_6-DMSO was irradiated with red light until the PSS was reached (77:23 *Z*:*E*, by ^{1}H NMR integration), before the titration experiment was conducted as described above. The PSS ratio was maintained throughout the titration for all derivatives. The binding constant for $\mathbf{1}^{\mathbf{Z}}$ derivatives to chloride were obtained by fitting the data, using a global fit procedure, to the following equilibria where $2K_1{}^{E}$ is fixed, and obtained from the previous titration with the *E* isomer.

$$\mathbf{1}^{\boldsymbol{E}} + \mathrm{Cl}^- \overset{2K_1{}^{E}}{\rightleftharpoons} \mathbf{1}^{\boldsymbol{E}}\cdot\mathrm{Cl}^-$$

$$\mathbf{1}^{\boldsymbol{Z}} + \mathrm{Cl}^- \overset{K_1{}^{Z}}{\rightleftharpoons} \mathbf{1}^{\boldsymbol{Z}}\cdot\mathrm{Cl}^-$$

$[\mathbf{1}^{\mathbf{E}}] + [\mathbf{1}^{\mathbf{Z}}] = 1$ mM; $[\mathbf{1}^{\mathbf{Z}}] = 0.77$ mM; $[\mathbf{1}^{\mathbf{E}}] = 0.23$ mM

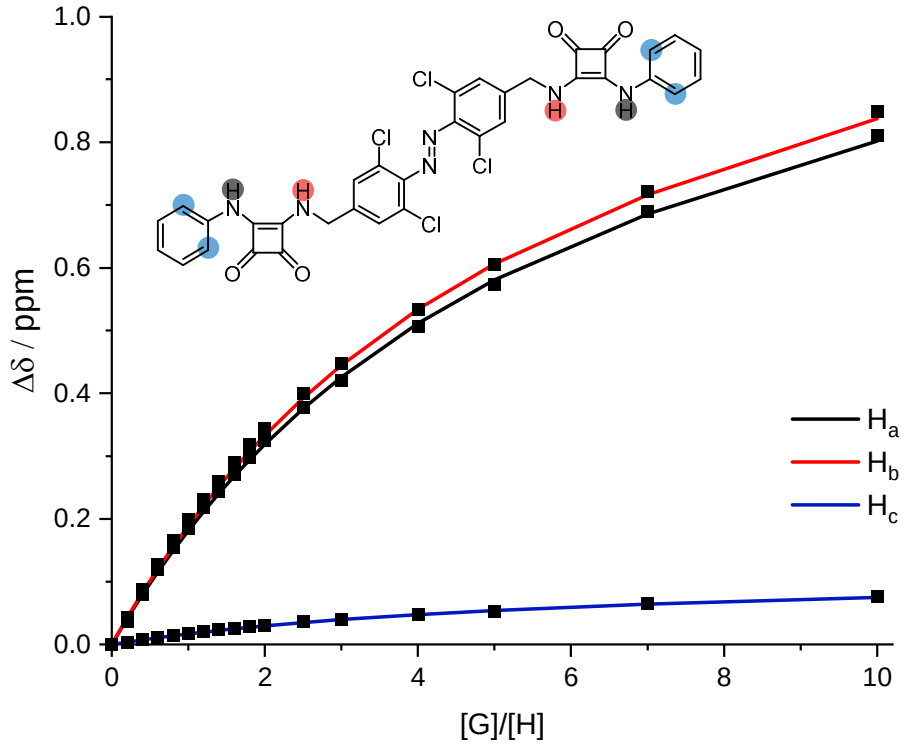

Figure S91. Plots of chemical shift changes of ***E*-1a** upon addition of TBACl. Shifts are normalised by subtraction to give an initial shift of 0.

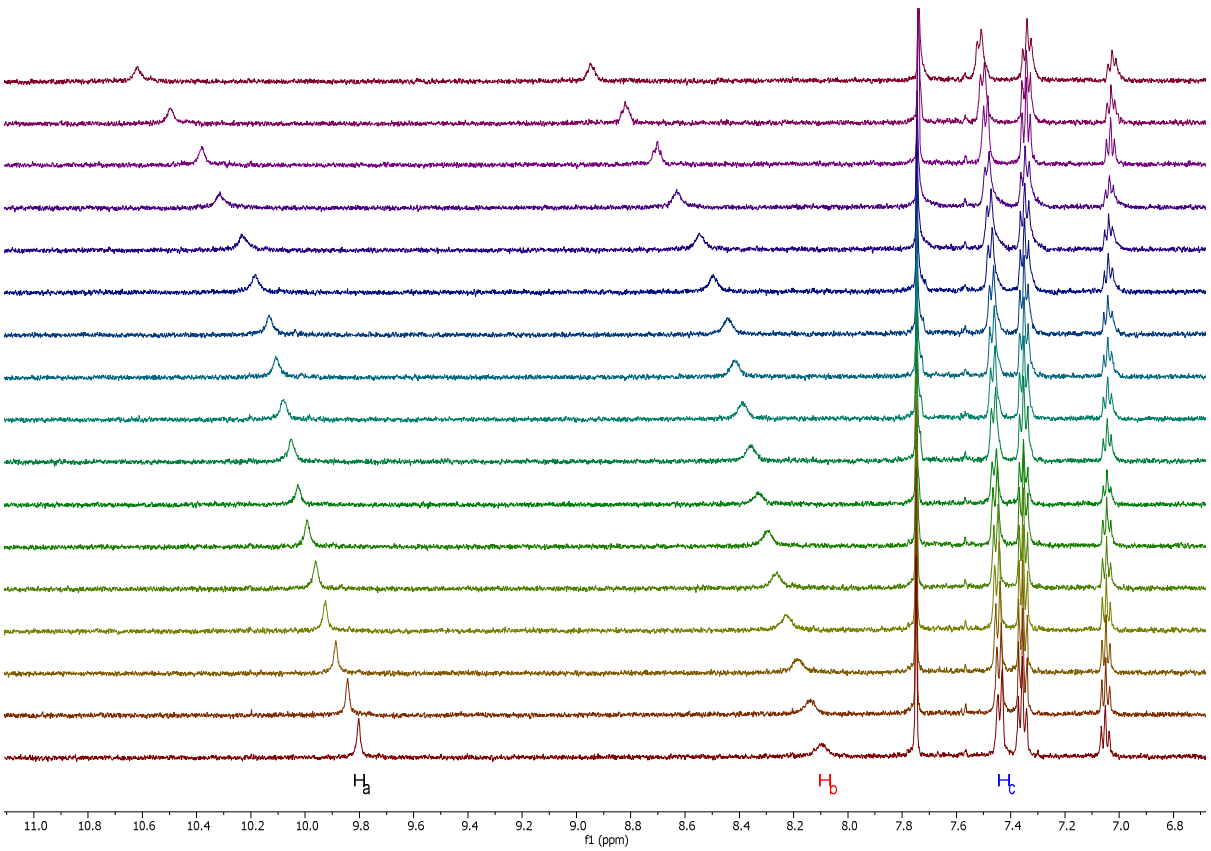

Figure S92. Stacked partial ^{1}H NMR spectra of ***E*-1a** with increasing equivalents of TBACl

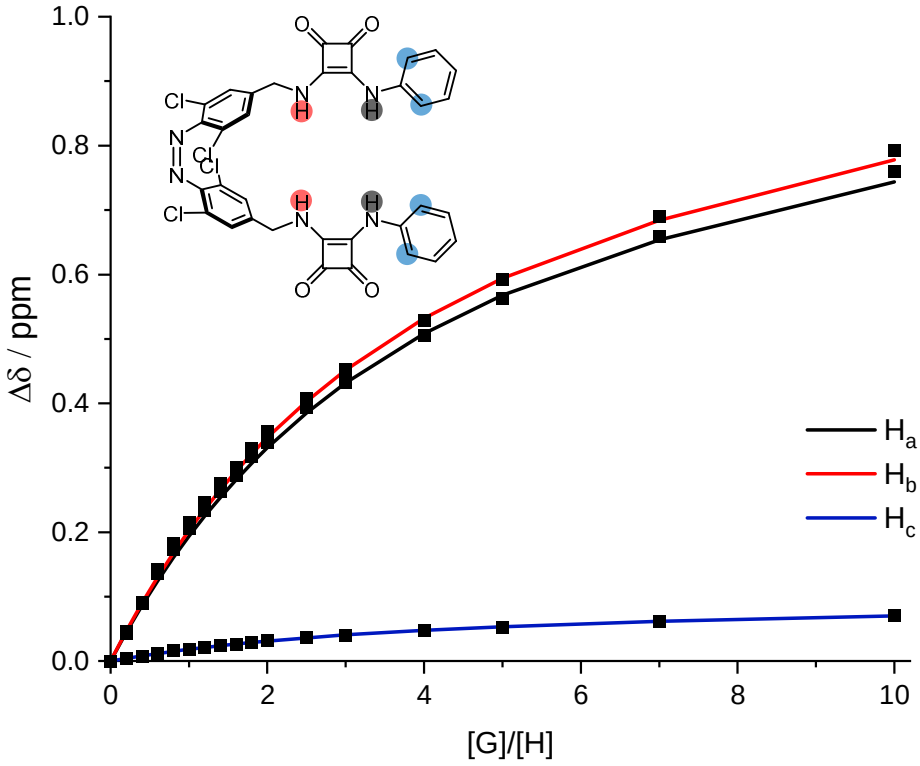

Figure S93. Plots of chemical shift changes of ***Z*-1a** upon addition of TBACl

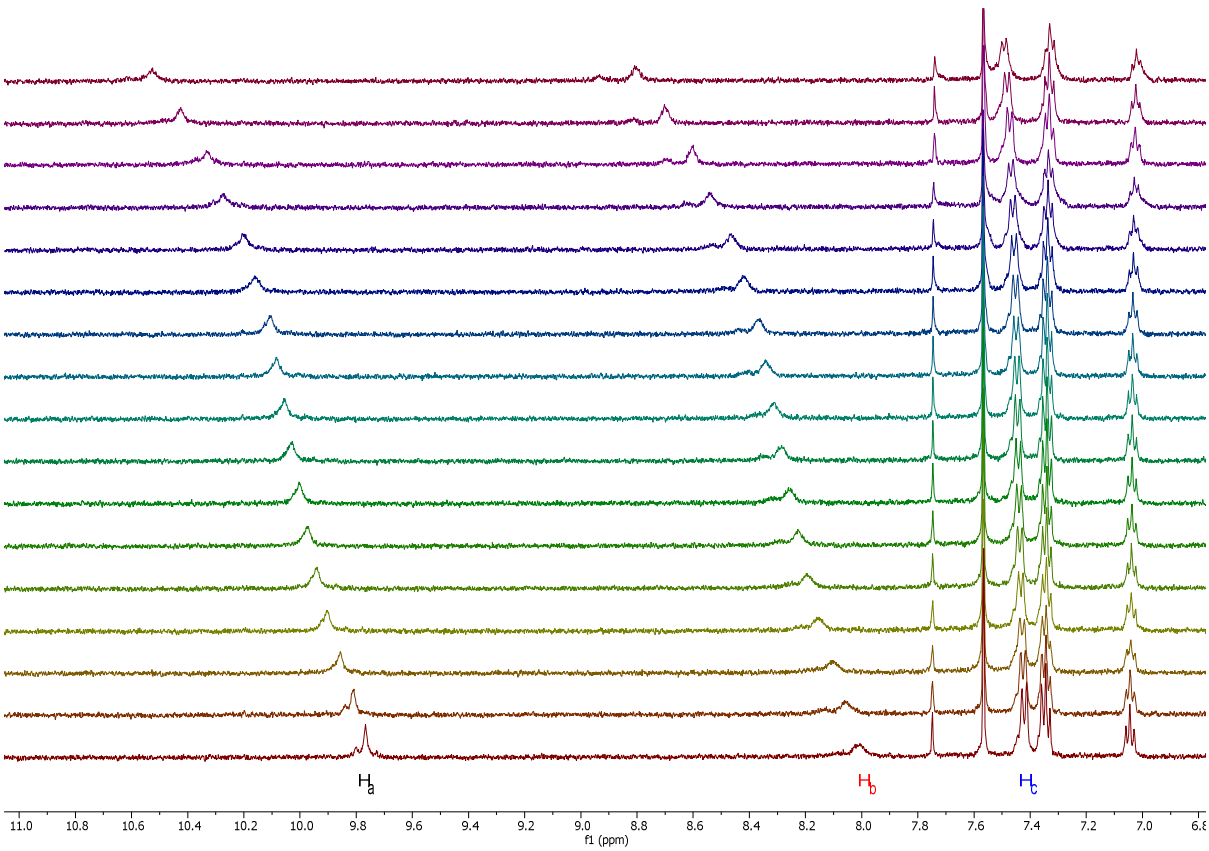

Figure S94. Stacked partial ^{1}H NMR spectra of ***Z*-1a** with increasing equivalents of TBACl

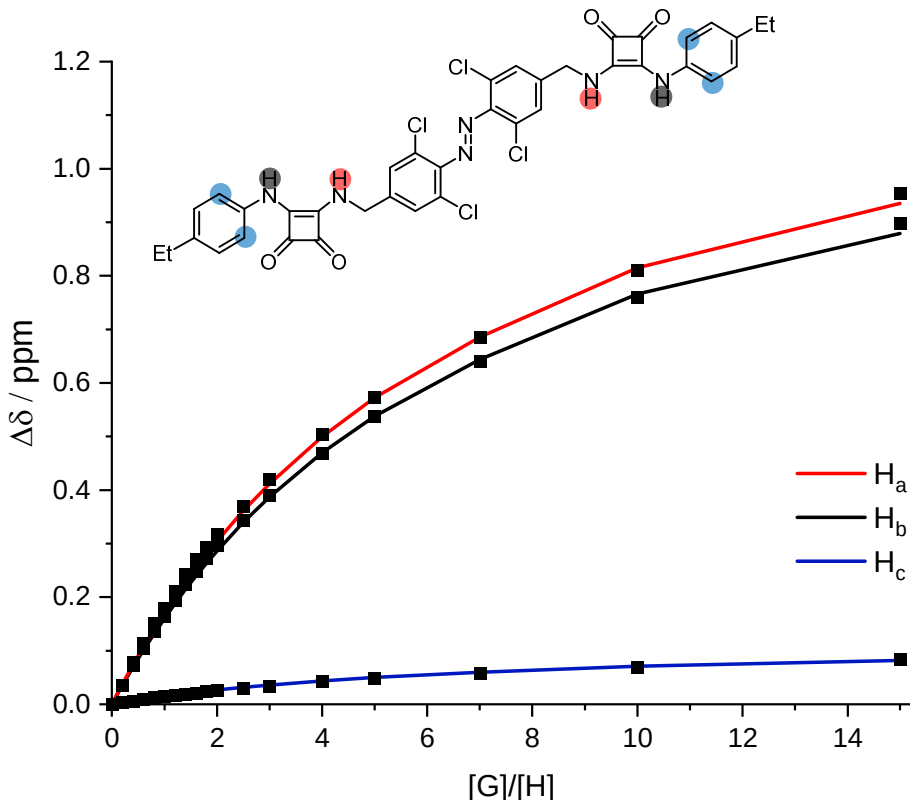

Figure S95. Plots of chemical shift changes of ***E*-1b** upon addition of TBACl

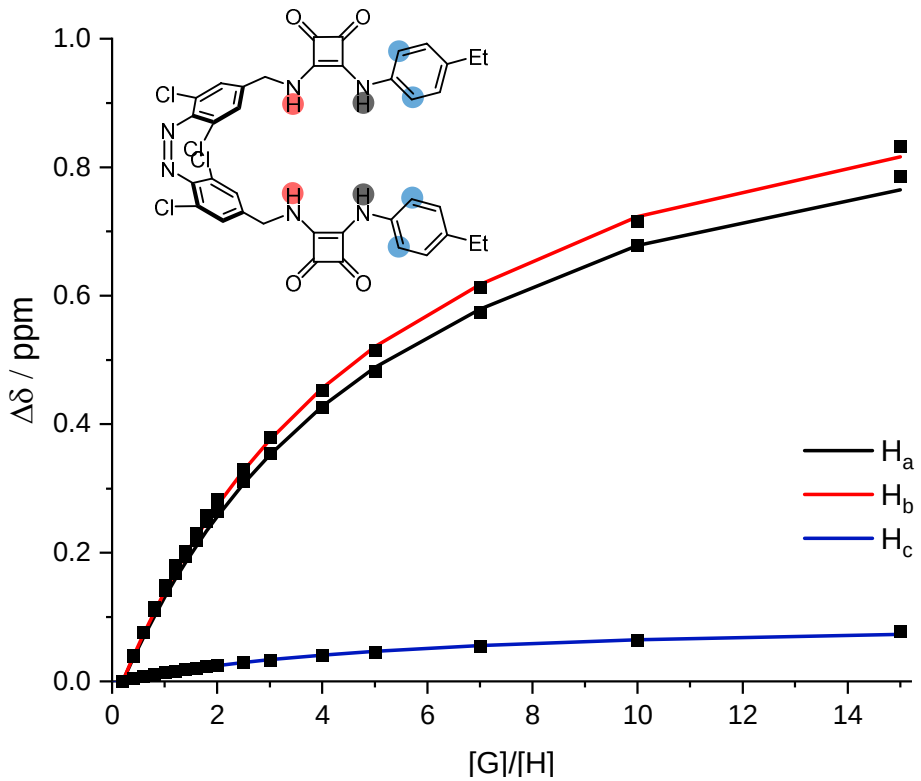

Figure S96. Plots of chemical shift changes of ***Z*-1b** upon addition of TBACl

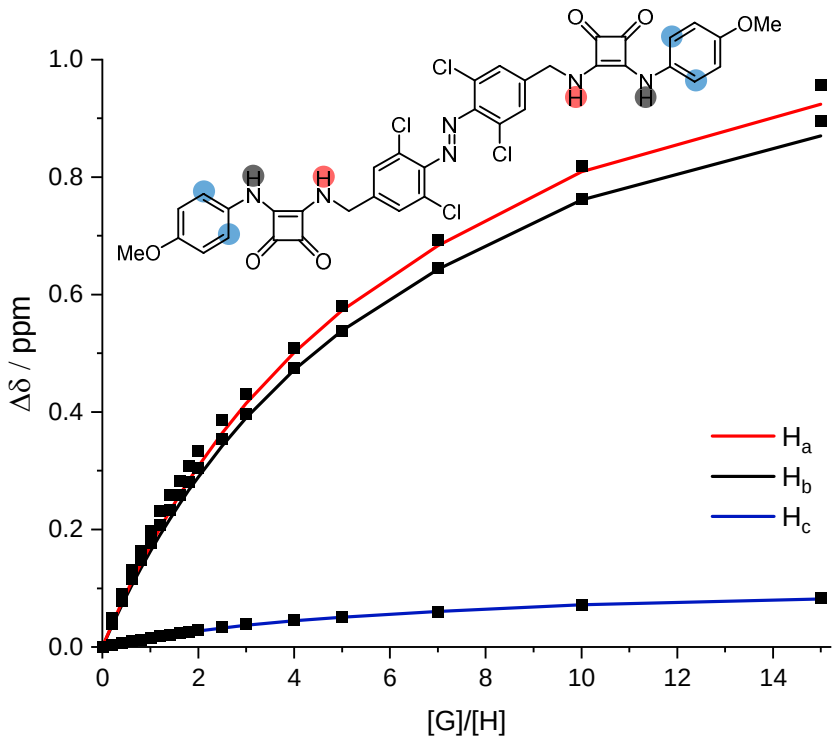

Figure S97. Plots of chemical shift changes of ***E*-1c** upon addition of TBACl

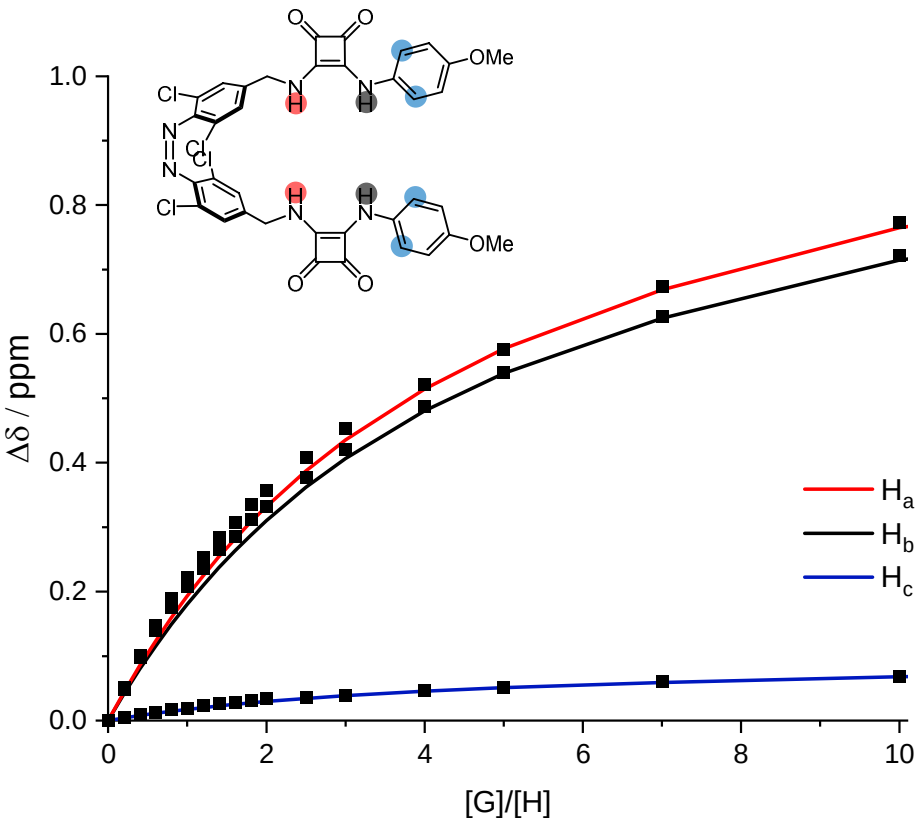

Figure S98. Plots of chemical shift changes of ***Z*-1c** upon addition of TBACl

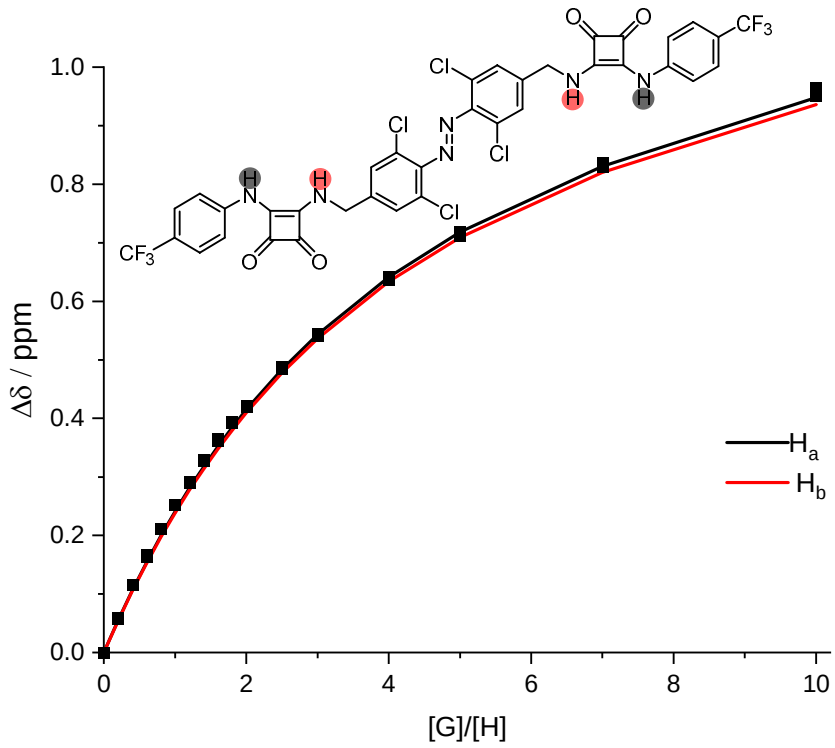

Figure S99. Plots of chemical shift changes of ***E*-1d** upon addition of TBACl

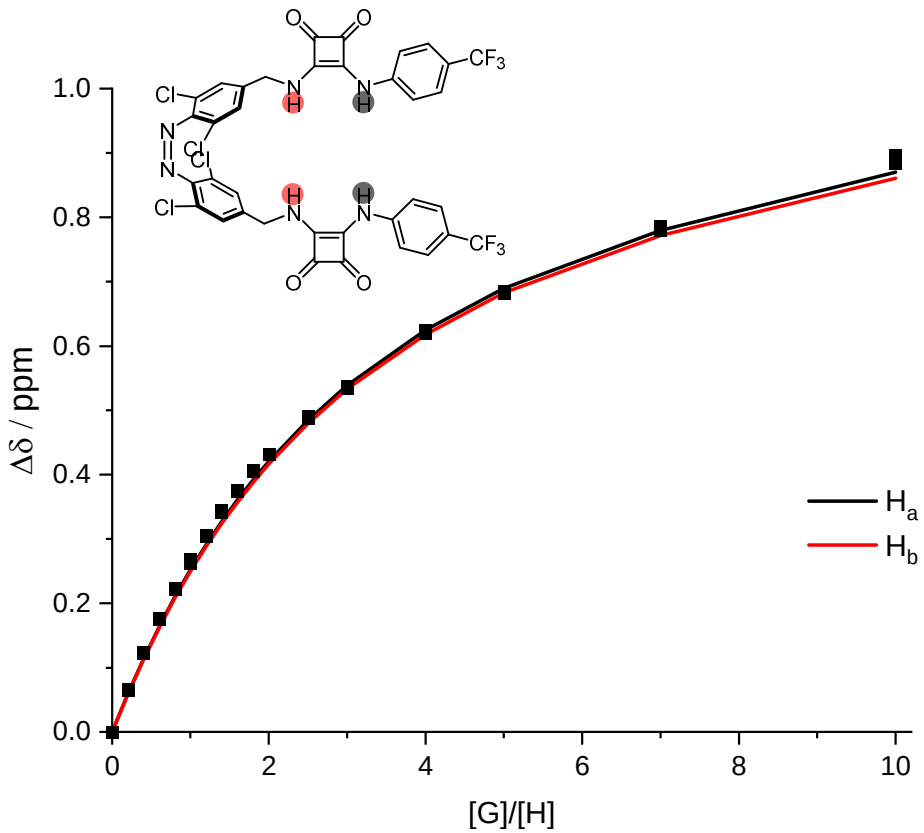

Figure S100. Plots of chemical shift changes of ***Z* -1d** upon addition of TBACl

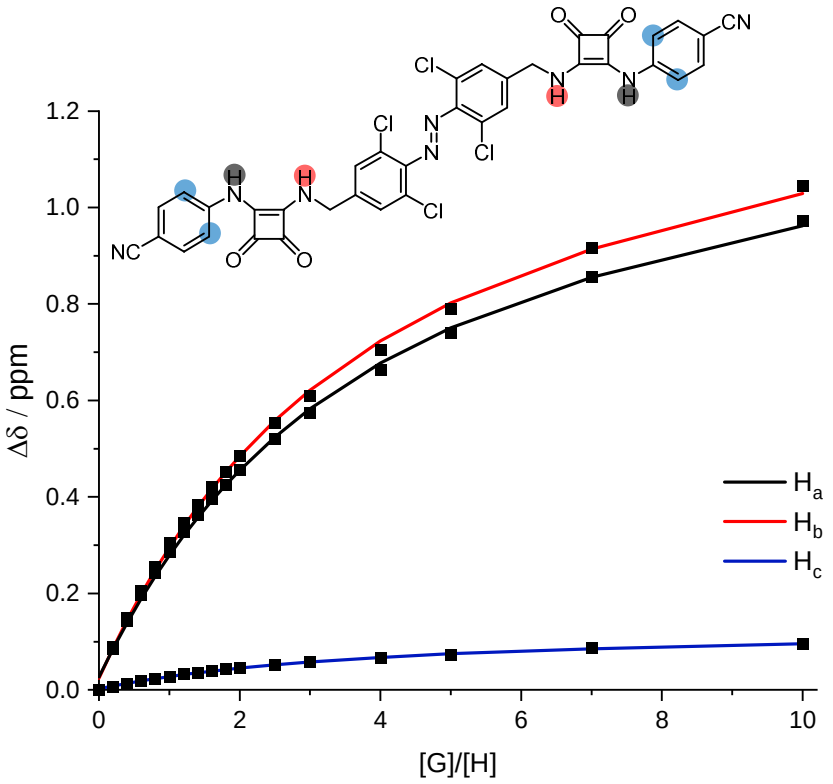

Figure S101. Plots of chemical shift changes of ***E*-1e** upon addition of TBACl

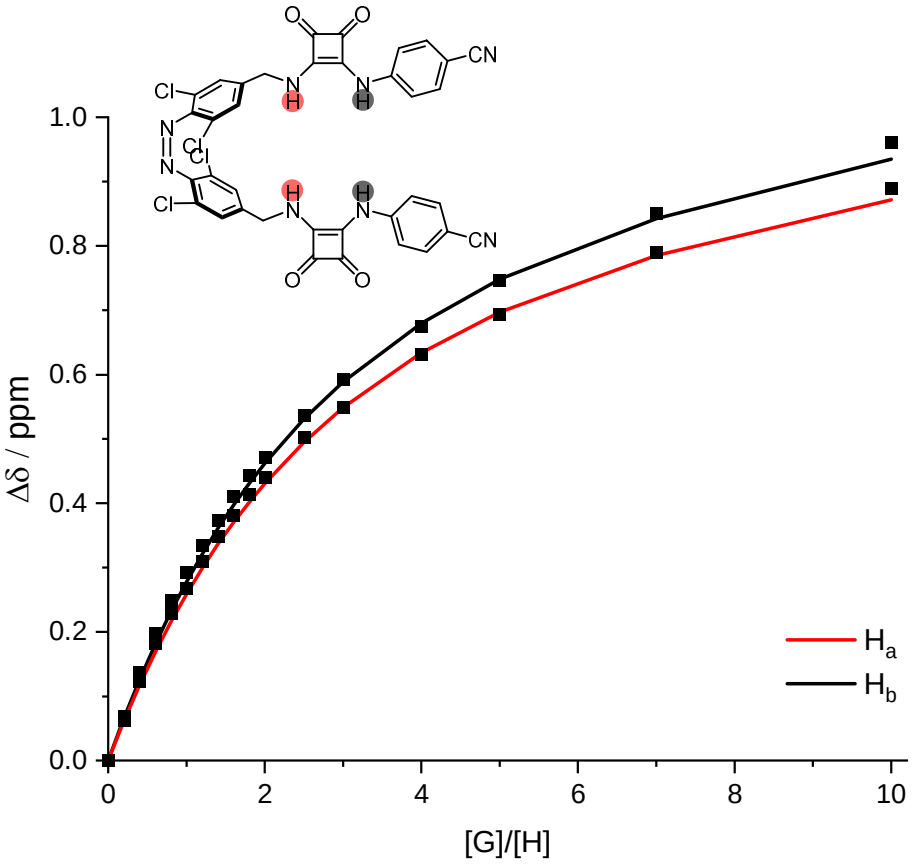

Figure S102. Plots of chemical shift changes of ***Z*-1e** upon addition of TBACl

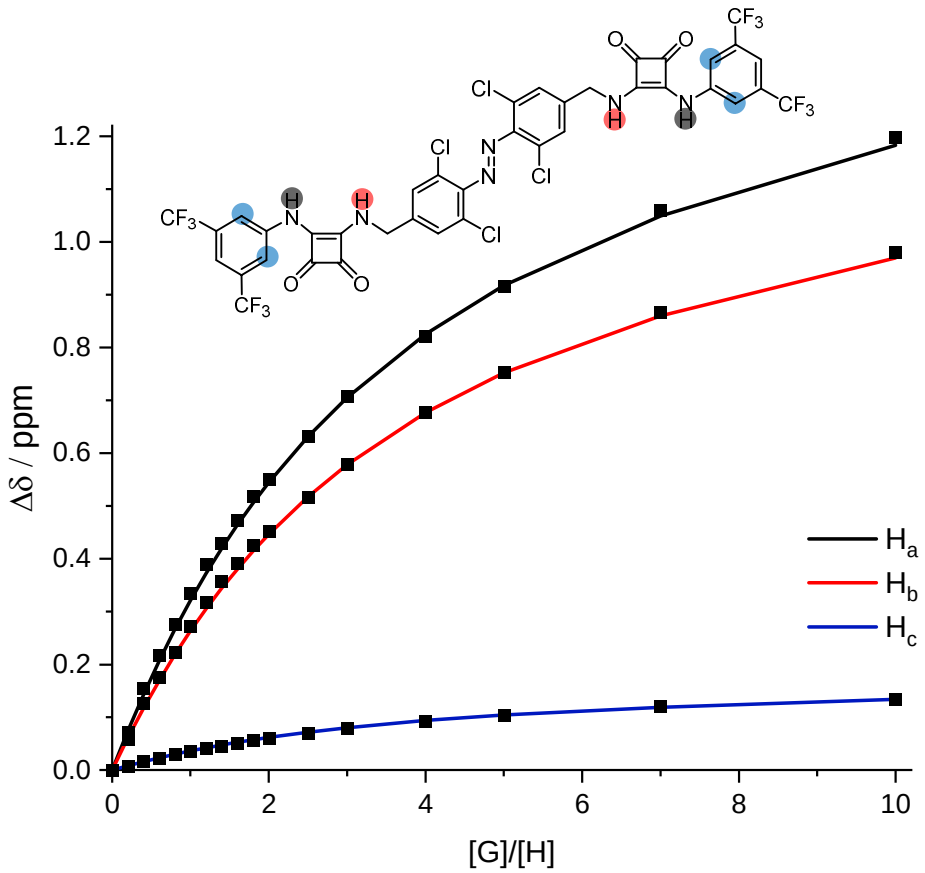

Figure S103. Plots of chemical shift changes of ***E*-1f** upon addition of TBACl

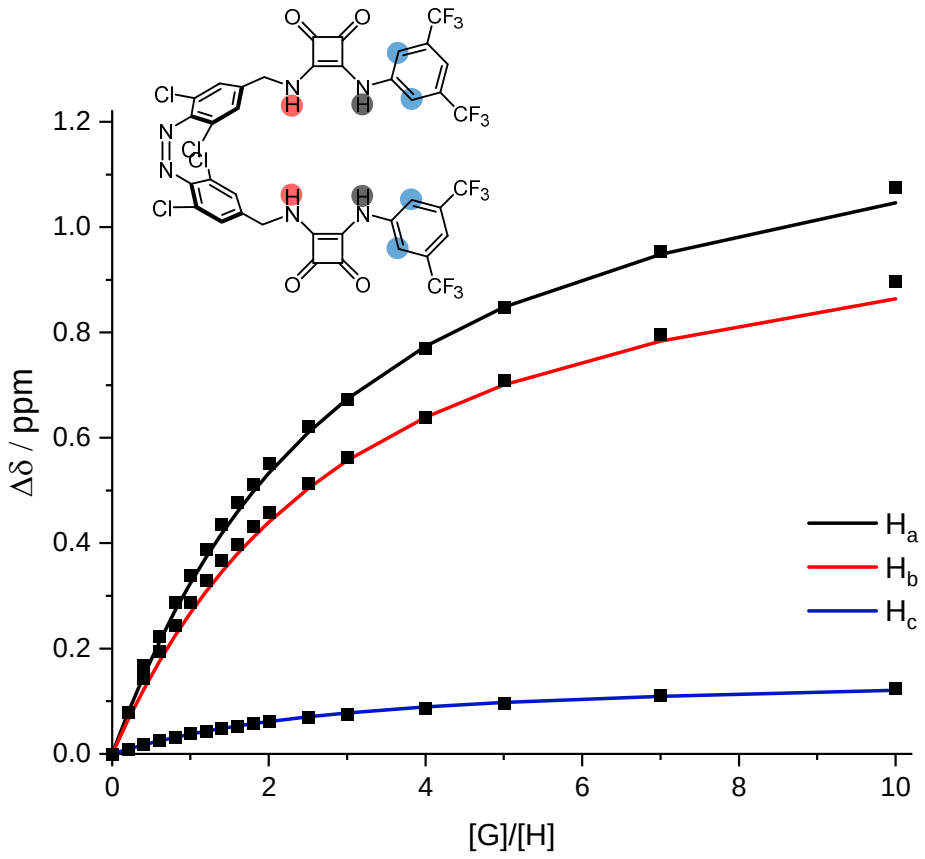

Figure S104. Plots of chemical shift changes of ***Z*-1f** upon addition of TBACl

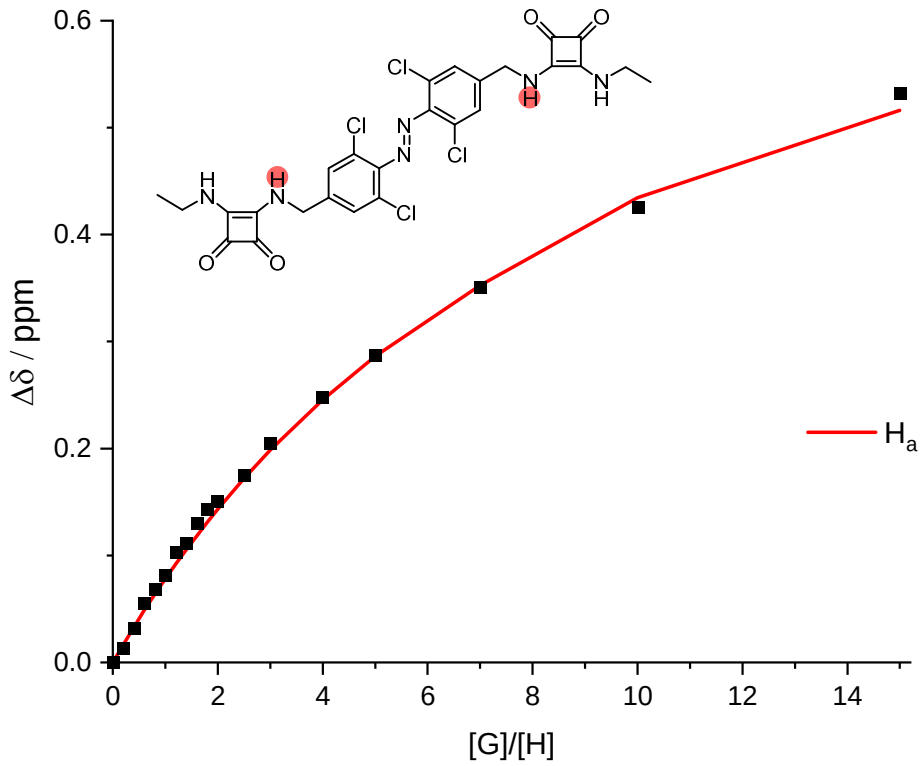

Figure S105. Plots of chemical shift changes of ***E*-1g** upon addition of TBACl

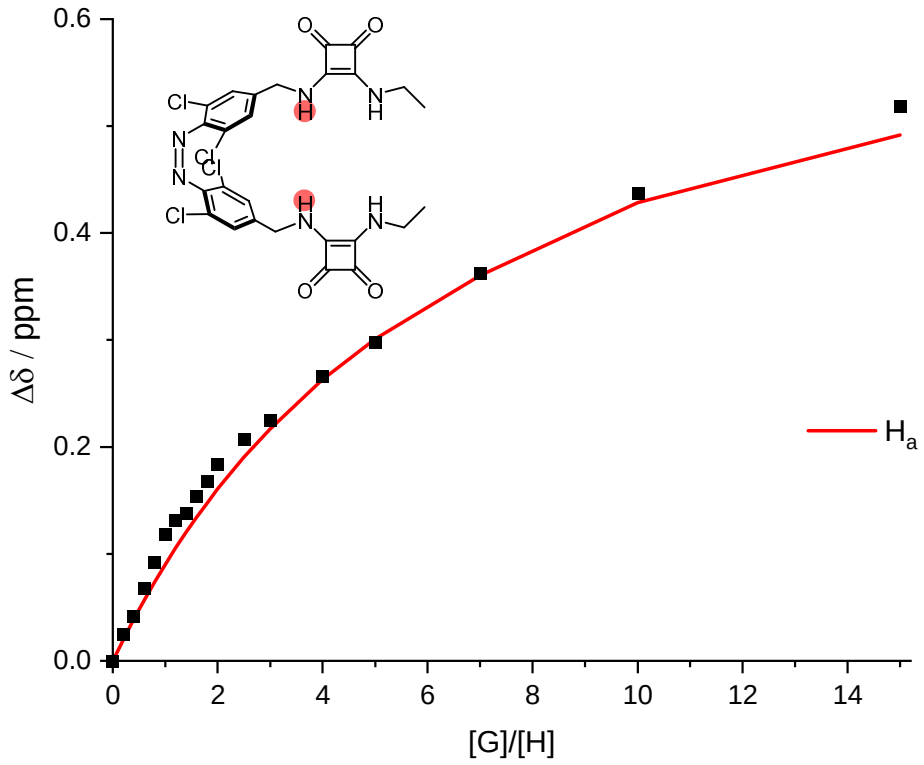

Figure S106. Plot of chemical shift changes of ***Z*-1g** upon addition of TBACl

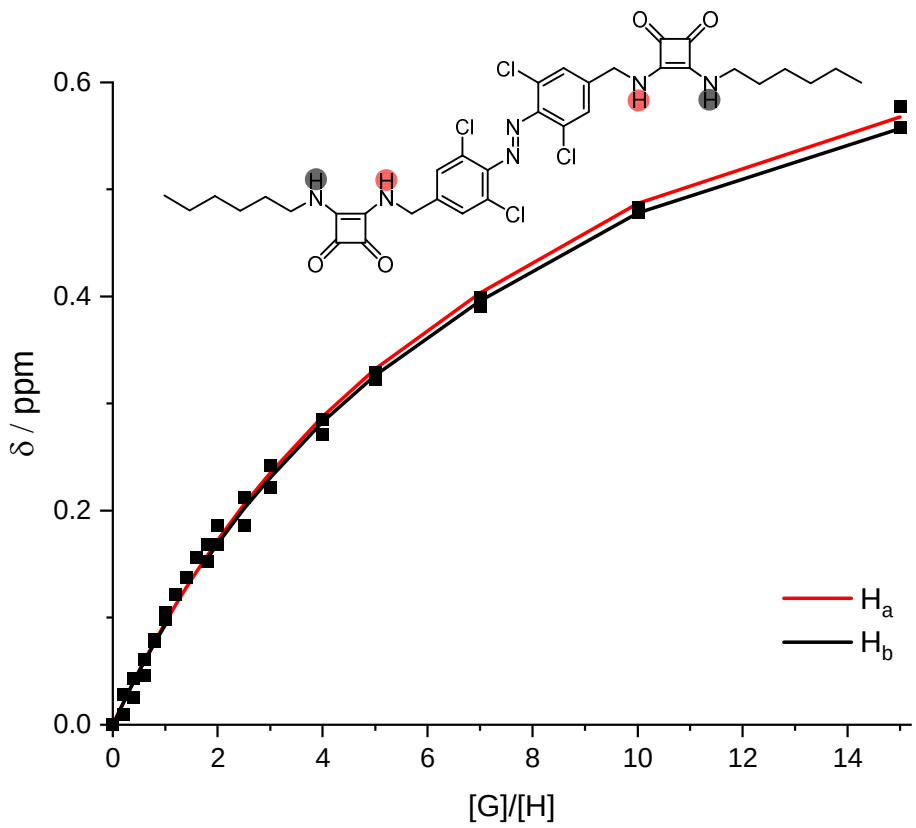

Figure S107. Plots of chemical shift changes of ***E*-1h** upon addition of TBACl

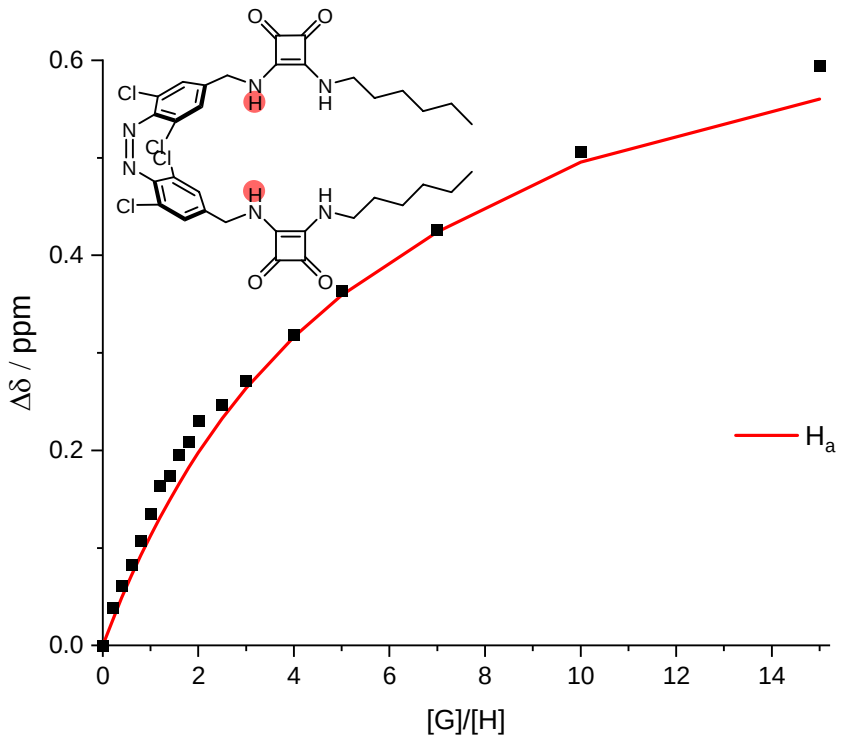

Figure S108. Plot of chemical shift changes of ***Z*-1h** upon addition of TBACl

6 Anion transport studies

Vesicle preparation

A thin film of lipid (1-palmitoyl-2-oleoyl-*sn*-3-phosphatidylcholine POPC, egg-yolk phosphatidylglycerol EYPG or dipalmitoyl phosphatidylcholine DPPC) was formed by evaporating a chloroform solution under a stream of nitrogen gas, and then under high vacuum for 6 hours. The lipid film was hydrated by vortexing with the prepared buffer (100 mM NaCl, 10 mM HEPES, 1 mM 8-Hydroxypyrene-1,3,6-trisulfonic acid trisodium salt (HPTS), pH 7.0). The lipid suspension was then subjected to 5 freeze-thaw cycles using liquid nitrogen and a water bath (40°C), followed by extrusion 19 times through a polycarbonate membrane (pore size 200 nm) at rt. Extrusion was performed at 50°C in the case of DPPC lipids. Extra-vesicular components were removed by size exclusion chromatography on a Sephadex G-25 column with 100 mM NaCl, 10 mM HEPES, pH 7.0. Final conditions: LUVs (2.5 mM lipid); inside 100 mM NaCl, 10 mM HEPES, 1 mM HPTS, pH 7.0; outside: 100 mM NaCl, 10 mM HEPES, pH 7.0. Vesicles for the sodium gluconate assay were prepared by the same procedure, substituting NaCl for NaGluconate in the buffer solution.

Transport assays with HPTS

In a typical experiment, the LUVs containing HPTS (25 μL, final lipid concentration 31 μM) were added to buffer (1950 μL of 100 mM NaCl, 10 mM HEPES, pH 7.0) at 25°C under gentle stirring. A pulse of NaOH (20 μL, 0.5 M) was added at 20 secs to initiate the experiment. At 80 s the test transporter (various concentrations, in 5 μL DMSO) was added, followed by detergent (25 μL of Triton X-100 in 7:1 (v/v) H_2O-DMSO) at 300 secs to calibrate the assay. The fluorescence emission was monitored at λ_{em} = 510 nm (λ_{ex} = 460/405 nm). The fractional fluorescence intensity (I_{rel}) was calculated from Equation S4, where R_t is the fluorescence ratio at time *t*, (ratio of intensities 460 nm / 405 nm excitation) R_0 is the fluorescence ratio at time 77 s, and R_d is the fluorescence ratio after the addition of detergent.

$$I_{rel} = \frac{R_t - R_0}{R_d - R_0} \qquad \textbf{(S4)}$$

The fractional fluorescence intensity (I_{rel}) at 290 s just prior to lysis, defined as the fractional activity *y*, was plotted as a function of the ionophore concentration (*x* / μM). Hill coefficients (*n*) and EC_{50} values were calculated by fitting to the Hill equation (Equation S5),

$$y = y_0 + (y_{max} - y_0).\frac{x^n}{EC50^n + x^n} \qquad \textbf{(S5)}$$

where y_0 is the fractional activity in the absence of transporter, y_{max} is the fractional activity in with excess transporter, *x* is the transporter concentration in the cuvette.

Exposure of the sample to the excitation beam was minimised by closing the shutter immediately after each measurement, and using a short integration time (0.05 s) / narrow excitation band pass (5 nm). The extent of *Z* to *E* isomerisation under these conditions during the anion transport assays was estimated to be <5% by analysis of the UV-vis spectra of sample subjected to the assay measurement conditions.

For each compound as the *E* and Z isomer, Hill plots were fitted to at-least 8, and up to 12 data points spanning the required concentration range, and each individual concentration was repeated at-least twice and averaged (>16 independent measurements per isomer).

Experiments with DPPC lipids were conducted in the same way. For elevated temperature studies, the sample was equilibrated at 45°C (using the Peltier temperature controller) for 5 minutes prior to initiating the experiment.

The effect of external ion exchange was explored by using a previously reported assay.[5-7] These experiments were carried out by adding the POPC vesicle solution (prepared as above) to buffer (100 mM MX, 10 mM HEPES, pH 7.0), where M = Li, Na, K, Rb (X = Cl), and X = Cl, Br, I, NO_3 (M = Na). In the case of NaI buffer, 5 mM $Na_2S_2O_3$ was also added.

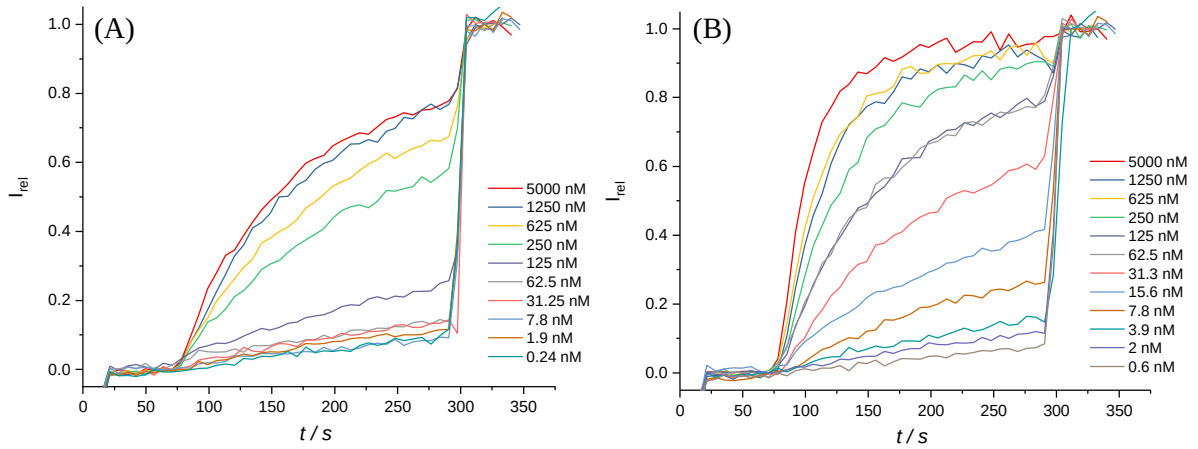

Figure S109. Original data for HPTS assay for (A) ***E*-1a** (B) PSS ***Z*-1a** (77%)

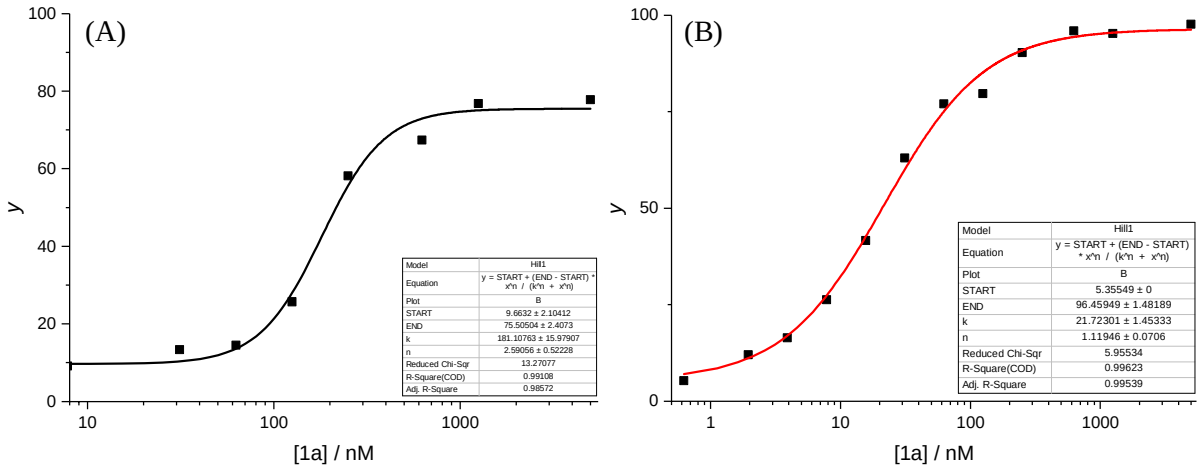

Figure S110. Hill plot for (A) ***E*-1a** (B) PSS ***Z*-1a** (77%)

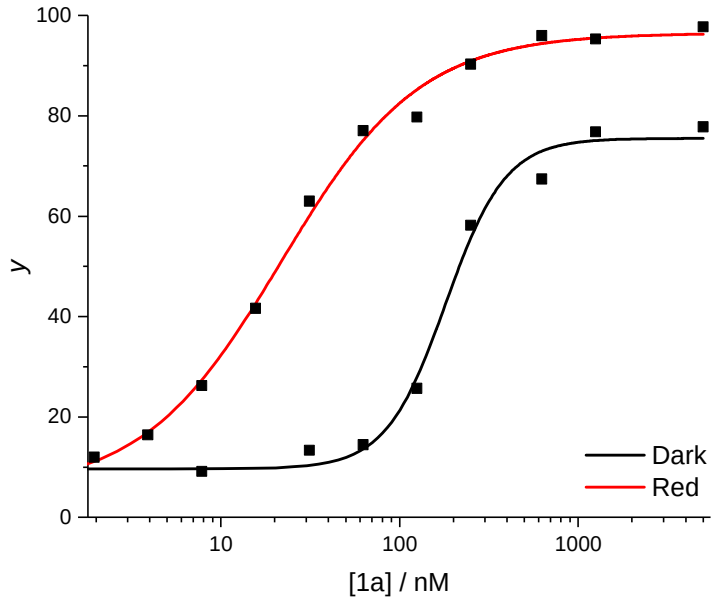

Figure S111. Stacked EC_{50} data of ***E*-1a** and PSS ***Z*-1a** (77%)

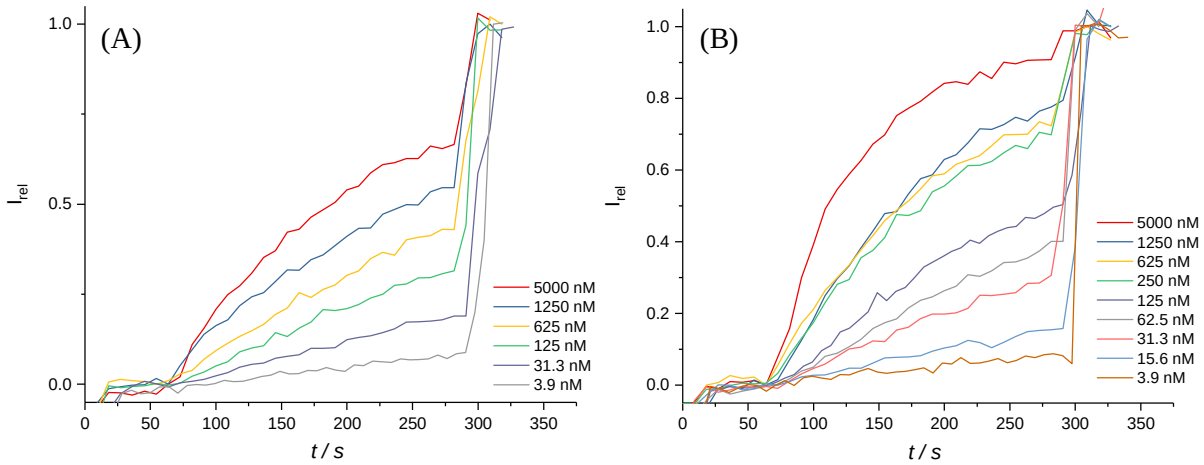

Figure S112. Original data for HPTS assay for (A) ***E*-1b** (B) PSS ***Z*-1b** (77%)

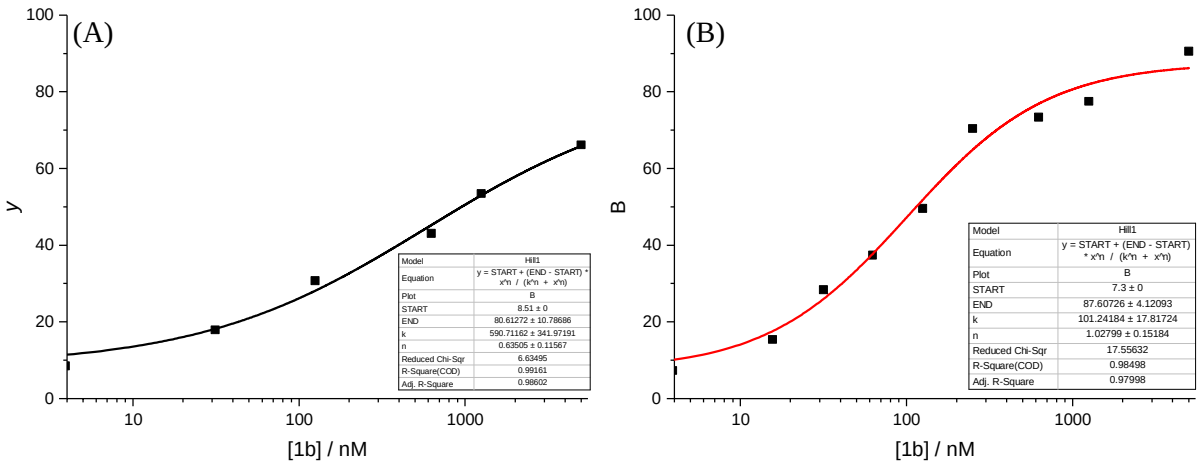

Figure S113. Hill plot for (A) ***E*-1b** (B) PSS ***Z*-1b** (77%)

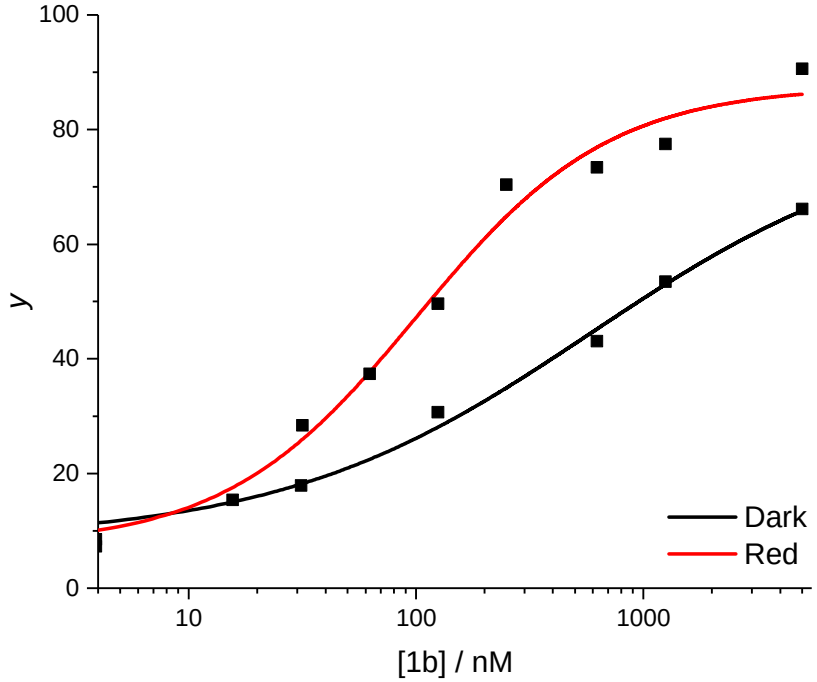

Figure S114. Stacked EC_{50} data of ***E*-1b** and PSS ***Z*-1b** (77%)

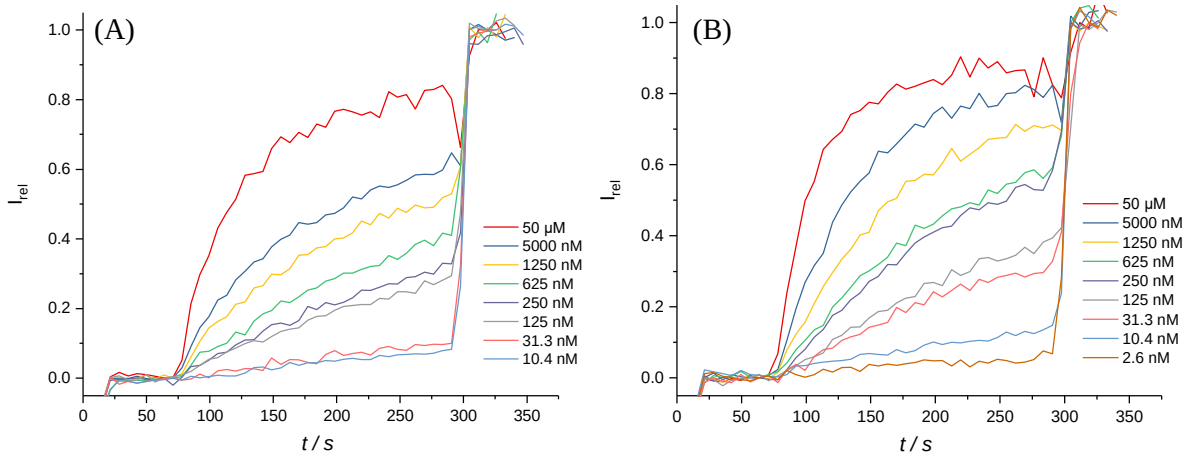

Figure S115. Original data for HPTS assay for (A) ***E*-1c** (B) PSS ***Z*-1c** (77%)

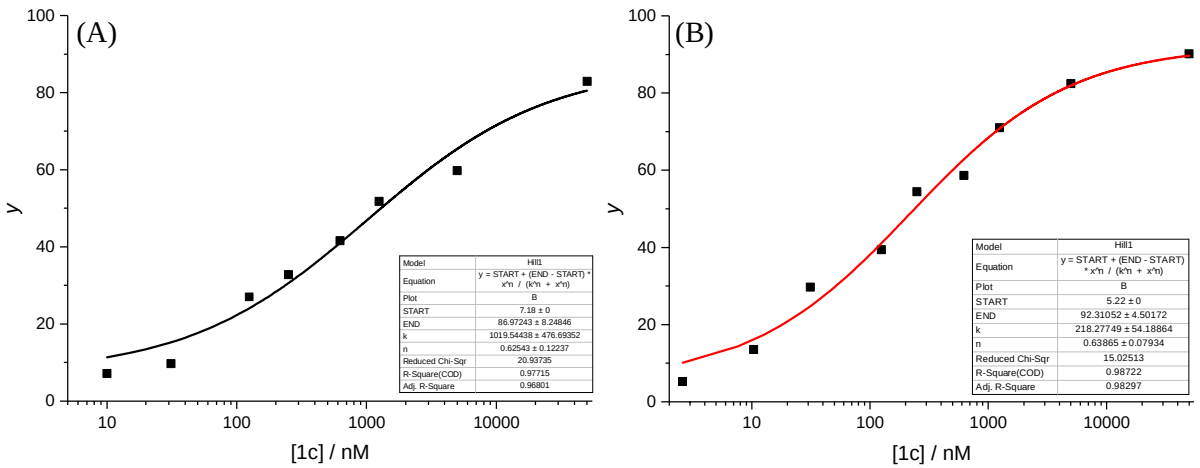

Figure S116. Hill plot for (A) ***E*-1c** (B) PSS ***Z*-1c** (77%)

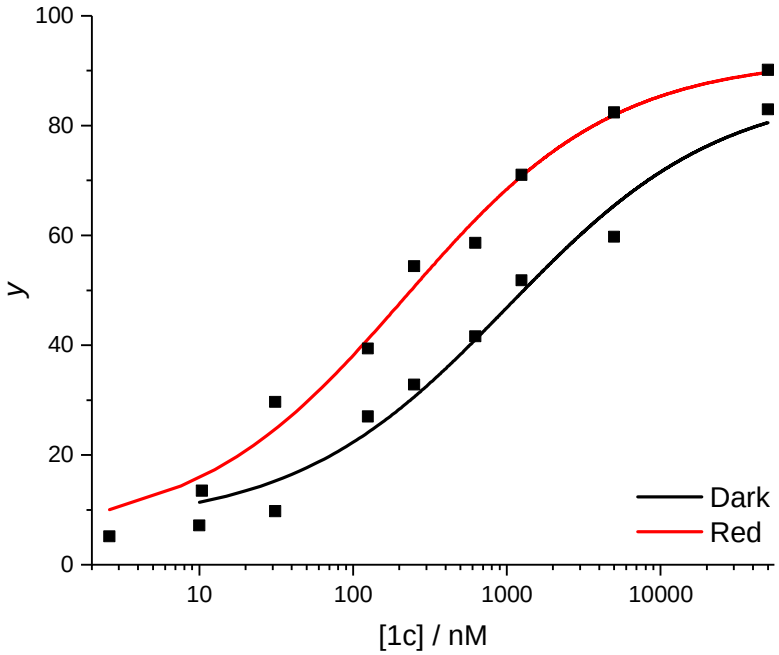

Figure S117. Stacked EC_{50} data of ***E*-1c** and PSS ***Z*-1c** (77%)

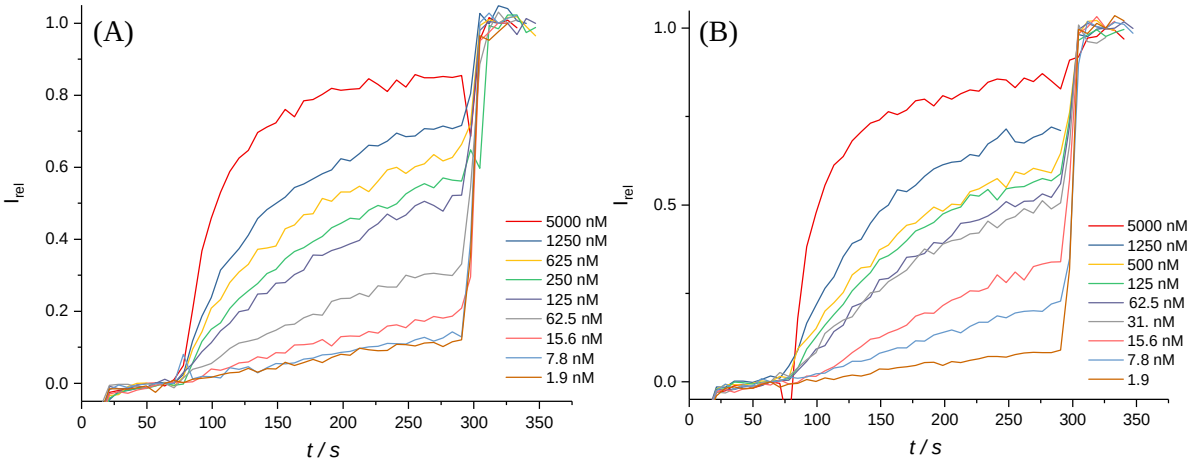

Figure S118. Original data for HPTS assay for (A) ***E*-1d** (B) PSS ***Z*-1d** (77%)

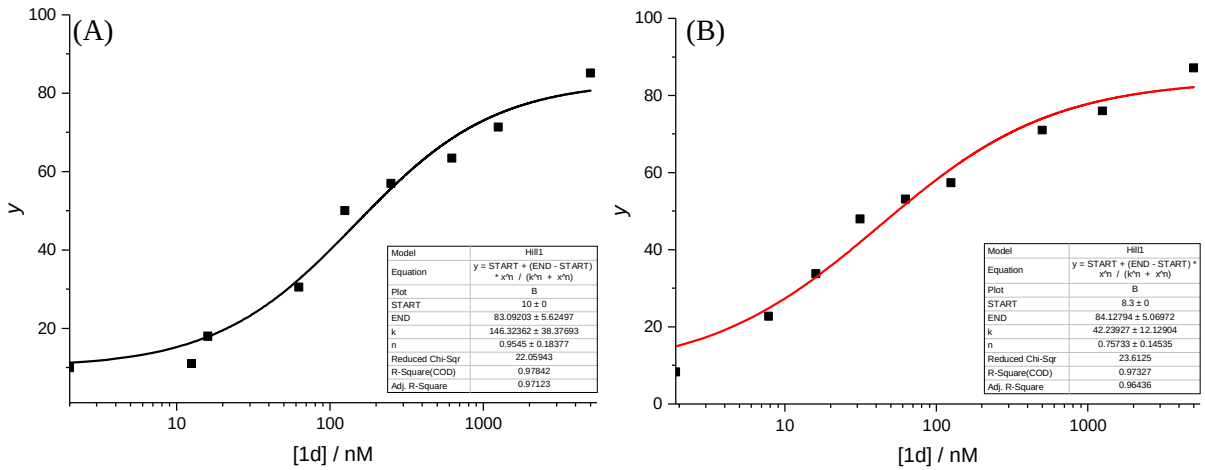

Figure S119. Hill plot for (A) ***E*-1d** (B) PSS ***Z*-1d** (77%)

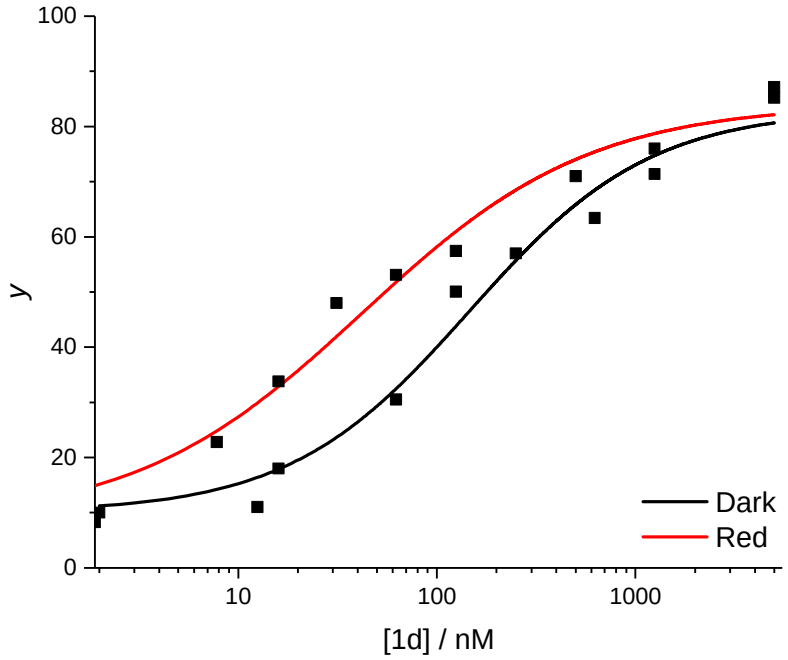

Figure S120. Stacked EC_{50} data of ***E*-1d** and PSS ***Z*-1d** (77%)

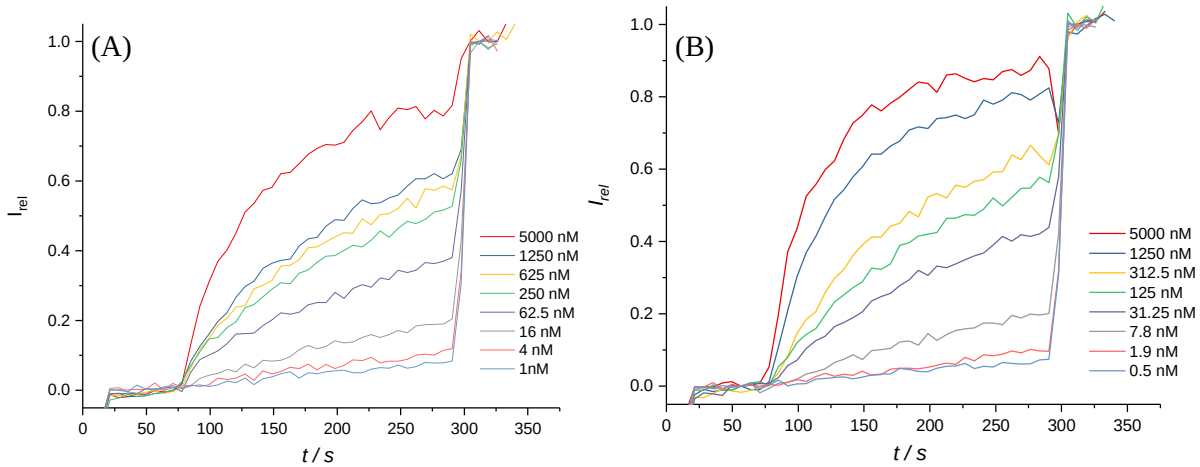

Figure S121. Original data for HPTS assay for (A) ***E*-1e** (B) PSS ***Z*-1e** (77%)

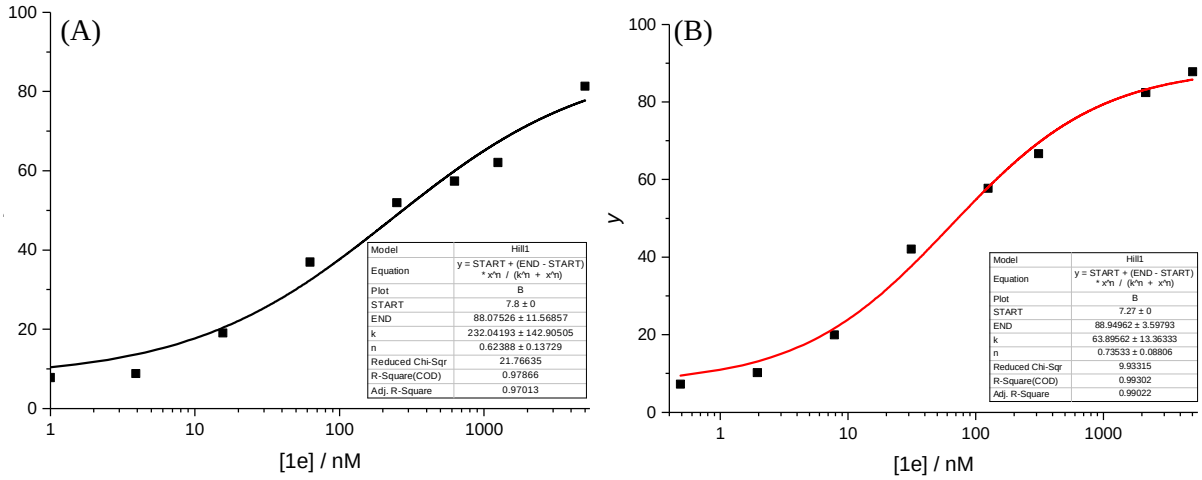

Figure S122. Hill plot for (A) ***E*-1e** (B) PSS ***Z*-1e** (77%)

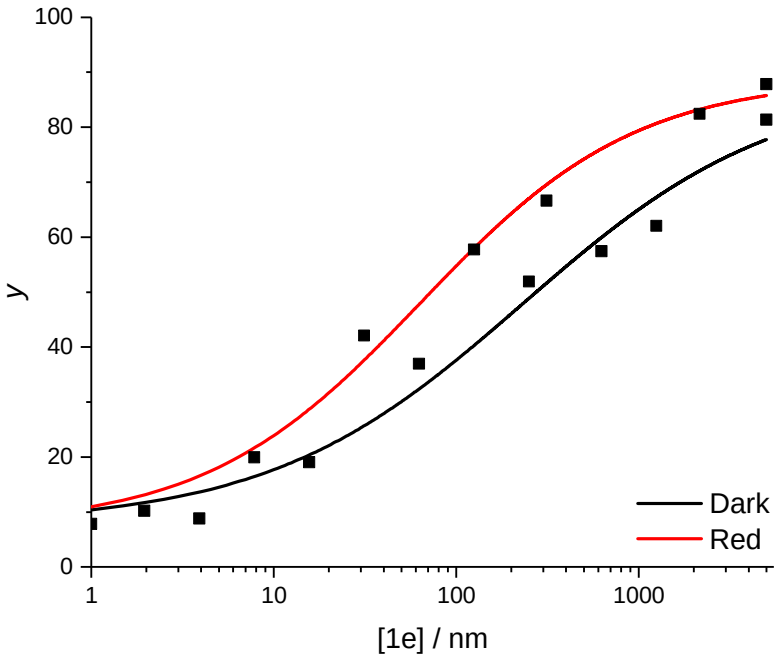

Figure S123. Stacked EC_{50} data of ***E*-1e** and PSS ***Z*-1e** (77%)

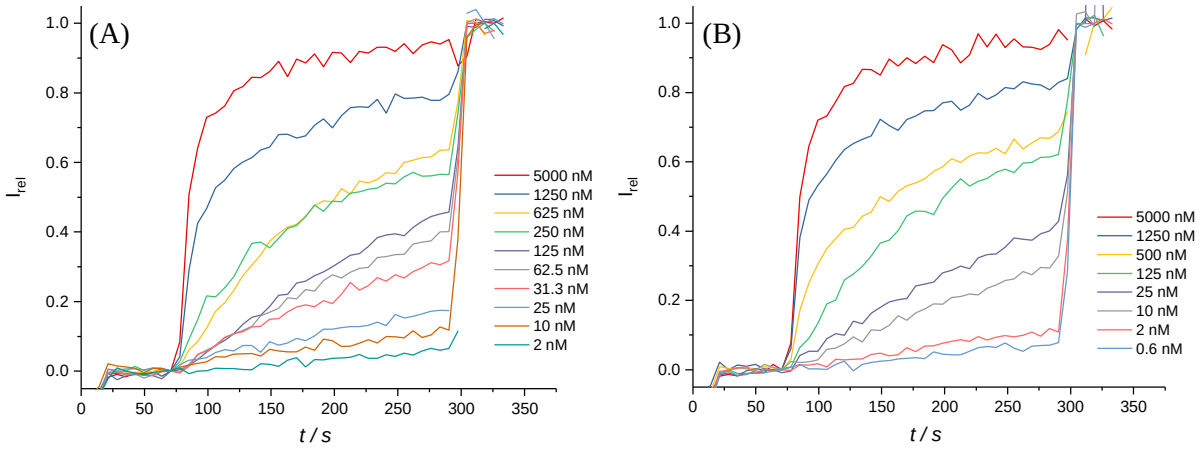

Figure S124. Original data for HPTS assay for (A) ***E*-1f** (B) PSS ***Z*-1f** (77%)

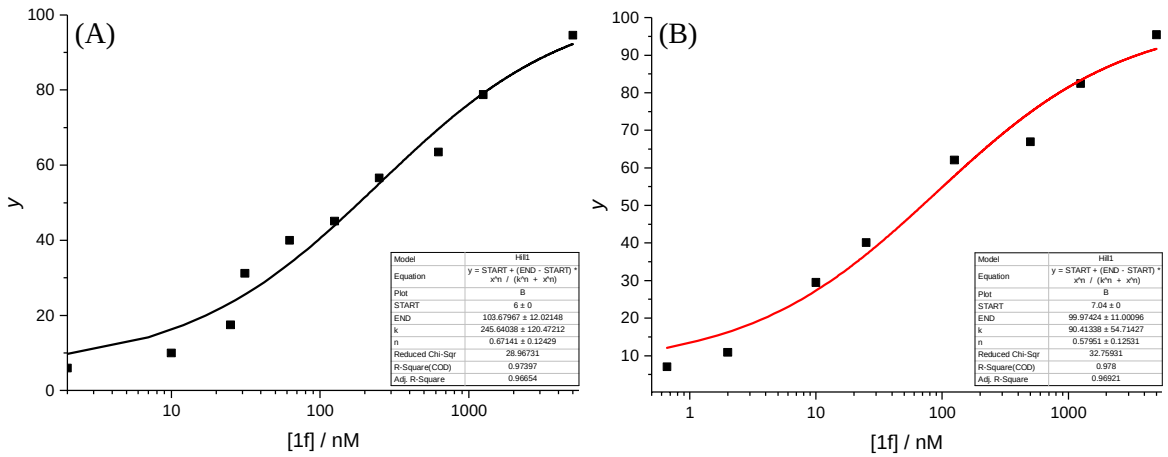

Figure S125. Hill plot for (A) ***E*-1f** (B) PSS ***Z*-1f** (77%)

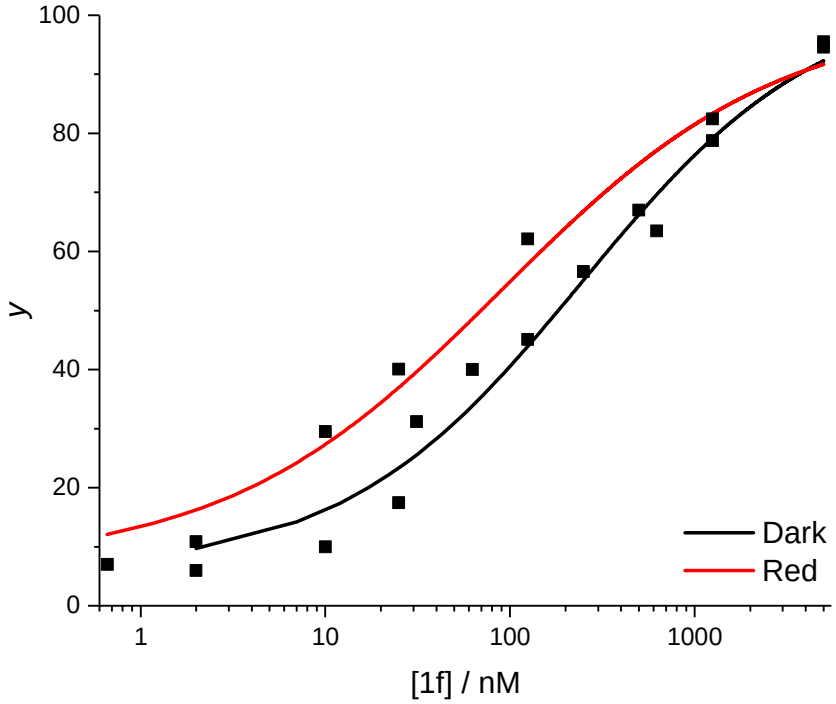

Figure S126. Stacked EC_{50} data of ***E*-1f** and PSS ***Z*-1f** (77%)

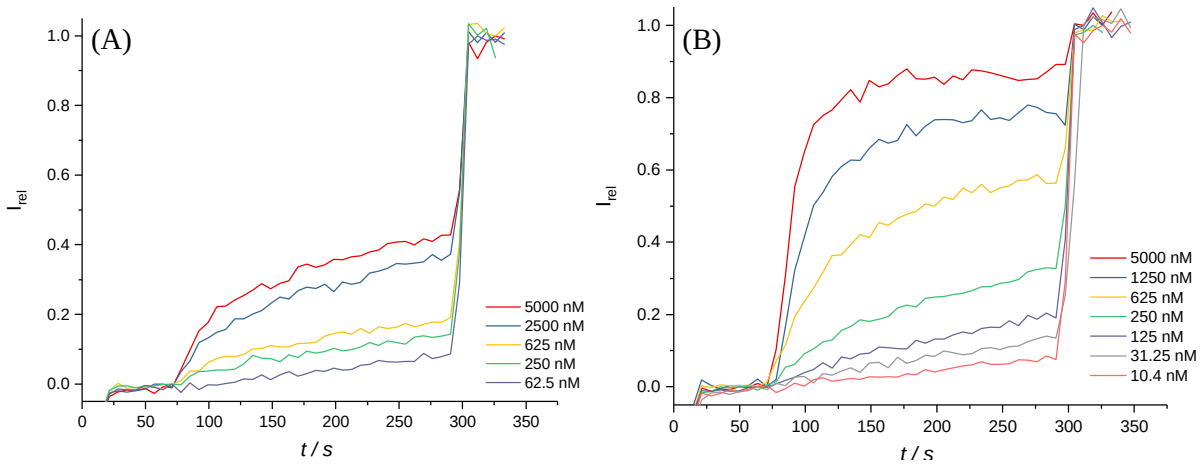

Figure S127. Original data for HPTS assay for (A) ***E*-1g** (B) PSS ***Z*-1g** (77%)

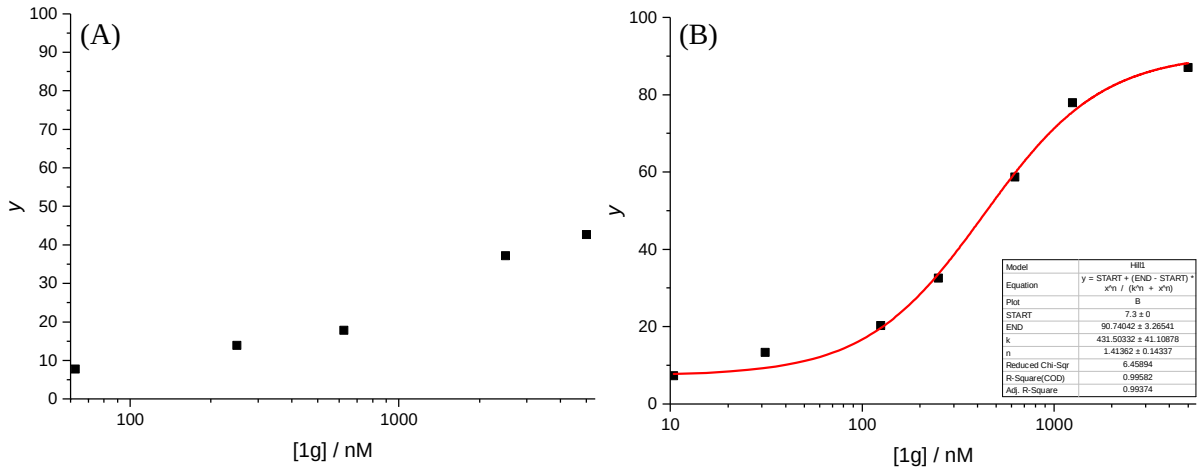

Figure S128. Hill plot for (A) ***E*-1g** (B) PSS ***Z*-1g** (77%). Insufficient activity of ***E*-1g** for Hill analysis.

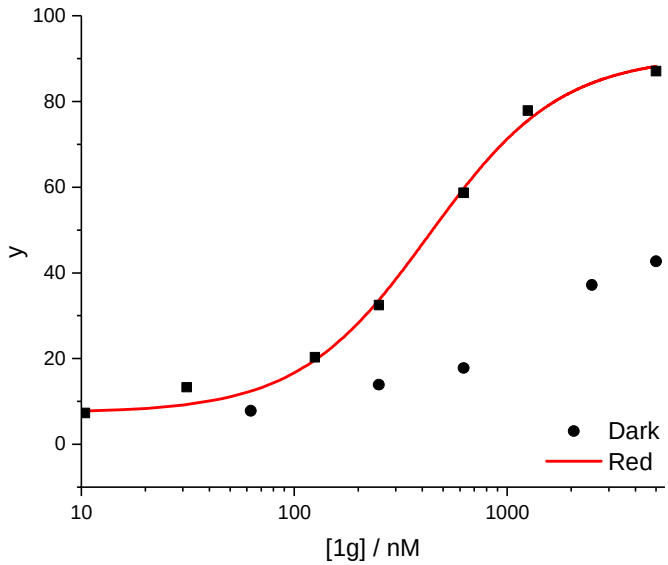

Figure S129. Stacked EC_{50} data of ***E*-1g** and PSS ***Z*-1g** (77%)

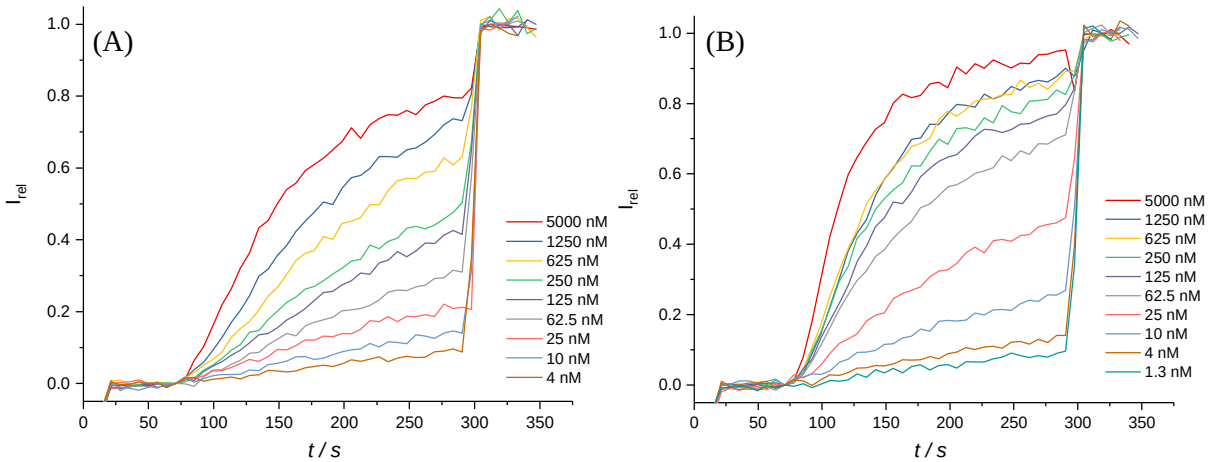

Figure S130. Original data for HPTS assay for (A) ***E*-1h** (B) PSS ***Z*-1h** (77%)

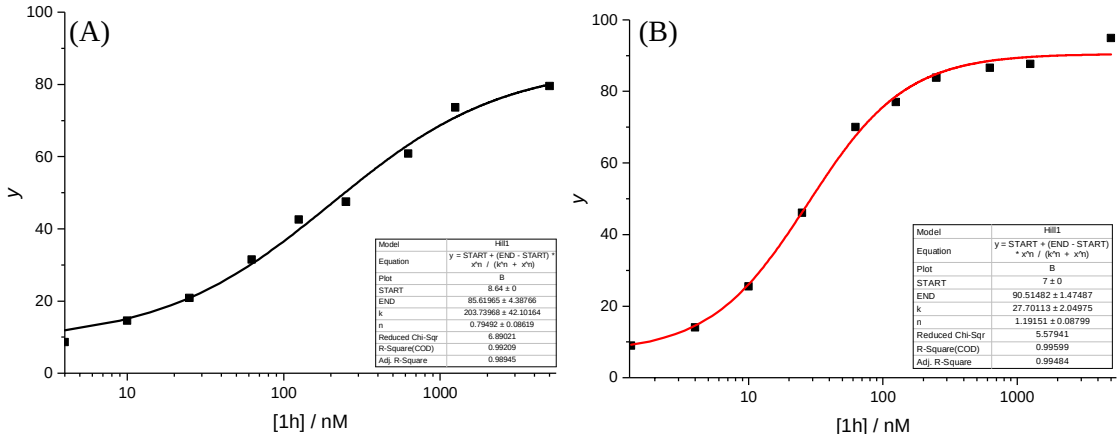

Figure S131. Hill plot for (A) ***E*-1h** (B) PSS ***Z*-1h** (77%).

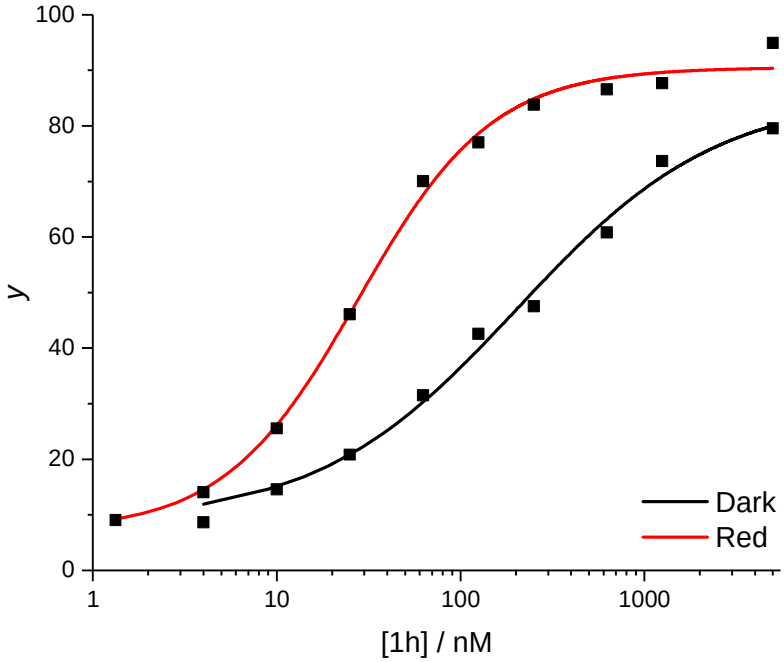

Figure S132. Stacked EC_{50} data of ***E*-1h** and PSS ***Z*-1h** (77%)

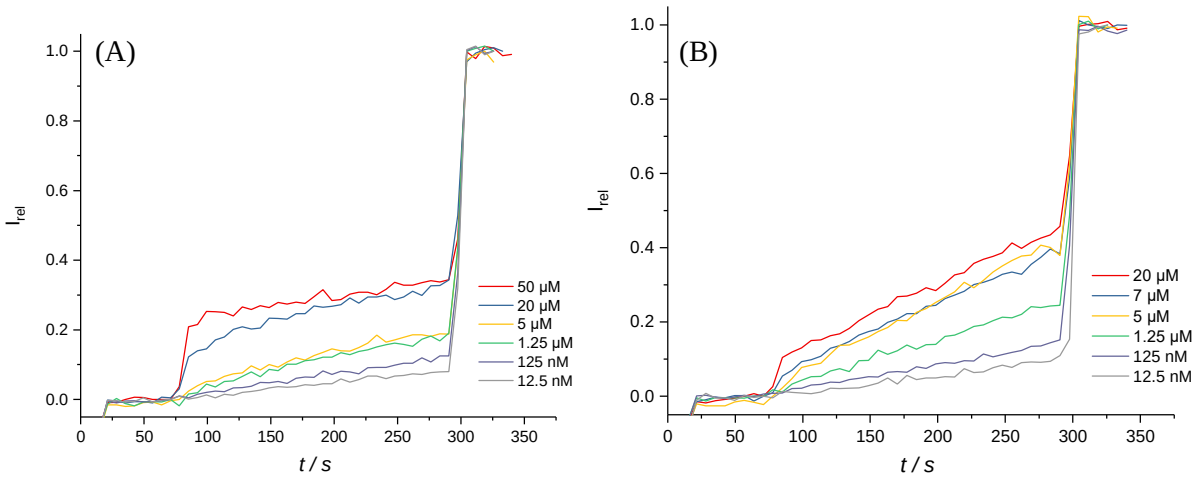

Figure S133. Original data for HPTS assay for (A) ***E*-1i** (B) PSS ***Z*-1i** (77%)

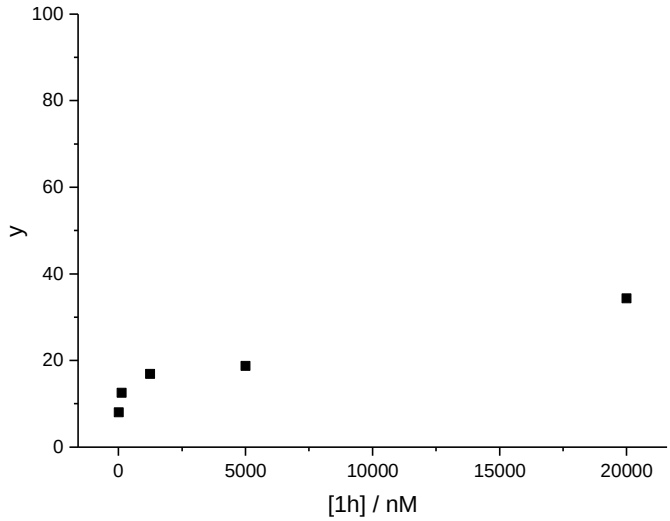

Figure S134. Maximal activity plot for ***E*-1i.** Insufficient activity of for Hill analysis.

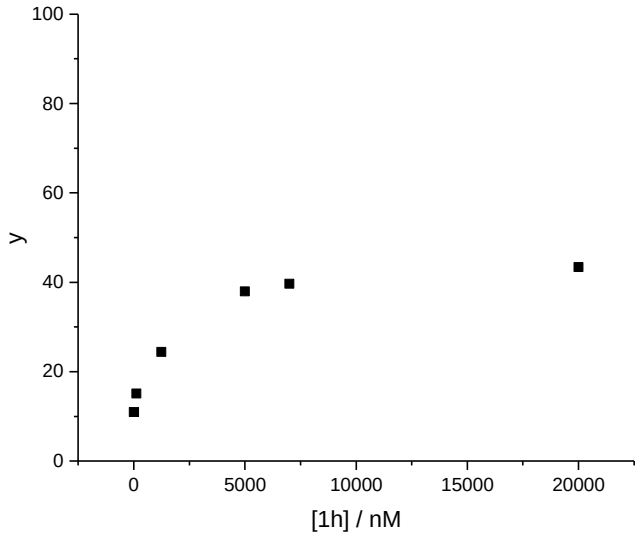

Figure S135. Maximal activity plot for PSS ***Z*-1i** (77%). Insufficient activity of for Hill analysis.

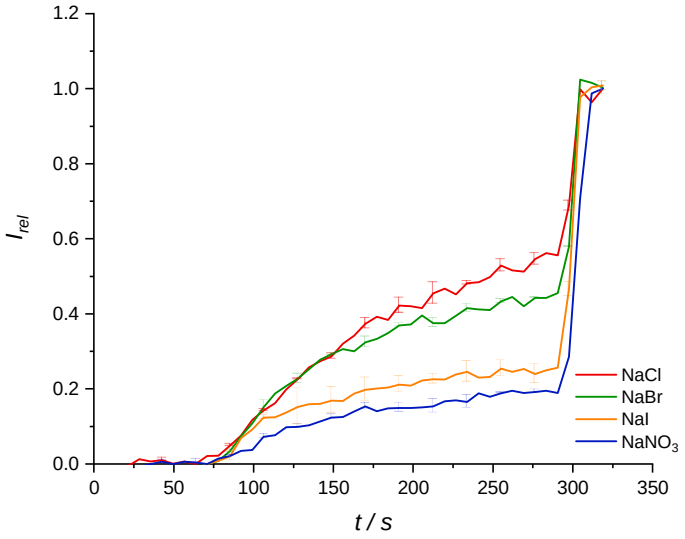

Figure S136. HPTS assay of ***Z*-1a** at 62.5 nM carrier concentration and varying external anion (external buffer 100 mM Na^+X^-, 10 mM HEPES; 5 mM $Na_2S_2O_3$ was added in the case of X = I). Error bars represent standard deviations and shown every four data points for clarity.

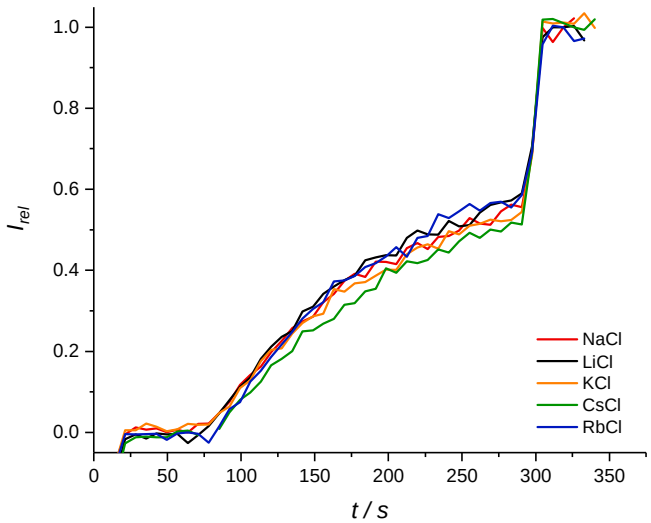

Figure S137. HPTS assay of ***Z*-1a** at 62.5 nM carrier concentration and varying external cation (external buffer 100 mM M^+Cl^-, 10 mM HEPES). Error bars omitted for clarity. For errors in fractional activities (relative intensity just prior to lysis) see article Figure 5.

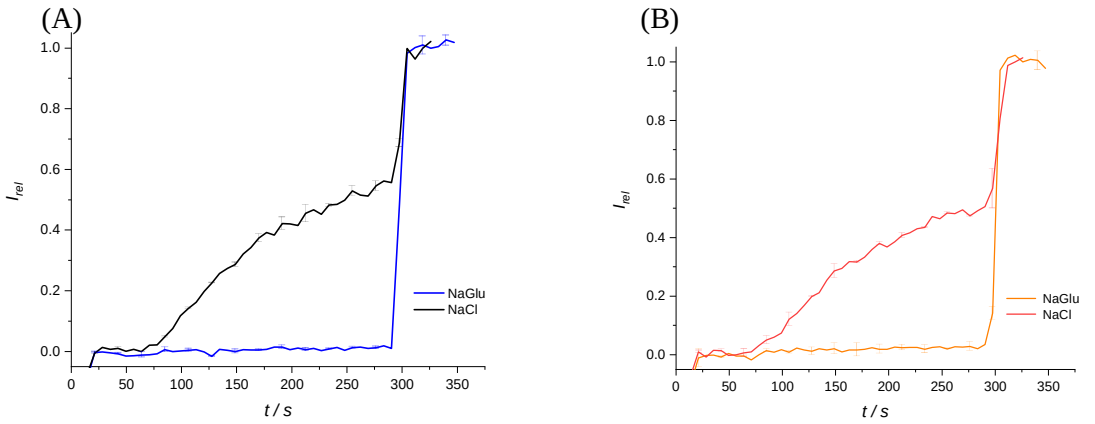

Figure S138. HPTS assay using 100 mM sodium gluconate vs 100mM NaCl for (A) ***E*-1a** at 200 nM carrier concentration and (B) ***Z*-1a** at 62.5 nM carrier concentration. Error bars represent standard deviations and shown every four data points for clarity.

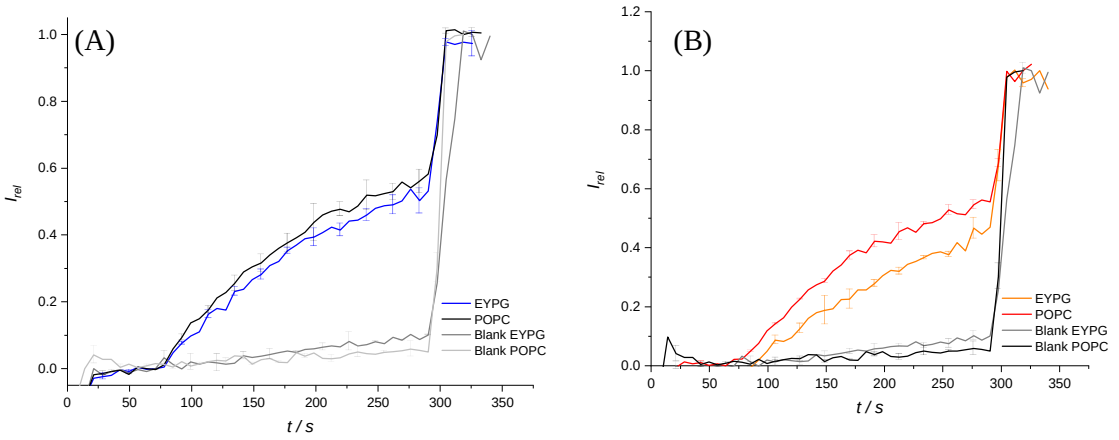

Figure S139. HPTS assay using EYPG LUVs for (A) ***E*-1a** at 200 nM carrier concentration and (B) ***Z*-1a** at 62.5 nM carrier concentration. Error bars represent standard deviations and shown every four data points for clarity. Blank runs are shown for comparison.

Calcein leakage assay

POPC vesicles were prepared containing calcein (Internal buffer: 100 mM NaCl, 10 mM HEPES, 100 mM calcein, pH 7.0. External buffer: 100 mM NaCl, 10 mM HEPES, pH 7.0). Each transport experiment was carried out as follows; the calcein-containing POPC vesicles (25 µl, 2.5 mM) were suspended in the external buffer (1925 µL, 100 mM NaCl, 10 mM HEPES, pH 7.0) at 25°C and gently stirred. At 60 s, the carriers were administered in 5 µL DMSO. The assay was calibrated at 250 s with detergent (25 µL of Triton X-100 in 7:1 (v/v) H_2O-DMSO). The time-dependent change in fluorescence intensity (λ_{ex} = 490 nm, λ_{em} = 520 nm) was monitored, and normalised according to Equation S6:

$$I_{rel} = \frac{I_t - I_0}{I_{max} - I_0} \qquad \textbf{(S6)}$$

where $I_0 = I_t$ before transporter addition, $I_{max} = I_t$ after lysis.

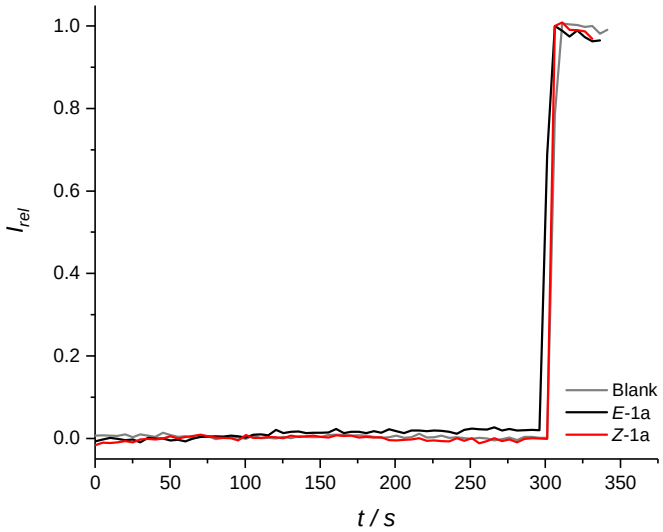

Figure S140. Calcein leakage assay: change in relative fluorescence intensity over time of **1a** at 5 µM carrier concentration.

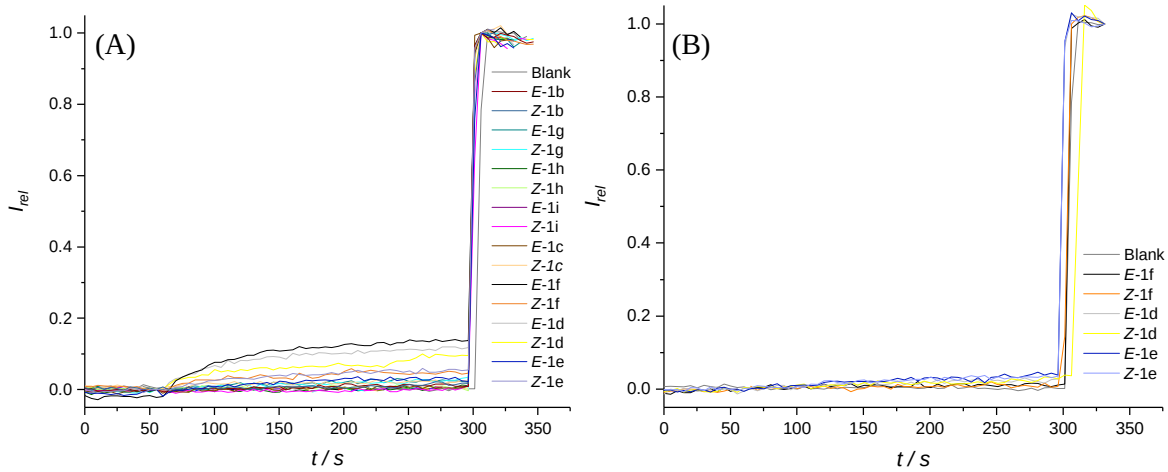

Figure S141. Calcein leakage assay: change in relative fluorescence intensity over time of (A) **1b-i** at 5 µM. Compounds that showed some leakage at 5 µM (**1d-f**) were repeated at 500 nM (B), relevant to actual transport assay concentrations, and where leakage was negligible.

7 In-situ photo-switching and ISE experiments

Vesicle preparation

A thin film of 1-palmitoyl-2-oleoyl-*sn*-3-phosphatidylcholine (POPC) lipid was formed by evaporating a chloroform solution under a stream of nitrogen gas, and then under high vacuum for 6 hours. The lipid film was hydrated by vortexing with the prepared buffer (489 mM NaCl, buffered to pH 7.0 with 5 mM sodium phosphate salts) The lipid suspension was then subjected to 9 freeze-thaw cycles using liquid nitrogen and a water bath (25°C), followed by extrusion 21 times through a polycarbonate membrane (pore size 200 nm) at rt. Extra-vesicular components were removed by size exclusion chromatography on a Sephadex G-25 column with 489 mM $NaNO_3$, buffered with phosphate salts to pH 7.0. After collecting, the vesicles were diluted to 30 mL in 489 mM $NaNO_3$/pH 7.0 phosphate buffer. Final conditions after dilution: LUVs (1 mM lipid); inside: 489 mM NaCl, buffered to pH 7.0 with 5 mM

sodium phosphate salts; outside: 489 mM $NaNO_3$, buffered to pH 7.0 with 5 mM sodium phosphate salts. Lipids were used within 24 hrs, and stored in the fridge between experiments. Samples were warmed to room temperature prior to use.

UV-vis of the vesicle samples containing **1a** following red and blue light irradiation (JASCO V-770 UV-Visible/NIR Spectrophotometer, using a 60 mm integrating sphere to reduce light loss from scattering, scanning 400-700 nm), revealed, as for solution studies, increased intensity of the n-π^* transition of **1a** at 440 nm with red light irradiation, which was reversed with blue light (Figure S142). This provided evidence for *in-situ* switching of $\mathbf{1a}^{E}$ in the membrane using the same LUV conditions used for the ion transport assay. This was confirmed by an additional NMR experiment, in which following red-light induced photo-switching the sample was extracted into $CDCl_3$, diluted with d_6-DMSO and the spectrum recorded (Figure S143). This provides an estimate for the extent of photo-switching when carried out in the vesicles used for the ISE assay, which was found to be ~45 % of that achieved in DMSO solution (65:35 *E*:*Z*).

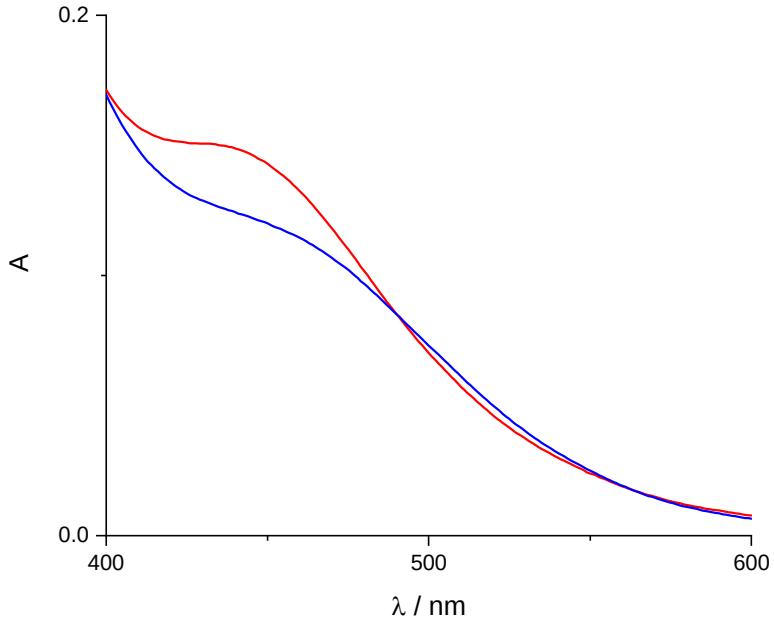

Figure S142. Partial UV-vis spectra of 15 mol% **1a** in POPC vesicles (containing 489 mM NaCl, suspended in 489 mM $NaNO_3$, and buffered with phosphate salts at pH 7.0) following 625 nm red (red line) and 455 nm blue (blue line) irradiation.

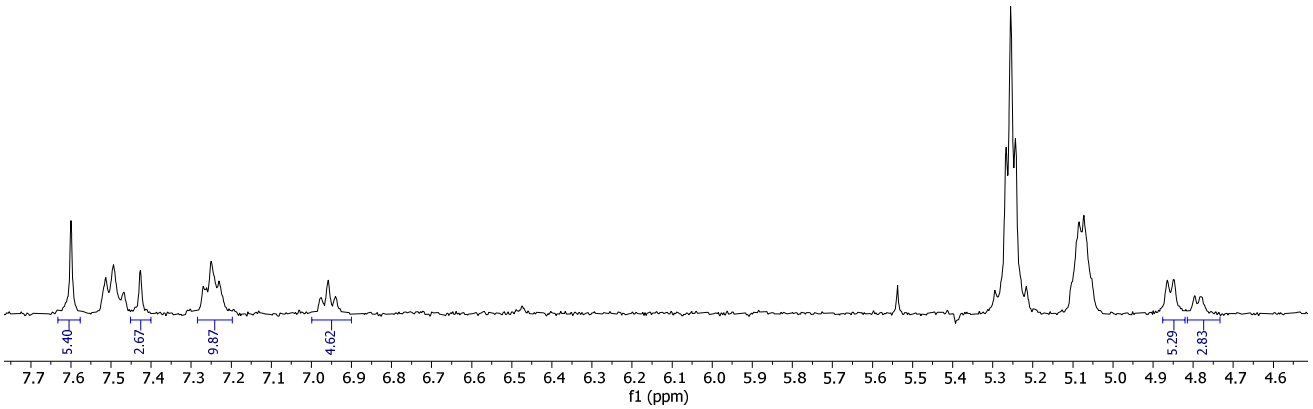

Figure S143. Partial ^{1}H NMR spectrum (3:2 d_6-DMSO/$CDCl_3$) of 15 mol% **1a** in POPC vesicles (containing 489 mM NaCl, suspended in 489 mM $NaNO_3$, and buffered with phosphate salts at pH 7.0, lipid concentration 1 mM) following 625 nm irradiation and extraction into $CDCl_3$

Electrode calibration

The chloride selective electrode (Thermo Scientific™ Orion™ ionplus® Sure-Flow® Solid State Combination ISE) was soaked in 1000 ppm chloride for extended periods (>1 hr) until readings were stable. Before each run, the electrode was calibrated by recording the potential of known chloride concentrations. The readings (mV) were converted to chloride activity using the modified Nernst equation (Equation S7), where y is chloride activity, x is potential (mV) and a and b are parameters to be determined and c=0.

$$y = a - b\ln(x + c) \qquad \textbf{(S7)}$$

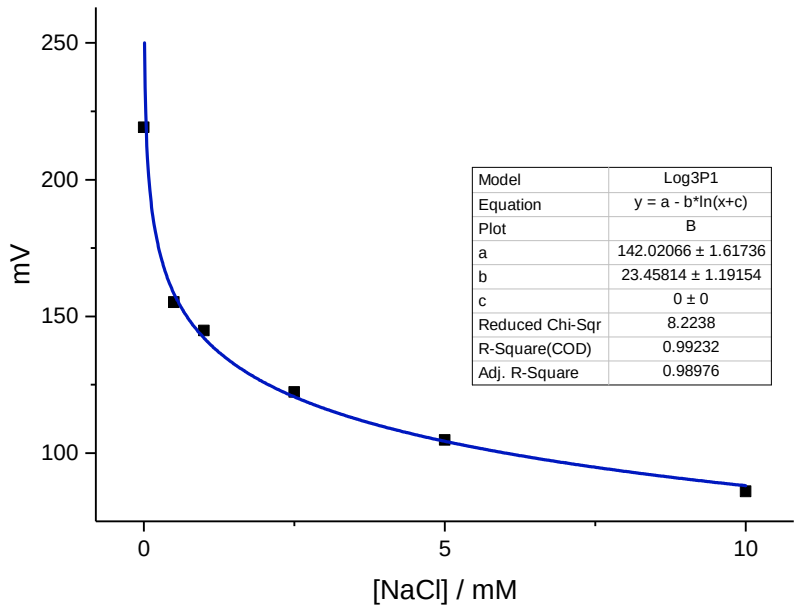

Figure S144. ISE calibration curve

Transport assays with ISE

Vesicle suspensions (1.5 mL, 1 mM lipid) were added to a 17 mm diameter vial, and gently stirred. The transporter (1 mM stock solution) was added in DMSO (7.5 μL, 0.5 mol% relative to lipid) after 60s, and the voltage was monitored over time, and converted to chloride concentration using **equation S7**. Observed initial transport rates calculated by a linear fit are: **1a**$^{Z,\ PSS}$: 1.6×10^{-5} M s^{-1}; **1a**^{E} 5.0×10^{-7} M s^{-1}

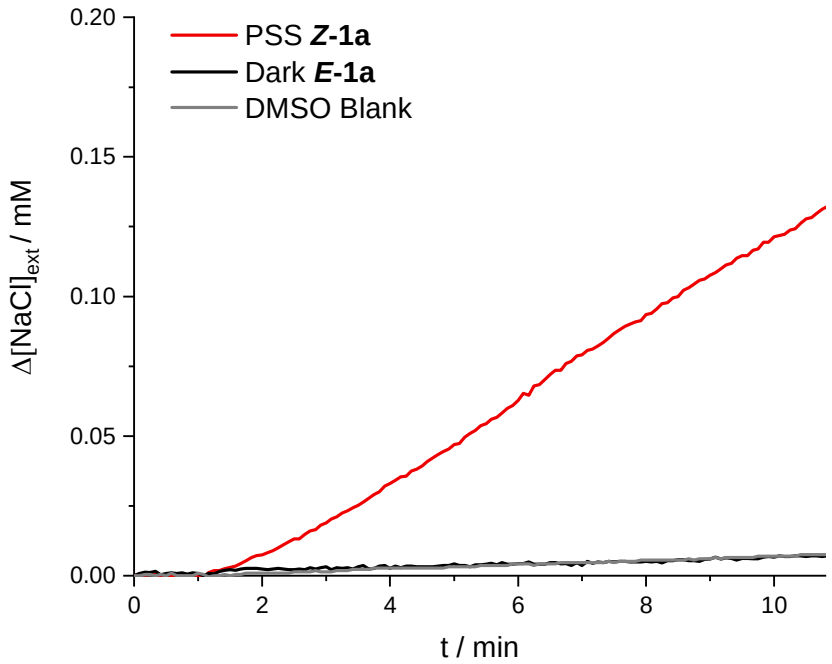

Figure S145. Ion transport of **1a** (0.5 mol% relative to lipid) from POPC vesicles containing 489 mM NaCl, suspended in 489 mM $NaNO_3$, and buffered with phosphate salts at pH 7.0. Chloride efflux from POPC vesicles monitored by chloride-selective ISE. Data points: vesicle exterior Cl^- concentration

***In-situ* photo-switching of ion transport**

Vesicle suspensions (4.5 mL, 1 mM lipid) were added to a 17 mm vial, and gently stirred. The electrode is placed as high as possible into solution, to minimise interference with light from the LEDs (Fig S146). For each run, the electrode is held at the same angle, stirring rate held constant (300 rpm), and calibration curves using **equation S7** are made before and after each run to ensure consistency. The electrode must not be disturbed during the run (vibrations, movement etc).

Transporter **1a** as the dark adapted *E* isomer or control squaramide **S1** is added as a 1 mM stock solution in DMSO (22.5 μL, 0.5 mol% relative to lipid) at 60s and voltage was monitored over time. The sample was continually irradiated as follows: red at 2 minutes, blue at 9 minutes, red at 16 minutes, blue at 23 minutes. Results are calibrated with **equation S7**. The relative rate enhancement achieved by direct irradiation of the transporter in vesicles, k_{red} / k_{blue} was approximately 10 under these conditions.

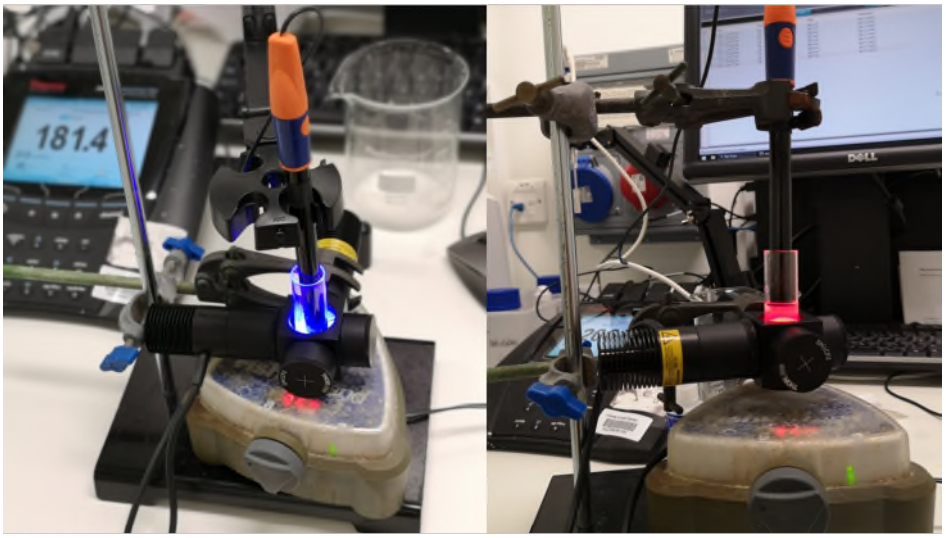

Figure S146. Experimental setup for ISE.

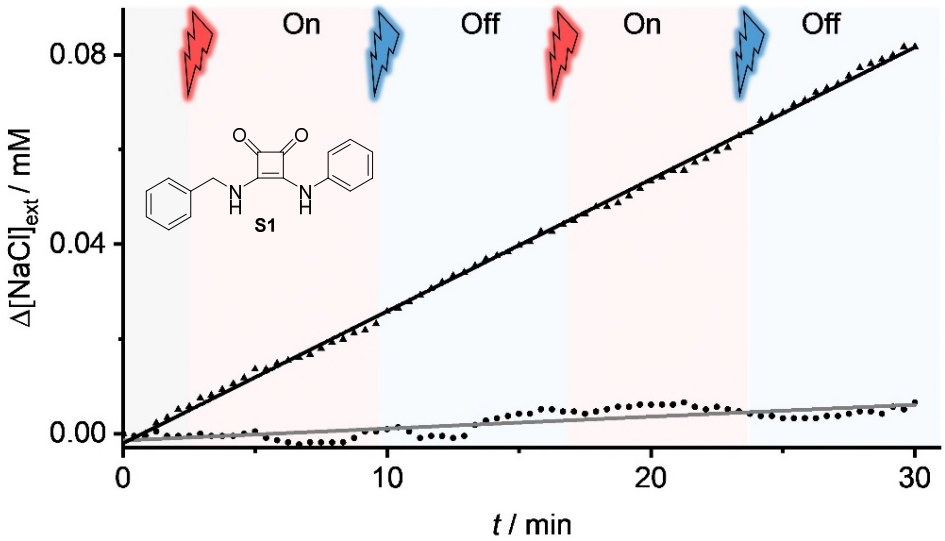

Figure S147. Ion transport of S**1** (▲) (0.5 mol% relative to lipid) added at t = 0 min and DMSO (●) from POPC vesicles containing 489 mM NaCl, suspended in 489 mM $NaNO_3$, and buffered with phosphate salts at pH 7.0. Chloride efflux from POPC vesicles monitored by chloride-selective ISE. Colours indicate commencement of sample irradiation using 625 nM (0.9 W, red) or 455 nm (1.1 W, blue) LEDs.

To estimate the efficiency of the *in-situ* generation of the transport-active *Z* isomer that occurs in the photo-switchable transport experiment (Article Figure 7), the ion transport rate in the "ON" state were compared to that for direct addition of the PSS mixture (77% Z, obtained by pre-irradiating the DMSO stock solution of **1a**^{E} to achieve the PSS; Figure S145):

$$k_{\text{obs,in-situ}} / k_{\text{obs,direct}} = 0.45$$

This agrees with results from NMR analysis (Figure S143). An analogous experiment using the HPTS ion transport assay afforded similar results. In this assay, carrier **1a**^{E} (62.5 nm) was added to the POPC LUVs containing HPTS. The cuvette was then placed in a cuvette holder (Figure S75) and irradiated with red light (625 nm, ~0.9 W) for the stated duration. The cuvette was placed in the fluorescence

spectrometer, a pulse of NaOH was added to start the transport experiment, and 25 μL of Triton X-100 in 7:1 (v/v) H_2O-DMSO used to calibrate the assay at the end point (Figure S148). Under these conditions, maximum activity was achieved after 5 minutes irradiation. The ratio of the fractional fluorescence intensity (I_{rel}) at 290 s just prior to lysis, defined as the fraction activity *y*, revealed a ratio $y_{in\text{-}situ}$ / $y_{external}$ of 0.45 after 2 mins and 0.55 after 5 mins irradiation.

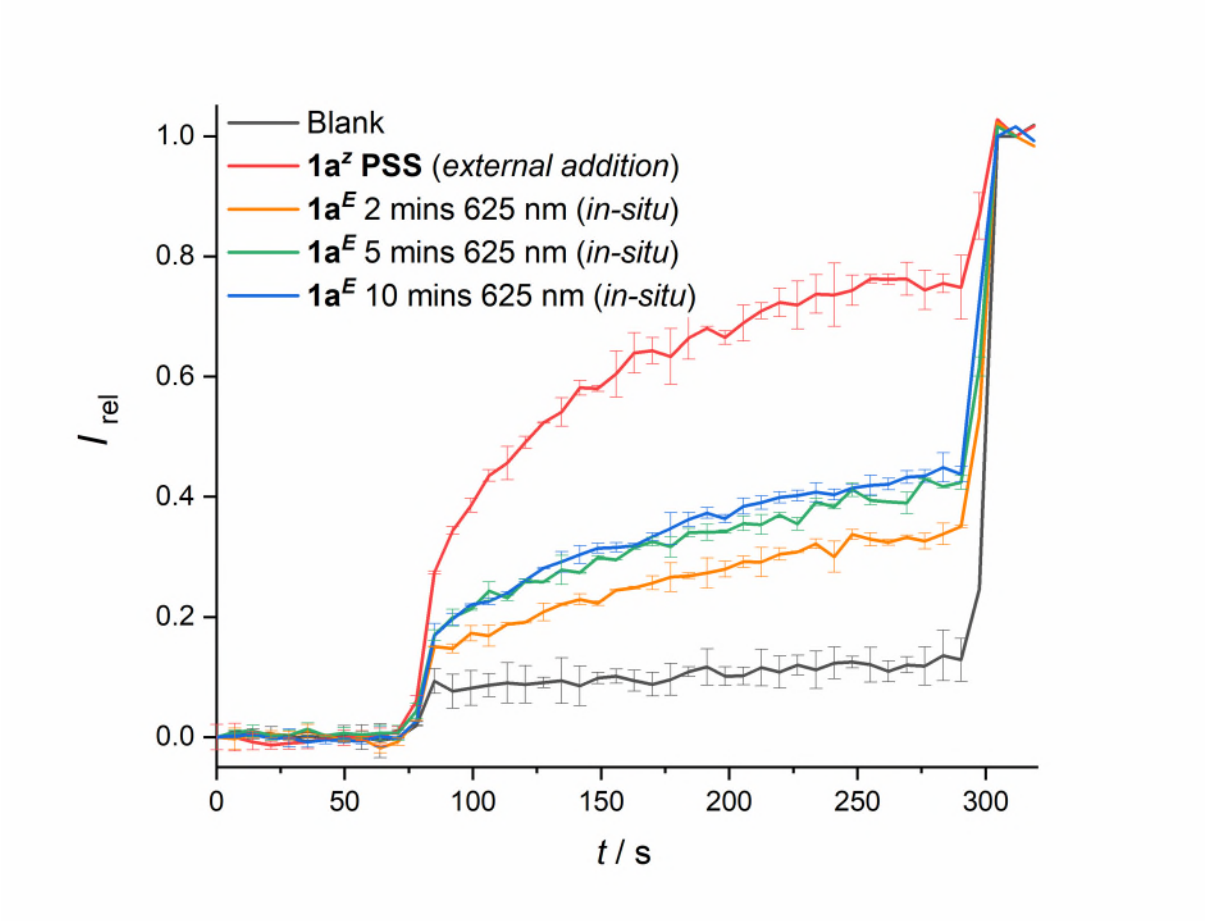

Figure S148. HPTS assay for *in-situ* photo-switching of **1a**^{E} (62.5 nM) following 2 (orange), 5 (green) and 10 (blue) minutes of irradiation with 0.9 W 625 nm red light. Red data: external addition of **1a**^{Z,PSS} following photo-isomerization in DMSO.

8 References

(1) Dai, L.; Su-Xi, C; *Advanced Synthesis and Catalysis* **2011**, 13, 2137–2141
(2) Yang, C.; Wang, J.; Liu, Y.; Ni, X.; Li, X.; Cheng, J.; *Chemistry – A European Journal* **2017,** 23, 5488–5497
(3) Kuzmic, P., *Anal. Biochem.* **1996**, 237, 260–273.
(4) Hunter, C. A.; Anderson, H. L.; *Angew. Chem. Int. Ed.* **2009**, 48, 7488–7499
(5) Sakai N, Houdebert D, Matile S. *Chem. Eur. J.* **2003**, 9, 223–232
(6) Sakai, N.; Matile, S.; *J. Phys. Org. Chem.* **2006**, 19, 452–460
(7) Ren, C.; Chen, F.; Ye, R.; Ong, Y. S.; Lu, H.; Lee, S. S.; Ying, J. Y.; Zeng, H.; *Angew. Chem. Int. Ed.* 2019, 58, 8034-8038